Towards Sustainable Heating

The Impact of Integrating District Heating Networks with Electricity Systems

MSc Thesis

Bas Kempkes

Delft University of Technology

Towards Sustainable Heating

The Impact of Integrating District Heating Networks with Electricity Systems

by

Bas Kempkes

Date:	**April 30, 2025**
	To be defended in public on: May 14, 2025
Student number:	4927427
Thesis comittee	
First supervisor:	Prof. Dr. Ir. L. de Vries, TU Delft
Second supervisor:	Dr. A. F. Correljé, TU Delft
External supervisors:	R. Godderij, EBN
	B. Schroot, EBN
	T. van Melle, EBN
Faculty:	Faculty of Technology, Policy & Management, Delft
MSc:	Complex System Engineering & Management

:

Acknowledgement

This thesis marks the end of my Master's in Complex Systems Engineering and Management at the TU Delft and, along with it, the end of my time as a student. After several years of studying, learning, and growing, I now feel ready to take the next step into working life.

I would like to sincerely thank my TU Delft supervisor, Laurens de Vries, for his continuous support and guidance throughout this thesis. The regular discussions were both insightful and motivating. The constructive feedback helped me improve my work significantly. I would also like to thank Aad Correljé for his helpful input and thoughtful reflections that strengthened the academic framing of this thesis.

From Energie Beheer Nederland (EBN), I want to sincerely thank Raymond Godderij, Barthold Schroot, and Timme van Melle. Your insights, guidance, and time have been a great help in shaping the practical side of this research. I'm especially grateful for your willingness to engage with the technical and modeling aspects of the thesis. I would also like to thank other EBN colleagues who contributed their knowledge or were available for questions along the way. Beyond the professional input, I appreciated the nice and welcoming office atmosphere. The fun office moments were a welcome balance during intense thesis phases.

Conducting my thesis within a company setting was a privilege. It gave me the opportunity to work on a real-world challenge, connect my academic knowledge with practice, and gain valuable experience for the future. Without this collaboration, this final part of my studies would have felt much heavier. I am glad to have experienced it in this way.

Lastly, I want to thank my family and friends for their continuous support, not just during this thesis, but throughout my entire study. Your help and company made my time as a student incredibly enjoyable, and without it, reaching this milestone would have been much more difficult.

Thank you all.

Bas Kempkes
April 2025

Executive Summary

Introduction

The heating sector in the Netherlands accounts for 41% of national energy consumption and remains heavily reliant on fossil fuels, with 89% of heat demand currently met by non-renewable sources. Due to climate goals and the Dutch Climate Agreement, a transition to sustainable heating alternatives is essential. District heating networks, particularly those utilizing heat sources such as geothermal energy and thermal storage, have been identified as key components of this transition. However, a core challenge remains: the mismatch between heat supply and demand, especially due to seasonal fluctuations.

Research approach

This study investigates how a heating system can be integrated with the electricity system to improve performance and minimize operational costs. This study focuses on how low-cost electricity and thermal storage can balance supply and demand. The central research question is:
What are the potential synergies of integrating and optimizing a heating system with an electricity system, to minimize operational cost and improve system performance?

To address this question, a techno-economic optimization model is developed using the open energy modeling framework (oemof) in Python. The objective is to minimize operational costs while evaluating the role of high-temperature aquifer thermal energy storage (HT-ATES) and power-to-heat solutions in improving system flexibility, efficiency, and sustainability. A real-world case study of Delft is analyzed in four experimental scenarios: fixed electricity pricing, dynamic market-based pricing, grid capacity constraints, and grid reinforcement.

Main findings

The key findings from this study are:

- Dynamic electricity pricing improves system responsiveness and storage costs. Heat pumps can be operated during off-peak hours, using low-cost electricity to charge the HT-ATES. This reduces reliance on gas-fired backup systems and improves cost efficiency. However, since total system costs are still dominated by CAPEX and fixed OPEX, the impact of operational savings from dynamic pricing alone remains limited.
- Thermal storage proves to be a valuable system component. By enabling energy to be stored in the form of heat, it facilitates load shifting and temporal decoupling between electricity consumption and heat demand. This significantly reduces fossil fuel reliance, particularly during periods of grid congestion. Thermal storage systems also act as long-duration, controllable electricity consumers, capable of absorbing renewable energy surpluses during periods of high production and reducing electricity demand during peak hours. This not only improves the performance of the heating system but also supports the stability and resilience of the electricity grid. In general, thermal storage creates strong synergies between the heating and electricity sectors and enhances the flexibility of the integrated energy system.
- Electricity grid constraints impose substantial limitations on electrified heating systems. During peak hours, electric systems may be restricted, leading to increased dependence on fossil fuels. Systems with larger heat pumps and well-sized storage are more resilient in these conditions, as they can shift electricity consumption to off-peak hours.While grid reinforcements are essential to prevent these limitations, the associated costs are economically justified in most scenarios. In the short term, thermal storage provides a viable and cost-effective mitigation strategy to alleviate pressure on the electricity grid.
- The research reveals a fundamental trade-off between capital expenditure, system flexibility, and CO_2 emissions. Larger systems are more robust, reduce emissions, and perform better under

stress conditions, but require higher upfront investments. Smaller systems are less expensive but also less adaptive and therefore remain more dependent on fossil fuels.

Recommendations

This research leads to several recommendations for the design and implementation of future district heating systems. First, thermal energy storage should be actively supported through investment subsidies or regulatory mechanisms. Its system-wide value in improving flexibility, reducing peak demand, and enabling the use of sustainable heat sources makes it an important aspect of resilient systems. Secondly, early coordination between heat developers, grid operators, and public authorities is essential. The rollout of heating networks must be closely synchronized with electricity infrastructure planning to prevent grid congestion and ensure that connection capacity is sufficient to support increasing levels of electrification. Lastly, the development and adaptation of smarter more responsive system designs to enhance flexible behavior. These systems should be capable of adjusting electricity consumption based on grid conditions and price signals. Regulatory frameworks or market mechanisms that reward flexible operation can play a key role in achieving this. Together these measures will help to ensure that heating system investments are both economically sound and aligned with long-term sustainability and energy transition goals.

Contents

List of Figures

List of Tables

1
Introduction

1.1. Problem definition

In recent years, the need for a transition toward sustainable energy systems has become more apparent due to the growing effects of climate change. Addressing climate change requires a large-scale shift to renewable energy sources, reducing dependence on fossil fuels [37]. In the Netherlands, heating accounts for a significant share of total energy consumption: 41% of the national energy demand is dedicated to heating [22]. A large portion of this heat is still sourced from fossil fuels, with 89% of demand met by non-renewable sources, as illustrated in Figure 1.1 [22, 64]. Consequently, the heating sector is a major contributor to CO_2 emissions, highlighting the urgent need for substantial improvements to develop a future-proof heating system.

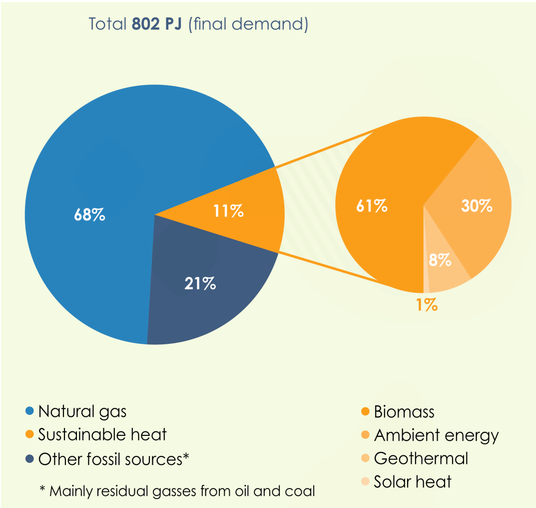

Figure 1.1: The sources of heat in the Netherlands [22]

To achieve carbon neutrality by 2050, the Dutch government has implemented regulations to make residential and commercial buildings more energy efficient. By 2030, it aims to transition 1.5 million households to sustainable heating systems and increase the share of renewable energy sources [50]. According to the Climate Agreement, all buildings must be heated sustainably by 2050, eliminating the use of natural gas [69]. The Dutch government recognizes district heating networks as high-potential alternatives for replacing fossil-fuel heating systems, particularly systems that involve renewable heat sources. The use of district heating is expected to eventually supply up to 50% of the heat demand for residential buildings and households [36]. As it enables large-scale utilization of heating resources, including geothermal energy and industrial waste heat [2].

A challenge that arises in the transition to a sustainable heating system is the mismatch between heat supply and demand. The heat demand pattern shows alternating high and low peaks throughout both daily cycles and seasonal changes. Characterized by high demand peaks during winter and low demand during summer[32]. Without an effective solution, this seasonal imbalance creates operational and economic challenges for district heating networks.

To address the strong seasonal mismatch, large-scale heat storage can be a solution to balance the system. Aquifer thermal energy storage (ATES) presents a promising approach. ATES allows surplus heat generated in summer to be stored underground and use during periods of high demand [8]. Currently, most existing district heating networks operate at high temperatures. Yet, conventional ATES systems are limited to storing temperatures up to 30°C, restricting their direct application in high-temperature district heating networks. Although future networks are expected to operate at lower temperatures, thanks to better building insulation. In the meantime, a solution is needed for high-temperature systems. A potential alternative is high-temperature aquifer thermal energy storage (HT-ATES), which allows heat storage at temperatures up to 90°C. HT-ATES can offer a potential solution to address the mismatch between heat supply and demand, improving potentially the flexibility, sustainability, and efficiency of the district heating network [43]. As shown in Figure 1.2, thermal storage helps buffer heat from various sources, offering greater flexibility and better utilization of surplus energy.

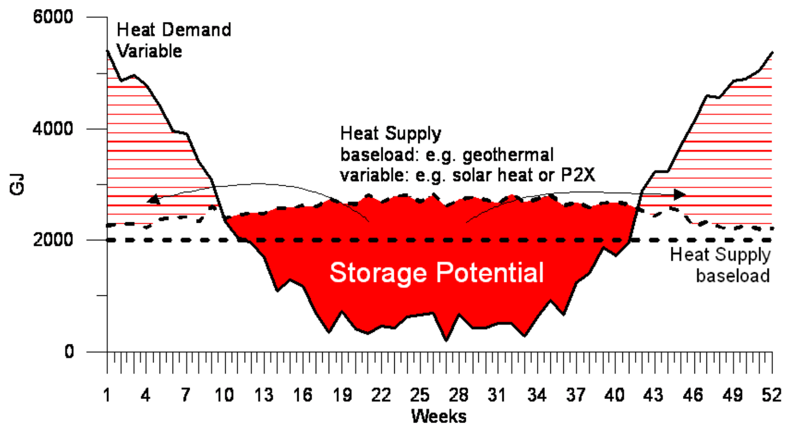

Figure 1.2: Seasonal thermal energy storage [33]

District heating networks can draw heat from several technologies, including geothermal wells, ambient heat, and industrial waste heat. Additional technologies that function as heat sources are heat pumps and e-boilers, which also function as a coupling element between the electricity and heating sector [45]. The transition from fossil fuels to renewable heating technologies introduces uncertainties and operational challenges in both sectors. A possible concern is the increasing electricity demand associated with electric heat technologies. The additional demand could cause additional strain on the electricity grid, especially during peak load periods [3]. Moreover, fluctuating electricity prices add volatility and unpredictability to the system [49]. Introducing storage possibilities can help mitigate these challenges. An important factor in ensuring the feasibility of district heating systems is the cohesion between the heating and electricity sectors. Currently, these sectors often operate independently, resulting in missed opportunities for synergy [6, 60].

A potential approach for increasing the efficiency of renewable energy sources is to use a multi-energy system (MES). In an MES, excess electricity can be stored as heat and could potentially increase the resilience of the heating sector. Integrating district heating networks with the electricity grid can improve overall energy efficiency by enabling better balancing of supply and demand [46]. For example, power-to-heat (P2H) technologies allow surplus renewable electricity to be converted into storable heat during periods of high generation [2]. Integrating these systems can possibly create a more efficient allocation of energy resources, where supply and demand are better balanced [60]. However, the large-scale deployment of HT-ATES systems faces several challenges. The combination of the heating and electricity sectors results in complex interactions between the heating sector and the electricity sector, introducing several uncertainties and technical complications.

1.2. Literature review

The integration of HT-ATES technology into district heating networks presents both opportunities and challenges, as outlined in the previous section. The literature review identifies existing research on multi-energy systems that incorporate thermal energy storage and explore uncertainties and possibilities for integrating HT-ATES within district heating systems.

1.2.1. District heating networks

District heating systems have evolved over the past decades. Early-generation district heating systems relied on fossil fuels such as coal, gas, or oil. During the 21st century, the focus shifted toward more sustainable solutions. With renewable heating technologies and CO_2 reduction playing a central role in research and policy-making [47]. These networks are expected to play a vital role in the energy transition, particularly when integrated with smart energy sources [48]. To ensure both economic and sustainable viability, the role of energy storage is increasingly important. Thermal energy storage can potentially improve the business case for district heating networks. The exact role depends on factors such as temperature levels, network size, heat production methods, storage technologies, and broader energy scenarios [72].

1.2.2. Role of thermal energy storage

Thermal energy storage has been recognized for its ability to mitigate the mismatch between heat supply and demand [32]. ATES systems, commonly used for low-temperature underground storage, have been extensively deployed in the Netherlands. In particular, in large commercial buildings to provide flexibility and be able to supply heat in the winter and cooling in the summer.

However, for the implementation of high-temperature storage further research is necessary to assess the feasibility of such projects. Drijver et al. (2012) [20] identified low recovery efficiency and technical challenges as the main barriers in previous HT-ATES projects. Since then, significant technological advances have been made. High temperatures sources such as geothermal wells and industrial waste heat can now be stored more efficiently. This enables the deployment of storage alongside baseload heat sources, reducing reliance on peak-load technologies like gas boilers, thereby decreasing CO_2 emissions and improving the year-round use of geothermal resources [8].

Beyond technological improvements, various research initiatives have assessed the feasibility of HT-ATES. The WINDOW research consortium, which followed the European-funded HEATSTORE project, conducted geological suitability studies for multiple HT-ATES locations [19]. National programs, including WarmingUP and its successor WarmingUP GOO, have provided deeper insights into the technical, legal, and economic feasibility of HT-ATES within the Dutch context. [31, 58]

A study by Zwamborn et al. (2022) [77] compared various potential HT-ATES locations in the Netherlands. The study analyzed their geological, legal, and economic feasibility. It concluded that, under specific conditions, HT-ATES can be economically competitive with other future-proof heating technologies. Similarly, Liu (2019) [43] and Daniilidis et al. (2022) [15] emphasized that integrating HT-ATES improves the techno-economic performance of district heating networks by lowering overall heat production costs and reducing CO_2 emissions.

Overall, multiple studies suggest that HT-ATES has the potential to become a valuable seasonal energy storage solution. When integrated with geothermal wells, industrial waste heat, or power-to-heat (P2H) technologies, it can help balance supply and demand, mitigate seasonal mismatches, and provide peak-load flexibility [21]. However, successful large-scale deployment requires suitable geological conditions, supportive regulations, and favorable economic environments.

1.2.3. Multi energy system design

The design of the energy system is decisive for how different elements within a district heating network interact with each other, which determines the system's overall effectiveness [61]. Many studies have investigated the interaction between district heating networks and the electricity sector. Integrated energy systems are considered important for future planning to improve energy efficiency and system flexibility. District heating networks offer the potential for a more sustainable heating sector, as they enable the integration of various energy technologies and storage solutions. This ultimately improves the overall efficiency of the heat supply compared to other renewable alternatives [63]. Consequently, multi-energy systems (MES) are regarded as a cornerstone of future sustainable heating networks. They offer advantages such as high energy efficiency, enhanced flexibility, improved grid balancing, and significant sustainability benefits [6, 14, 38, 44, 60, 63, 76].

Sectoral coupling has increased the importance of power-to-heat (P2H) technologies. P2H technologies convert excess renewable electricity into heat, with the ability to store and utilize this energy later in the year[9, 66, 76]. This characteristic is particularly valuable due to the intermittency of renewable energy sources, which makes it challenging to balance supply and demand. To address this challenge, additional flexibility solutions, such as P2H and HT-ATES are important to ensure reliable grid balancing services [38]. To achieve an effective operable system, the heating and electricity networks need to be used more efficiently. However, a major barrier remains the lack of suitable tools that can simultaneously capture the detailed operating parameters of both networks [5]. The design and coupling of multiple energy technologies, along with defining the correct technical parameters for both the heating and electricity sectors remain a complex challenge.

1.2.4. Comparison of similar studies

Various studies do highlight the benefits of multi-energy systems while also acknowledging the challenges associated with their integration. Different studies employ different methodologies for optimizing and modeling different MES configurations. These studies aim to identify optimal system designs and assess the feasibility of HT-ATES technology under different conditions. The key findings of these studies are summarized in Table 1.1, providing an overview of objectives, model outputs, temporal resolutions, and modeling horizons.

Study	Objective	Model Output	Time Step	Horizon
Capone et al. (2021) [12]	Multi-objective optimization: minimizing total operation cost; minimizing carbon emissions	System cost per day, heat load, Pareto curve	Minutes	1 day
Cheng et al. (2019) [14]	Minimizing total cost	Heat load, system costs	Not specified	Scenario-based
Desguers et al. (2024) [17]	Multi-objective optimization: maximizing energy efficiency; maximizing demand-side flexibility	Thermal efficiency, heat load, operational costs, emissions	10 min	20 years
Roest et al. (2021) [60]	Minimizing the levelized cost of heat	HT-ATES performance, heat demand with HT-ATES, MES efficiency	Hourly	10 years
Bakker & Roest (2023) [6]	Minimizing total cost	All costs, emissions, share of renewable energy	Hourly	20 years
Javnashir et al. (2022) [38]	Multi-objective optimization: minimizing heat production costs; maximizing revenue from electricity and balancing markets	Optimal DHN operation, revenue from markets	Hourly	3 years
Visser & Terwel (2024) [72]	Cost minimization	Distribution mix, CO_2 emissions, LCOH, grid congestion	Hourly	1 year
’t Westende & Dinkelman (2023) [2]	Multi-objective optimization: maximizing economic and sustainable performance	Economic and sustainability indicators	3 days	10 years

Table 1.1: Overview of objectives, model outputs, and design parameters in comparable studies.

Optimization modeling is the most commonly used approach, where the primary focus is on economic parameters. Multiple studies aim to minimize operational or total costs, while others incorporate objectives such as carbon emission reduction, energy efficiency, or flexibility improvements. Model outputs usually include system costs, heat loads, efficiencies, and emissions. Energy demand is in these cases often treated as a hard constraint rather than a flexible model output. Most studies use an hourly time step, as it aligns with the availability of weather and energy demand data. However, some studies utilize higher resolutions (minutes to 10-minute intervals) for more detailed operational modeling. The time span also vary: some research focuses on single-year modeling, while others assess long-term feasibility over multiple years. Overall, while the majority of studies strive for cost minimization, this does not always lead to the most sustainable outcomes. This reflects the ongoing challenge of balancing economic feasibility with sustainability objectives when deploying MES and HT-ATES solutions.

1.3. Research gap

Despite the growing interest in HT-ATES and its potential role in multi-energy systems, several critical knowledge gaps remain. These gaps primarily concern the integration of heating and electricity systems and the impact of electricity market dynamics on heat storage. Most existing studies treat heat and electricity networks as separate systems, with limited exploration of their synergies and joint operations. Although the potential of HT-ATES to improve system flexibility is often acknowledged, few studies examine its interaction with electricity markets. In particular, the effects of low-price electricity availability on heat storage, heat generation, and overall system feasibility remain underexplored.

As electrification in heating networks increases, access to the electricity grid will not always be guaranteed. Network congestion and infrastructure limitations could restrict available grid capacity. However, much of the current research assumes unrestricted electricity access and neglects the impacts of grid constraints, connection limits, and network tariffs. Investigating the interaction between heating systems and electricity grids, particularly under constrained conditions, is therefore essential to fully understand their operational and economic implications.

Integrating an HT-ATES offers several potential advantages, such as reducing dependence on high-cost peak electricity, improving system flexibility, and supporting sustainable heat. However, integration also introduces design challenges. Technical frameworks must become more complex, and economic incentives must be carefully structured to ensure efficient system operation. Additionally, the influence of different future energy scenarios, fluctuating energy prices, and policy incentives on technical design choices remains insufficiently studied. As the complexity of MES increases, there is a growing need for research that guides different investment strategies, especially in the sizing of key technologies to create flexible and resilient systems. This research aims to address these gaps by examining the interactions between heat storage and grid stability. By better understanding how these systems can work together, this study will provide insight into developing efficient, flexible, and future-proof heating systems capable of withstanding varying weather and market conditions.

1.4. Research objective

This research seeks to address the identified knowledge gaps related to the integration of heating and electricity systems. The focus is on understanding the synergies and interactions between these sectors through the design and evaluation of an integrated district heating network. Specifically, the study will analyze a district heating network that incorporates geothermal energy as baseload, thermal energy storage, and power-to-heat applications. Various technological configurations will be compared to determine their cost-effectiveness, flexibility, and sustainability. A particular emphasis will be placed on how low-cost electricity can be leveraged for heat generation and storage, while also accounting for electricity grid limitations.

The primary goal is to minimize the operational costs of the district heating network while integrating different technologies to create a resilient, future-proof system. The choice to focus primarily on operational costs is motivated by the fact that variable costs are crucial for the generation of heat. Every hour, a new merit order will be established based on marginal production costs, allowing the system to select the most cost-effective heat generation option, independent of installed capacity. Prioritizing operational costs enables the identification of efficient system designs under dynamic market conditions.

However, it is important to acknowledge that minimizing operational costs may have implications for the CAPEX. The size of key components, such as P2H installation and geothermal capacity, is directly influenced by system design choices. A larger P2H installation may enable greater flexibility in using cheap electricity, but could increase upfront investment costs. Similarly, the required size of a geothermal well may be impacted by system integration strategies. Although the study does not optimize the technologies for their CAPEX, it recognizes the interplay between investment decisions and long-term operational savings, which will be included in the results.

A particular focus will be on the utilization of low-cost electricity for heat generation and storage, as well as the limitations of the electricity grid. The aim of the system is thus to minimize the operational costs for the heating network to provide as cheaply as possible heat to consumers. By aiming for minimal operational costs, the economic incentives become central in this research. Thereby, the feasibility and scalability of the system will be researched. Furthermore, the research will assess the influence of varying energy scenarios. This includes fluctuating electricity prices, grid limitations, and the integration of renewable energy for the technical and economic performance. By examining these aspects, the objective of this research's is to provide new insights into the role of integrated heating and electricity systems while achieving cost minimization, operational efficiency, and sustainability. This leads to the following main research question:

What are the potential synergies of integrating and optimizing a heating system with an electricity system, to minimize operational cost and improve system performance?

1.5. Sub research questions

To answer the main research question, the report is structured around four key sub-questions. Each sub-question addresses a specific aspect of the integration between the heating and the electricity system. With the complexity of the analysis increasing progressively. The following sub-research questions are formulated:

- How can a heating system be designed to optimize electricity usage and heat demand with a fixed electricity price?
- What is the impact of real-time electricity prices on the optimal heating system design?
- How do network capacity constraints on the electricity grid affect the optimal layout of the heating system?
- How do economic incentives need to be designed to influence the heating system for optimal performance?

The first sub-question establishes a baseline model by analyzing a heating system in a simplified scenario with fixed electricity prices. This allows identification of fundamental system parameters, such as the size of HT-ATES, geothermal wells, and P2H applications. By understanding system performance in a stable pricing environment, this step provides a reference point for later analyses involving dynamic factors.

The second sub-question introduces real-time electricity prices into the model. This step investigates how varying electricity prices influence the ideal operation of the heating system, including decisions about when to generate heat or store heat. Considering the increasing volatility of electricity prices due to growing shares of renewable energy, this analysis is crucial for designing resilient systems.

The third sub-question examines the effects of electricity grid capacity constraints, such as limited connection capacity or network congestion. As the heating sector becomes more electrified, grid limitations will increasingly impact heating system design and operations. This part of the study explores how such constraints influence the optimal system configuration.

Finally, the fourth sub-question analyzes how economic incentives, such as pricing schemes and network tariffs, can encourage more cost-efficient and sustainable operation of integrated heating systems. By incorporating economic incentives into the model, this research evaluates their role in guiding operational decisions.

By providing answers to these four sub-questions, this research aims to construct a general outline of how HT-ATES, P2H, and geothermal heating systems can be optimized to provide lower operational costs, greater flexibility, and greater resilience to future energy challenges.

1.6. Relevance

Research emphasizes the urgency of investigation in this area due to the increasing challenges of heat supply, as peak loads in the Dutch electricity grid must be reduced and electricity surpluses better utilized. This contributes to a more flexible and sustainable energy system.

This master thesis aligns closely with the objectives of the CoSEM program by researching the integration of district heating with the electricity market. Various learning aspects of the Energy track will be utilized. By addressing technical complexities, this research adds value to the MSc program's learning objectives, as it combines technical and societal aspects to optimize the balance between thermal energy storage and the electricity grid.

1.7. Report outline

The report is structured as follows. Chapter 2 discusses the methodology of the thesis, including the research approach, research methods, and key performance indicators. Chapter 3 introduces the district heating network model, starting with the conceptualization of the system. Subsequently, Chapter 4 presents the case study and outlines the key components of the model. This chapter also includes the verification and validation of the model. In Chapter 5, the experimental designs are explained, followed by Chapter 6, in which the results are analyzed. Chapter 7 contains the discussion, where the findings are further examined and the limitations of the study are addressed. Chapter 8 presents the conclusion of the thesis. Lastly, Chapter 9 presents a personal reflection on this master thesis.

2 Methodology

Building on the research questions introduced in Chapter 1, this chapter explains what kind of research approach is used to simulate the performance of various district heating configurations. It details the model structure, assumptions, and evaluation metrics used to analyze system behavior.

2.1. Research approach

The objective of this research is to determine the optimal configuration of a district heating system that minimizes operational costs while reliably meeting heat demand. This objective must be achieved within the limits of network constraints, regulatory requirements, and economic incentives. Consequently, the chosen research approach must be able to identify an efficient generation mix, integrate relevant technical and institutional constraints, and evaluate the effects of network tariffs and policy mechanisms. Given the uncertainties of future energy systems, the approach needs to be flexible, allowing for the incorporation of different energy scenarios and the evaluation of their effects. The research aims to uncover unknown relationships and interactions within the system.

To achieve this, a modeling approach is employed. A modeling approach can effectively describe how different mechanisms interact and evolve over time. The problem focuses on minimizing operational costs, with a hard constraint of supplying heat demand. The problem is framed as an optimization task, specifically a mixed-integer linear programming (MILP) problem. This method allows optimal system configuration while respecting technical and economic constraints.

The heating system must meet the required heat demand in the most cost-effective way, leading to the formulation of a heat dispatch optimization model. The model examines the interconnections between the heating and electricity systems while accounting for specific constraints. For simplification, a deterministic energy system model is adopted, assuming fixed relationships between components. As a result, the model does not account for uncertainties as future heat and electricity demand scenarios are predefined.

The modeling approach offers a distinct advantage by enabling detailed simulation of various scenarios, providing insights that would be difficult to test in real-world conditions. Through these simulations, different strategies for integrating HT-ATES and electricity networks can be tested and refined [26]. However, the modeling approach also has limitations. Inaccurate assumptions can introduce errors, where even minor discrepancies in the model lead to significant deviations in the results. This highlights the importance of developing the energy model with precision and care. It is critical to acknowledge that no model can fully capture the complexity of real-world systems. A poorly defined model scope or inadequate data can result in output biases [65]. To mitigate these risks, the model will be validated through sensitivity analyzes and scenario verification to assess the impact of different assumptions [59].

2.1.1. Modeling framework

The model is developed following a structured step-by-step approach to ensure that all technical and economic aspects of the integrated system are thoroughly analyzed. This process is iterative, each step is validated by the next to minimize errors and refine assumptions. The modeling approach consists of five main phases as shown in Figure 2.1.

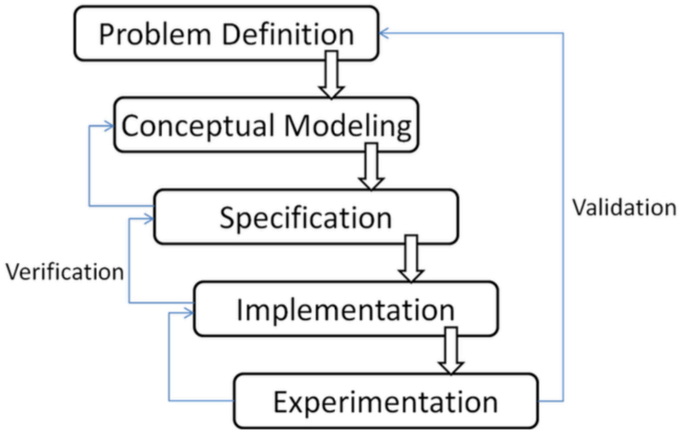

Figure 2.1: Modeling approach [13]

Problem definition
In this initial stage, the specific challenges and objectives of the district heating model are identified. This includes understanding the core requirements of the system and defining the problem. This step establishes the foundation on which the model is built, ensuring that it addresses both technical functionality and socio-economic factors.

Conceptual modeling The conceptual model phase transforms the problem statement into a structured design, identifying the most important elements of the district heating network. It includes primary components such as heat sources, storages, and connections to electrical grids. The system accounts for interactions between technical subsystems and socio-technical dimensions such as regulation on policies, market incentives, and customer choice.

Specification
In the specification phase, the conceptual model is translated into specific quantifiable parameters and rules that will guide the system's operation and performance. This means specifying technical specifications for components and functional parameters. This is done to fill in the conceptual framework with a strong, implementable design that suits technical feasibility as well as socio-economic integration.

Implementation
Implementation involves translating the specifications into a working simulation, including coding and data integration. The implementation is constructed iteratively to allow for adjustments based on verification from previous steps. The goal is to ensure that technical and economic system dynamics are accurately represented under realistic conditions.

Experimentation
Throughout the experimentation process, the model is tested by a series of simulations to verify its performance and analyze the impact of different scenarios. Iterative adjustments are made as more experience is acquired, refining the model to become more accurate and applicable to real scenarios. This phase not only validates the model but also identifies potential optimizations for district heating network operation under various future conditions.

2.2. Research methods

The research methods used in this thesis are divided into tools that identify the necessary input values for the model. The second are tools to model and simulate the integrated energy system.

2.2.1. Identifying uncertainties

In energy system modeling, uncertainties play a crucial role in determining the accuracy and reliability of the results. External factors such as fluctuating energy prices, evolving policies, and climate variability can significantly affect the design and operation of heating and electricity networks. To address these uncertainties, this study uses the Energy Transition Model (ETM). The ETM is an interactive open-source simulation tool designed to explore potential future energy systems. It provides a detailed representation of the Dutch energy market, allowing users to create custom scenarios by adjusting input parameters. Key features of the ETM include: the design of multiple future pathways, evaluating the impact of renewable energy integration, electrification trends, and researching different weather patterns.

The ETM provides a comprehensive analysis of regional and national energy systems. This covers aspects such as demand and supply for both electricity and heat. Also, the estimation of emissions and system efficiency can be simulated. The ETM enables to build scenarios designed for specific future years, incorporating technological advancements, regulatory changes, and economic factors. Another feature of the ETM is the ability to provide hourly heat demand profiles, electricity price series, and climate year data. By integrating historical climate variability, the ETM ensures that weather-dependent fluctuations in energy demand are realistically represented [25]. These detailed, dynamic datasets are crucial for constructing robust energy system scenarios, enabling the evaluation of how different weather patterns, policy developments, and market evolutions impact future heating and electricity networks.

2.2.2. Modeling tool

For system modeling, a custom optimization model is developed in Python. Python is selected for its flexibility, extensive libraries, and suitability for modeling complex multi-energy systems. Python offers an adaptable platform, facilitating the integration of multiple energy system modeling approaches within a cohesive framework. There are multiple open energy sources that can help with building a energy system framework. The core modeling framework in this study is based on the Open Energy Modelling Framework (oemof).

Open Energy Modeling Framework (oemof)

The oemof platform is a Python-based, open-source software toolbox for modeling and optimizing energy system. It is collaboratively developed by the Reiner Lemoine Institute (RLI), the Center for Sustainable Energy Systems (ZNES – University and University of Applied Sciences Flensburg), and Magdeburg University. The framework complies with the Best Practice Rules for Scientific Computing and adheres to the transparency Checklist for Energy System Models [57]. The key principle of the best practice rule is based on writing programs being for people where the computer is supposed to do the calculating work. Additionally, it is best to make incremental changes, and in the end collaborate with other users [75]. The transparency checklist refers to a framework that provides guidelines to ensure that energy models are clear, reproducible, and scientifically rigorous. Oemof is distributed with the MIT open-source license, allowing users to freely access, modify, and redistribute the framework. The framework is actively maintained on GitHub, with contributions from researchers and developers[51].

Oemof's modular structure supports a wide range of energy system applications, making it particularly useful for interdisciplinary studies between different energy systems. Its core library, oemof.solph, is specifically designed for creating and solving linear and mixed-integer linear optimization problems. The library is based on the Pyomo package, which enables the modeling of energy systems as networks composed of nodes and edges. Nodes represent components (producers, consumers, and processes), while edges define the relationship between nodes, including energy flows, and in- and outputs. The graph-based structure simplifies the representation of complex energy systems, and allows seamless integration of additional tools and libraries, facilitating the use of diverse modeling approaches [35].

Comparison with other modeling frameworks

While oemof offers a highly flexible, modular framework for energy system modeling, other tools also have their specific benefits and characteristics. Calliope is a user-friendly platform designed for high-level energy system planning. It excels in robust scenario analysis and enables users to evaluate energy systems across spatial and temporal scales. However, Calliope lacks the detailed domain-specific capabilities of oemof, particularly in modeling thermal properties and technologies. The second tool, OSeMOSYS, is a framework focused on long-term energy policy planning. It enables large-scale optimization with minimal computational requirements; however, it is less adaptable for interdisciplinary studies [35]. Specialized district heating tools like THERMOS and DiGriPy offer straightforward simulation and economic assessment capabilities for grid applications but do not support comprehensive multi-energy system modeling [73]. Proprietary tools such as ROKA3 and NEPLAN deliver precision in hydraulic simulations but sacrifice transparency and adaptability. Overall, oemof's balance of flexibility, extensibility, and focus on thermal integration makes it uniquely suited for this study, particularly for modeling integrated heating and electricity systems.

Integration and implementation

The custom model is developed iteratively through four phases. Each phase increases in complexity and realism, ensuring a structured and validated approach to modeling thermal-electric interactions, grid constraints, and cost dynamics. This phased approach ensures that the model evolves logically, starting with a basic heating system and culminating in a detailed cost optimization model. The custom model is designed to leverage two key features, firstly object-oriented and graph-based data structure. Which simplifies the representation of complex energy systems, which allows users to work efficiently with the model [40]. Secondly, seamless integration with external tools for easily extension of the model and integration with other modeling methods [52].

The first phase focuses on modeling the core heating system, laying the foundation for future expansions. This stage primarily determines the energy use and system sizing of key thermal components, as the HT-ATES, P2H applications, and heat demand from consumers. This will be done with the help of an extension of oemof, the library oemof.thermal provides tools for modeling thermal energy systems such as heating and cooling technologies. By addressing specific pre-processing and post-processing requirements, oemof.thermal expands the general capabilities of oemof.solph allowing for more detailed modeling of thermal flow processes[29]. At this stage, the main goal is to determine the optimal energy use and system sizing, ensuring the heating system can provide affordable and efficient heat to consumers. Electricity prices are assumed to be fixed in this phase.

In the second phase, the model is improved by incorporating real-time electricity prices. Adding a dynamic market element requires the system to react adaptively to price fluctuations at every time step. This increases the complexity of the model, since the model now calculates in each timestep the most cost-effective heating technologies. By adding more complexity to the model it transitions from a static cost minimization approach to an adaptive and market-responsive system that better represents real-world conditions.

The third step is to add grid constraints, ensuring that the energy system is within both the physical and economic limits of the electricity grid. This is a valuable addition, as it reflects the real-world grid capacity constraints, which can limit the level at which electrified heating technologies can be used. This addition makes the model more realistic, as it now accounts for both economic and technical constraints. With the physical network constraints, the model is converted from a cost-optimized model to a technically feasible energy system.

The final phase introduces network tariffs and grid reinforcements, refining the cost structure of electricity consumption. This phase shifts the model to a more detailed economic optimization enabling analysis of how financial incentives influence operational decisions.

2.2.3. Model variables

To clarify the structure of the optimization model used in this study, it is important to distinguish between endogenous and exogenous variables. Endogenous variables are determined within the model during the optimization process. These represent operational decisions made by the system to minimize cost or emissions, subject to technical and physical constraints. Exogenous variables, on the other hand, are provided as fixed inputs. These include scenario assumptions, weather data, environmental data, and system parameters that are not influenced by the optimization process but define the conditions under which the system operates. This classification helps to differentiate which aspects of system behavior result from the model optimization and which are based on predetermined assumptions and external calculations.

Model Element	Type	Description
Endogenous Elements		
Heat production	Endogenous	Model determines hourly operation to meet demand at lowest cost.
Charging/discharging of HT-ATES	Endogenous	Storage operation is optimized to use low-cost electricity and flatten demand peaks.
Electricity drawn from the grid	Endogenous	Determined based on pricing, grid limits, and heat demand.
Exogenous Elements		
Hourly heat demand	Exogenous	Based on external datasets; fixed per scenario.
Electricity prices	Exogenous	Scenario input reflecting different market behaviors.
Weather conditions	Exogenous	Affects heat demand and heat pump performance (COP).
Technology parameters	Exogenous	Equipment performance and cost values from literature and project inputs.
Grid capacity limits	Exogenous	Scenario-specific constraint for assessing congestion impact.
Network tariffs or incentive schemes	Exogenous	Used to evaluate financial viability and policy impacts.
Heat pump capacity	Exogenous	Set as a fixed parameter in predefined scaling scenarios.

Table 2.1: Overview of endogenous and exogenous variables in the optimization model.

2.3. Key performance indicators

To evaluate the performance and effectiveness of the integrated heating and electricity systems, a set of KPIs is used. These KPIs provide valuable insights into the environmental, technical, and economic performance of different designs and scenarios.

LCOH (€/MWh)
The Levelized Cost of Heat (LCOH) represents the average cost of producing one megawatt-hour (MWh) of heat over the entire lifecycle of the system. It includes capital investment (CAPEX), fixed operational costs (fixed OPEX), and variable operational costs (variable OPEX). Providing a comprehensive metric of the economic competitiveness of the system.

The LCOH acts as a financial benchmark for the feasibility of the projects. It indicates the minimum price at which heat must be sold to achieve a break-even point. It enables a standardized comparison between different heating solutions, supporting both the project feasibility analysis and long-term investment decisions. In this study, two variations of LCOH are analyzed. First, the *variable OPEX LCOH*, which includes the operational costs. These costs are primarily existent of 'fuel' costs such as electricity and gas. Second, the *total system LCOH* represents the complete cost structure (variable OPEX, fixed OPEX, and CAPEX and reflects the overall financial situation of the system.

CO_2 emission (kg/MWh)
Reducing carbon emissions is a key motivation for this research. Therefore, CO_2 emissions per megawatt-hour of produced energy are used as a critical environmental indicator. Lower emissions values indicate improved system sustainability and reduced reliance on fossil fuels. This metric provides direct insights into how effectively different system configurations contribute to the transition toward more sustainable energy sources.

3 District Heat Network

The Dutch electricity and heat markets are complex and interconnected systems. In this chapter, the heating network will be explained and the model is precisely defined. Understanding the interdependencies between these systems is essential. To achieve this, an in-depth exploration and conceptualization of the district heating network model will be conducted.

3.1. Conceptualization

The conceptualization of the model is based on a variety of sources, including academic literature, technical reports on district heating projects, and regulatory documents outlining sustainability objectives. Additionally, real-world case studies provide valuable information into technological decision-making and operational limitations. The district heating network model is constructed iteratively in four stages, with each stage increasing complexity and realism. The model's central aim is to portray the interaction dynamics among heating demand, electricity use, storage operation, and operating cost in a technologically viable and economic way.

3.1.1. Heating system

The heating system forms the foundation of the district heating network model. In this design, the focus is exclusively on the centralized district heating network rather than individual household heating solutions. The conceptual structure of the heating system is illustrated in Figure 3.1. Within this system, energy is generated using three primary sources: gas, electricity, and thermal heat. Electricity can be converted into heat and injected into the network with the help of a heat pump. Gas-fired boilers represent another method in which natural gas is combusted to produce heat. The third source is geothermal energy, where hot water is extracted from underground reservoirs to supply heat directly to the network [70].

A district heating system operates through a centralized network that distributes heat to multiple buildings through a chain of insulated pipes. Compared to individual household heating, where each building maintains its own boiler, a district heating network consists of a single closed-loop hot water circuit. The operation is cyclic: water is reheated at a centralized source (such as a geothermal facility, heat pump, or gas boiler) and then distributed through the network to residential and commercial consumers. In each building, a heat exchanger extracts heat from the circulating water for space heating. As the heat is extracted, the water temperature decreases, and the cooled water is returned to the district heating network. The returned water is then preheated at the central heat sources with the help of heat exchangers before being sent back into the network [30]. Water temperatures within the network fluctuate over time based on outdoor temperature conditions. During cold periods, lower ambient temperatures will require higher supply temperatures to meet heat demand. One advantage of a centralized system is that they enable effective heat distribution, reducing the need for individual gas boilers and give the option of integrating renewable heat sources.

The heating system consists of multiple integrated components, each fulfilling a specific role in main-

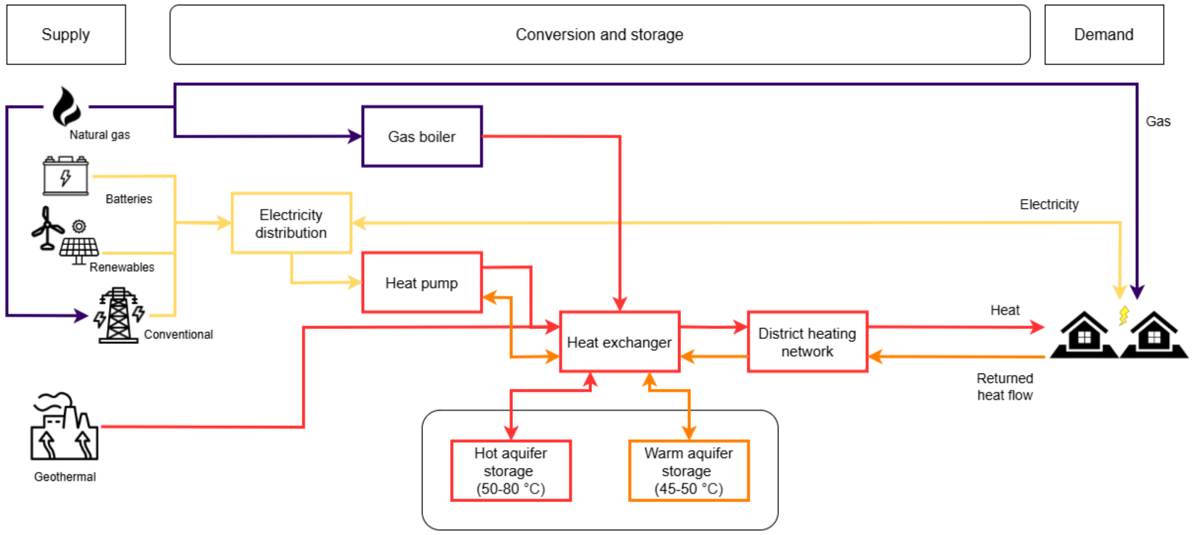

Figure 3.1: Conceptualization heating system

taining consumer heat demand. Geothermal energy is the primary heat source, providing a stable and CO_2-neutral base load. The surplus heat generated during summer months by the geothermal well can be stored in an HT-ATES system for later use. The HT-ATES functions as a seasonal energy buffer, storing heat during the summer and discharging it in winter when demand exceeds the direct geothermal output. To extract geothermal heat, electric submersible pumps (ESP) are used. Two main pump types are common in geothermal systems: line shaft pumps (LSP), typically used for high-temperature wells (150-200°C). For lower-temperature fluids (<120°C), ESP's are used. For this system, ESP's are chosen due to their compatibility with the specific geothermal well conditions. Given that ESPs experience increased wear with frequent on/off cycles, the model assumes a controlled operating range between 20% and 100% capacity, ensuring a longer pump lifespan and reduced maintenance costs [1].

The HT-ATES system requires a specific operational strategy for managing its charge and discharge cycles. During summer, heat is injected into the aquifer using an ESP. In winter, when additional heating is required, the stored heat is extracted from the HT-ATES and supplied to the network. This is necessary because the HT-ATES system cannot switch instantaneously between injection and extraction due to the characteristics of the ESP pump. Furthermore, over time, the temperature within the HT-ATES declines, and once it falls below a certain threshold temperature, it can no longer effectively supply the required heat.

The general principle of ATES systems is that groundwater will be used as thermal energy storage medium. An HT-ATES installation consists of two vertical water wells: a warm well and a hot well, typically located 100 – 300 meters apart to prevent interference between them [53]. Together, these wells form a doublet. During summer, groundwater is extracted from the warm well and heated via a heat exchanger. The heated groundwater is then injected into the hot well, creating a hot water bubble around it. In winter, the pump direction is reversed: hot groundwater is recovered from the hot well. The heat is extracted and the cooled water is reinjected into the warm well [34]. This cycle of storing heat in summer and recovering it in winter constitutes one full operational loop. The storage medium (typically a sand layer) is naturally sealed at the top and bottom by clay layers, making it an ideal medium due to its large capacity and natural insulation properties [53].

In addition to the geothermal source and HT-ATES, a heat pump is included to regulate the temperature of the district heating network. This P2H application enhances temperature control and improves the utilization of geothermal heat. The heat pump serves two main functions: boosting the temperature of geothermal heat and heating up the returned water in the network. For optimal geothermal capacity, the water injected back into the geothermal well must be cooled as much as possible, a task assisted by the heat pump. Additionally, when the required supply temperature for the district heating network is higher than the provided geothermal source, the heat pump raises the temperature to the necessary level.

An E-boiler is also incorporated to take advantage of periods when electricity is abundant and inexpensive. A gas boiler is includes as a backup to ensure reliability during peak demand periods. This combination of technologies allows the model to explore the effects of different configurations on system performance, operational costs, and sustainability outcomes.

To establish a baseline for evaluating the system performance, the first iteration of the model makes several simplifications. These include assuming a fixed electricity price, ignoring grid capacity constraints, neglecting network tariffs, and grid reinforcements. While these assumptions are not fully representative of real-world conditions, they provide a necessary starting point for understanding the core dynamics of the heating system before introducing more complexity. The first phase of the model directly addresses the research question: *How can a heating system be designed to optimize electricity usage and heat demand with fixed electricity prices?*

3.1.2. Incorporating electricity price dynamics

The second model iteration introduces real-time electricity prices, which is one of the main considerations when studying the interaction between electric and thermal systems. This addition makes it possible to investigate the influence of electricity price volatility on operational efficiency and profitability within the district heating system. Through this iteration, the following sub-question will be addressed: *How does real-time electricity price variability influence the operational efficiency and cost-effectiveness of the district heating system?*

One of the most significant effects of variable electricity prices is the dynamic reordering of heat production. In the first iteration, heat production was dictated mostly by system efficiency and technical constraints. However, with the introduction of variable electricity prices, the operational order of heat production technologies will depend on real-time costs. This is particularly relevant for P2H applications that adjust their operation according to price variation. By using low-cost electricity for heat generation and storage, the system can save operational costs while also improving sustainability. Moreover, fluctuations in electricity prices are often correlated with renewable energy availability, creating opportunities to utilize electricity surpluses. This link between electricity price volatility and renewable generation allows the model to assess the feasibility of drawing on surplus electricity, enhancing both cost-effectiveness and sustainability.

3.1.3. Integration in the electricity system

The third iteration expands the district heating network model to include a more detailed description of the electricity network with grid constraints and capacity limits. This modification allows the model to study how the dynamics of the grid influences the operation of heating technologies. The following sub-question will be answered: *"How do grid capacity constraints influence the operation of district heating technologies, and what are the implications for system efficiency and economic feasibility?*

Grid capacity refers to the maximum amount of power that the network can supply to a specific area. This capacity is limited by several factors, including transmission and distribution constraints, the availability of generation, and voltage stability. Transmission and distribution plants regulate how much power can be delivered safely without overloading the system. Electricity generation tends to be restricted by external sources, such as wind and solar energy. Voltage stability also poses challenges, overloaded transmission or distribution lines can cause voltage drops, leading to performance issues or equipment damage. Maintaining voltage within acceptable ranges becomes particularly difficult in systems with a high share of renewable energy, where variable demand and intermittent supply frequently cause imbalances [68].

The rapid adoption of electricity-based technologies, including heat pumps, electric vehicle charging, and the electrification of industries, has added further strain to the grid. In South Holland, both the medium-voltage network and TenneT's high-voltage grid have already reached maximum capacity levels in parts of the several regions. This requires urgent reinforcements of the electricity grid [24].

The current congestion in many regions highlights the difficulty of integrating heating technologies with the electricity grid and underscores the importance of accurately defining grid constraints. The integration between the district heating network and the electricity grid is modeled at both local and national levels. At the local level, electricity-intensive technologies such as heat pumps and electric boilers can significantly influence grid connection costs and electricity demand. These P2H applications require substantial power, increasing the risks for local bottlenecks. Addressing these constraints may involve reinforcing the grid infrastructure, which could lead to higher network costs. To evaluate these implications, the model simulates different scenarios with varying grid capacities. At the national level, the influence of the district heating network on grid stability is less direct. Instead, the generation mix, particularly the share of intermittent renewable sources, and overall electricity demand will largely determine national electricity prices. Thus, the model primarily focuses on how price signals driven by national-level conditions influence heating system operation.

The electricity grid is only significantly strained during a few moments throughout the year. It is designed to provide sufficient capacity at any given time, yet electricity consumption is highly variable. Demand typically peaks during cold periods or during specific hours of the day. Meanwhile, electricity feed-in peaks are highest during sunny or windy periods. In the built environment, peak demand moments are critical for determining the required transport capacity of the grid. These moments, when several high-demand technologies operate simultaneously, place the greatest strain on the network [56].

In the model, the grid capacity constraints ensure that electricity consumption of the district heating network does not exceed the technical and distribution limitations. In addition, the model accounts for planning and regulatory challenges that could restrict grid expansion within policy and spatial planning frameworks. It also considers the impact of peak hours by simulating scenarios with varying grid capacities At different times of the day, allowing for an evaluation of the economic implications of local bottlenecks. Incorporating these constraints ensures that the model accurately reflects the interactions between heating technologies and the electricity grid in real-world conditions. Given the growing challenges associated with grid congestion, it is increasingly important to adapt future system designs to account for these limitations.

3.1.4. Economic incentives

The final iteration of the district heating network model incorporates economic incentives, focusing on the effects of grid reinforcement. It investigates the impacts of pricing mechanisms such as network tariffs and the allocation of costs for future grid expansions. By introducing these market-based tools, the model explores how financial signals can alleviate system bottlenecks, optimize resource utilization, and enhance the overall economic feasibility of the heating system with the help of this sub-question.
How can economic incentives and pricing mechanisms optimize the operation of the district heating network while ensuring grid stability and financial feasibility?

The electrification of energy demand and the rollout of renewable energy require grid expansions across different grid levels. Grid reinforcement may involve modifying existing stations, adding new stations, laying additional cables, and adapting the grid structure [62]. Such reinforcements are crucial for addressing network constraints, improving future system costs, and enhancing network stability and reliability. Strengthening the grid also helps reduce the risk of network outages [11]. The responsibility for facilitating the growing demand for electricity transport lies with both the Transmission System Operator (TSO) and the Distribution System Operator (DSO). The Dutch electricity grid is divided into three levels: the high-voltage grid, consisting of 110 kV to 380 kV lines, operated by the TSO (TenneT). The medium-voltage grid which operates from 10 KV to 50 KV, is operated by the DSOs and serving large industrial users and renewable energy projects. The last sector is the low-voltage which consists of lines below 10 kV, which is also operated by the DSOs and is used for small users such as households and small companies [41, 62]. The technologies in the heating system are of such size that they will be connected to the medium-voltage grid.

The TSO and DSO recover the costs of grid reinforcement by implementing network tariffs. The financial burden of infrastructure expansion is ultimately passed on to end users. The TSO has a legal obligation to provide access to all parties who want to connect to the electricity grid. Current regulatory frameworks require the TSO to develop sufficient network capacity to meet the full transport demand of all connected users, regardless of how often these peak loads occur [10]. This can lead to overdimensioning, where infrastructure is sized to accommodate rare peak events, potentially resulting in suboptimal cost-effectiveness from a societal perspective. The challenge lies in balancing short-term and long-term investments, as the growing need for capacity cannot always be met due to grid constraints. In this context, HT-ATES could potentially serve as a valuable resource to help mitigate network congestion.

From a producer perspective, the model investigates how network tariffs and grid reinforcements affect the economic feasibility of the heating system. It evaluates whether the current pricing structures offer sufficient incentives for TSOs and DSOs to invest in grid improvements that benefit society. Moreover, the model assesses the role of HT-ATES in mitigating the effects of grid congestion. A key component of this iteration is the incorporation of network tariffs that reflect grid capacity limitations. These tariffs are intended to induce consumers to shift demand away from peak periods, and thereby reduce strain on the electricity grid. Since current electricity prices do not reflect congestion costs, the tariffs introduce an additional charge for electricity consumption during periods of high demand. To further align incentives with system stability, the model also integrates regulatory and policy constraints designed to promote low-carbon heat generation and maximize the utilization of renewable energy sources. By evaluating how different pricing structures impact decision-making within the system, the model investigates the impact of tariff adjustments on the system's behavior.

3.2. System uncertainties

The future of the heating market is characterized by uncertainties from evolving technological, economic, and policy conditions. The uncertainties arise from factors such as fluctuating energy prices, the intermittency of renewable generation , climate variability, and decarbonization trends. Addressing these uncertainties is crucial for designing an optimal and robust heating system. Some of the most important uncertainties include;

- Energy price variability
  Electricity and other energy carriers such as natural gas are priced by market forces, regulatory choices, and geopolitical factors. The price scenarios in this research need to be linked with variables as temperature, heat demand, and electricity generation's emission intensity in order to connect the right energy prices to the right variables.
- Renewable energy integration
  The growing share of renewable energy sources introduces variability in power production, impacting grid reliability and electricity pricing. This intermittent period provides an opportunity to utilize surplus electricity for P2H applications but also introduces difficulties in ensuring an assured supply in periods of low renewable generation.
- Heat demand dynamics
  Heat demand is strongly correlated with weather patterns and seasonal variations. Warmer winters and better isolation may reduce the overall heat demand. However, a large connection to the district heating network can increase the heat demand in these networks.
- Policy and regulatory changes
  National and EU-level policies, such as CO_2 pricing, renewable energy subsidies, and emissions caps, directly affect the economic and operational features of heating systems.

To address these uncertainties and build resilient heating systems, it is important to study a number of future energy scenarios. These scenarios should consider potential variations in critical parameters such as electricity prices, grid constraints, and renewable energy share. To facilitate this process, the Energy Transition Model (ETM) has been used as a tool. It offers a variety of analytical opportunities, including energy scenarios based on weather, electricity price forecasting, energy mix simulation, and optimization software for systems. In this research, the KEV 2030 scenario of the ETM has been applied. This scenario forms the foundation of the current policy scheme and forecasts of the Dutch energy system in 2030, renewable energy expansion, fossil fuel phase-outs, and electricity demand [55]. Using this scenario, the research is aligned with national objectives and provides realistic insights into how the district heating system could operate within the broader energy context of the Netherlands.

4 Model implementation

Building on the conceptual system design introduced in Chapter 3, this chapter translates the conceptualization into a model application. A specific case study is used to implement and validate the district heating network model. The case study provides a real-world application of the model, demonstrating its feasibility, performance, and adaptability to a multi-source heating system. Following the case description, the model implementation details are outlined, explaining how the system's characteristics are incorporated into the optimization framework.

4.1. Case description

To analyze the integration of various heat sources and storage technologies, a case study is selected based on an ongoing district heating expansion in Delft. This location is particularly relevant as a result of the development of both a geothermal well and an HT-ATES system.

4.1.1. Case study: Delft

The TU Delft campus is currently undergoing a transformation of its heat supply infrastructure. A geothermal well is being developed on the campus, which will supply sustainable heat to the TU Delft district heating system. The geothermal well will also be connected to the Open Warmtenet Delft (OWD), a new district heating system is under development. This transition presents a special opportunity to investigate how different heating technologies interact in a mixed urban and institutional context.

The geothermal well will have a production temperature of 79°C. and reach a depth of approximately 2,200 meters. The well will be used to supply heat to the TU Delft and OWD [28, 54]. However, the geothermal source alone will not be sufficient to meet peak demand, necessitating the integration of additional heat technologies. An HT-ATES system will provide seasonal heat storage. The characteristics of the HT-ATES system target a storage capacity of 20–40 TJ, equivalent to a thermal volume of 300,000–600,000 m^3 [39]. The unit will be installed at a depth of 120–180 meters, and the efficiency of the system will depend on geohydrological conditions that influence heat retention and thermal losses [16].

The district heating infrastructure in Delft consists of two distinct networks, each with different supply and return temperature characteristics. This variation is due to the different heating purposes of the networks, with the TU Delft network primarily serving university buildings. The OWD network mainly serve residential areas. Consequently, the two networks have different return temperature requirements, which vary depending on outdoor temperatures. During colder periods, lower outdoor temperatures will require higher supply temperatures to meet the heat demand. Both networks operate within a supply temperature range of 70–90°C, but their return temperatures differ. [16, 39]. The TU Delft has a return temperature of 55-65°C [16], whereas the return temperature for the OWD is between 50-60°C [39]. As illustrated in Figure 4.1, the return temperatures of the two networks exhibit opposite trends, which can be attributed to differences in building insulation and heat exchanger efficiency. The OWD network experiences an almost parallel temperature drop. The TU Delft network features more efficient cooling when outside temperatures rise. Future improvements in the buildings insulation may allow for reductions in supply temperatures, which could enhance the efficiency of heat sources such as geothermal energy [27].

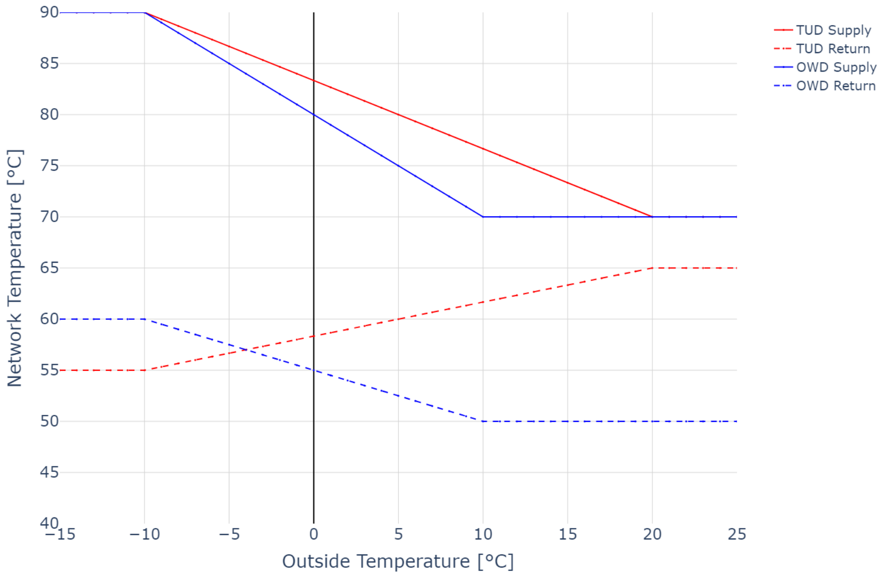

Figure 4.1: Supply and return temperature for OWD and TUD [39]

The Delft case provides a relevant real-world context for testing the theoretical model developed in Chapter 3. The presence of an operational geothermal well and the planned deployment of HT-ATES offer a unique opportunity to study integrated heating systems in a mixed-use environment. The insights derived from this localized case study will help answer the broader research question by establishing the analysis for realistic system constraints.

Heat demand

The current annual heat demand of the TU Delft campus is estimated to be between 160 and 190 TJ/year. As ongoing insulation improvements and energy-saving measures are implemented, this demand is expected to decline. In 2040, the projected demand stabilizes at 80 TJ/year. For the Open Warmtenet Delft, heat demand will grow over the next decades. By 2030, the heat demand for OWD is expected to be 120 TJ/year, driven by urban development, population growth, and additional adoption of district heating. By 2040, demand is projected to increase further, reaching between 200 and 400 TJ/year [16]. The primary heat source for OWD network is expected to be the geothermal well. In the future, additional heat supply will be provided by industrial residual heat from the Rotterdam harbor. The residual heat will be carried by the WarmtelinQ, a new heat pipeline from the Rotterdam harbor to The Hague[54]. The expected demand projections are illustrated in Figure 4.2.

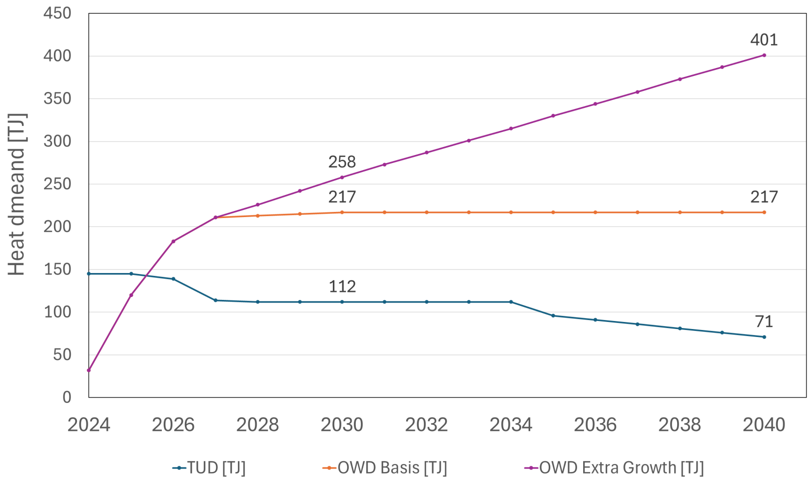

Figure 4.2: Heat demand perspective [39]

In addition to annual trends, hourly heat demand profiles for TU Delft and OWD provide valuable insights into seasonal and daily variations. Figure 4.3 shows the daily average demand profiles for the projected year of 2030, with the corresponding outside temperature for the reference year of 2019. During the summer months, heat demand for the TU Delft campus drops significantly, reaching zero in July and August. This sharp decline occurs because campus buildings shut down their heating systems during this period, when there is no need for space heating, and university operations are at a reduced level due to summer break [39]. The OWD network, which predominantly serves residential areas, exhibits less seasonal fluctuation compared to the TU Delft network. In the OWD network domestic hot water consumption is included whereas for the TU Delft this is not included, this explains the demand in the summer months [25].

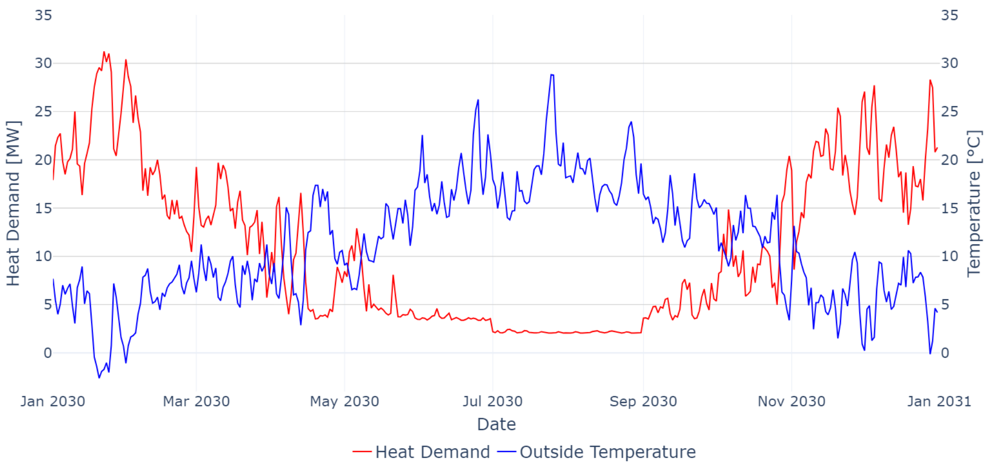

Figure 4.3: Daily average of the temperature and heat demand

4.1.2. Weather profiles

The model incorporates two distinct weather profiles, each representing different climatic conditions that influence heat demand and electricity prices. These profiles allow for scenario-based analyses, ensuring that the model accounts for both typical and extreme weather conditions. By simulating multiple weather years, the model evaluates how different meteorological patterns affect system performance, cost efficiency, and the feasibility of integrating renewable energy sources.

Weather conditions significantly impact both heat demand and electricity prices, two critical inputs in the optimization model. For instance, cold winters lead to increased heat demand, requiring higher heat generation. Periods of low renewable energy availability ('Dunkelflaute') can result in higher electricity prices, affecting the economic dispatch of heat-generating technologies. The two weather profiles are summarized in Table 4.1.

Weather Profiles	Weather Year	Description
def	2019	default
W1	1987	Dunkelflaute during extreme cold winter

Table 4.1: Weather Profiles and Descriptions

Electricity prices are closely linked to weather patterns due to the fluctuating availability of wind and solar energy. The model incorporates hourly electricity prices from the day-ahead market. The different weather scenarios are introduced to analyze the robustness of the system under various meteorological conditions. Weather directly influences both heat demand and renewable energy generation. The chosen weather years capture a range of extreme conditions.

4.2. Key concepts of the model

In the previous Chapter a conceptualization of the model was given, in this section the implementation of the key concepts in the python model will be described.

Model requirements

The primary goal of this model is to optimize the dispatch of heat generation technologies, ensuring that heat demand is met at the lowest possible cost. Variable costs are defined for all system components, allowing the model to determine the optimal distribution of heat generation based on a merit-order approach. At each timestep, the merit order ensures that the cheapest available technology is dispatched first, prioritizing cost efficiency.

To achieve this, the model must:

- Economically optimal heat generation: The model must calculate and minimize the cost of heat generation for two distinct district heating networks, reflecting their specific characteristics.
- Support scenario analysis: Variables within the model must be easily adjustable to allow comparison of multiple scenarios, including variations in energy prices, demand, and system configurations.
- Simulate a comprehensive system: The model incorporates key components such as a heat pump, a geothermal well, an E-boiler, and an HT-ATES. These technologies are integrated to supply heat at the lowest possible cost while adhering to technical, environmental, and operational constraints.
- Incorporate thermodynamic principles: The oemof framework ensures thermodynamic consistency by basing its components on mass and heat transfer equations.
- Reflect temporal variations: With an hourly resolution over the modeled period, the system captures temporal variations in demand, supply, and operational parameters, providing a realistic depiction of network behavior.

Objective function

The primary objective of the model is thus to minimize the variable costs while meeting the required heat demand, The objective function C_{var} focuses on the cost components associated with system operation, where a hard constraint is included to ensure that the heat demand always will be delivered. Including operational and maintenance costs, electricity costs, and environmental costs. Mathematically, it can be expressed as:

$$\min [C_{\text{var}}]$$

Where the variable costs can be divided into four main components:

1. Total operational and maintenance costs $C_{\text{o\&m}}$: These costs account for the ongoing expenses related to the system's operation.
2. Total Electricity costs C_{elec}: These represent the cost of electricity required to operate the system, calculated based on hourly electricity prices from the day-ahead market.
3. Total gas costs C_{gas}: These represent the cost of gas required to operate the system, calculated based on fixed gas prices.
4. environmental costs C_{env}: These include penalties for CO_2emissions, incorporating externalities associated with greenhouse gas emissions.

The objective function can be expressed as:

$$\min [C_{\text{O\&M}} + C_{\text{electricity}} + C_{\text{gas}} + C_{\text{environment}}]$$

Expanding this, total variable costs are defined as:

$$C_{\text{var}} = \sum_t (c_{\text{i}}^{\text{O\&M}} \cdot q_{\text{i},t}^{\text{heat}}) + \sum_t (P_{\text{t}}^{\text{elec}} \cdot q_{\text{i,t}}^{\text{elec}}) + (P_{\text{gas}} \cdot q_{\text{t}}^{\text{gas}}) + (P_{\text{CO}_2} \cdot \sum_t e_t)$$

where:

- $c_{\text{i}}^{\text{OPEX}}$: Operational and maintenance cost coefficients for each technology i.
- $q_{\text{i},t}$:Heat output of technology i at time t.
- $P_{\text{elec},t}$: Hourly electricity market price at time t.
- $q_{\text{elec},i,t}$: Electricity consumption of technology i at time t.
- P_{gas}: Gas price
- $q_{\text{t}}^{\text{gas}}$: Gas consumption at time t.
- c_{CO_2}: CO_2 price per kg of CO_2 emissions.
- e_t: CO_2 emissions from the system at time t.

This formulation ensures that the model accounts for both operational and environmental costs, reflecting the trade-offs between cost efficiency and sustainability.

Temporal resolution and horizon

The model has an hourly time resolution, allowing to capture intraday variability in heat demand, supply, and electricity prices. High temporal resolution is required to capture the dynamic nature of the district heating system in relation to the short-term dynamics of heat demand as well as the operation of the geothermal and HT-ATES systems. To provide a comprehensive analysis, the simulation horizon is set to represent a full year. This approach accounts for seasonal variations in heat demand and geothermal system output, ensuring the model captures the broader operational trends alongside finer short-term dynamics.

To optimize computational efficiency, temporal resolution should balance model accuracy with runtime. For most experiments, the minimum timestep of 1 hour is maintained as it aligns with the available datasets and ensures detailed outputs without compromising model functionality. However, to save time during certain analyses, such as verification and sensitivity testing, a daily timestep has been used. In these cases, daily averages were employed as input data, reducing the computational load while still providing sufficient accuracy for these specific purposes.

4.2.1. The district heating network

The district heating network serves as the backbone of the model, connecting heat generation technologies, storage systems, and end-users to deliver heat efficiently. To simplify the modeling process several key assumptions are made regarding the network's operation. These assumptions simplify the modeling process, where a difference can be made between a strong and weak assumption. Strong assumptions provide large differences from reality, where weak assumptions have a less significant impact but could still affect the accuracy of environmental and economic assessments.

- Losses in pipelines are a percentage of the demand:
  Heat losses in the district heating network pipelines are modeled as a fixed percentage of the total heat demand. In real-world this factor dependent on operational conditions such as flow rates, pipe insulation quality, or ambient temperature. Pipeline losses are estimated at 25% during the winter months and increase to 30% in summer, when the heat demand is lower and relative losses are higher.his is considered a weak assumption, as it simplifies modeling but introduces minor potential inaccuracies.
- Utilization of return temperatures:
  It is assumed that the return temperature from the district heating network is fully usable for heat pump operations. This allows the heat pump to recover and upgrade residual thermal energy, raising it back to the required supply temperature for redistribution within the network. This is also a weak assumption because this is often a good simulation of reality.
- Demand profiles are known and fixed: Heat demand profiles for all end-users are assumed to be predefined and deterministic, meaning there are no uncertainties in demand over time. This allows the model to focus on supply optimization. As a consequence there will be an undervaluation of the storage, as the model does not account for the operational flexibility that storage could provide in response to unexpected fluctuations in demand. This is classified as a strong assumption and must be considered when interpreting results, especially for scenarios where storage flexibility is critical.

Electricity generation

In the model, the hourly electricity prices are representable for future energy scenarios, where a source is constructed to simulate the electricity generation. Each electricity-consuming component, such as heat pumps, geothermal pumps, and the E-boiler, draws electricity from this source. The electricity prices are coupled with the electricity usage. The electricity source is further defined by different renewable sources, which affect the pricing of the electricity. Also, this differentiation affects the CO_2 emissions of the district heating network, The proportion of renewable electricity is dependent of the availability of renewable sources, which increases naturally if certain renewable sources are designed to deliver their electricity to the network. By linking electricity prices to these sources, the model captures the economic incentives for utilizing low-cost, low-emission electricity during periods of high renewable energy availability. Local grid capacity also results in realistic operating constraints for the model and highlights potential infrastructure investments to accommodate increased electrification.

To model the process while preserving its accuracy, several implications are made:

- Inelastic national electricity prices:
  The model assumes that electricity prices are fixed on a national scale and do not respond to changes in local electricity demand. This assumption is based on the assumption that the scale of the district heating network operation is insufficient to influence national electricity prices.
- No Negative Electricity Prices:
  The electricity price dataset used in the model does not include negative price events, as these are not computed in the Energy Transition Model. In real markets, negative electricity prices occur during periods of extreme surplus renewable generation.
- Electricity input:
  It is assumed that electricity from the source reaches the district heating network without losses during transmission or distribution. This simplifies the model by ignoring efficiency losses typically associated with grid infrastructure, because here is merely focused on the heating system and not the electricity system.

Flows and interconnection

The energy system model employs buses as the fundamental method to manage and transfer energy flows. A bus represents an energy carrier, balancing inputs and outputs to ensure the system remains stable. The model automatically balances all energies that flow into and out of a bus, so each bus represents a grid or a network. Two key buses are implemented in the model:

- Electricity Bus: This bus represents the electrical energy flows within the system and primarily serves as an input variable, supplying electricity to energy-demanding components such as heat pumps and E-boilers.
- Heat Bus: This bus represents the thermal energy flows and serves as the main output of the model. It delivers heat to meet the demands of the district heating network.

To enhance the model's flexibility, additional buses are added to characterize specific energy flows. For example, a 'heat bus geo' represents thermal energy originating from the geothermal well. This enables that heat sources within the system can be differentiated. All parts of the model are shown as distinct entities, and buses facilitating the interaction and energy exchange between the entities.

Heat exchanger

Heat exchangers play a crucial role in the model, enabling thermal integration between different system entities. They allow heat transfer from one flow to another, adjusting energy characteristics as necessary to ensure compatibility between sources and sinks. The model assumes the following characteristics for the heat exchangers:

- Equal flow rates:
  The flow rates on both sides of the heat exchanger are assumed to be equal, simplifying the system dynamics. When this is not the case for example for a sweet and salt water circuit this is calculated with the help of the fluid characteristics. This assumption simplifies system dynamics but may introduce minor inaccuracies in cases where flow imbalances significantly impact heat transfer efficiency.
- Incorporated heat losses:
  Small heat losses are included in the model to simulate real-world inefficiencies without sacrificing the model's simplicity. All heat exchangers have a constant 2°C heat loss as a realistic estimate of thermal degradation. While this approximation reflects typical heat exchanger inefficiencies, actual losses can vary depending on operational conditions such as temperature differences, pressure drops, and heat exchanger design.

4.2.2. Heat generation

The heat supply for the district heating network relies on multiple generation technologies, each with distinct operational characteristics and constraints. The primary components responsible for heat generation in the system are the geothermal well and the heat pump.

Geothermal well

The geothermal well provides a reliable base load for the district heating network. It is designed to operate flexibly within 20% to 100% of its maximum capacity. The ESP extracts saline groundwater from the reservoir with a temperature of 79°C. This water flows through a heat exchanger, after which it is cooled and reinjected into the cold well at 20°C. This is a closed-loop cycle that maintains the thermal balance of the reservoir [71, 74]. This system operates using a saltwater circulation flow, where the specific density and heat capacity of the water influence the thermal calculations. The maximum production flow rate from the well is 394 m^3/h, while the reinjection flow is slightly lower at 388 m^3/h. This discrepancy arises because water expands when heated; thus, the injected volume is lower than the extracted volume.

The heat exchanger transfers thermal energy from the salt water circuit to a sweet water circuit, which connects to the heat pump and the district heating network. The corresponding flow rate is 367 m^3/h [23]. During this process, a 2°C temperature loss occurs across the heat exchanger, resulting in a geothermal output temperature of 77°C. To achieve the required reinjection temperature of 20°C, the system relies on a heat pump to sufficiently cool the return flow. Without the heat pump, the district heating return flow would typically only cool the geothermal water by approximately 25°C, which would limit extraction efficiency. A larger temperature difference (ΔT) enables greater heat extraction, thereby increasing the geothermal system's thermal output. The geothermal output process is shown in Figure 4.4. The thermal output is determined using the fundamental heat transfer equation:

$$P_{\text{max}} = \dot{m} \cdot c_p \cdot \frac{(T_{\text{prod}} + 273.15) - (T_{\text{inj}} + 273.15)}{10^6}$$

Applying this equation, the maximum thermal power output of the geothermal well is 25.2 MW, while the minimum operational heat output is 4.9 MW at a flow rate of 75 m^3/h. The ESP system requires electrical energy to pump geothermal water to the surface, with electricity consumption calculated based on flow rate, heat capacity, water density, and injection pressure. The efficiency of the ESP is expressed through a COP of 55.15, which considers both the production and injection pumps. Although the actual COP fluctuates with variations in injection pressure. These variations are minor, allowing for an assumed constant COP in the model.

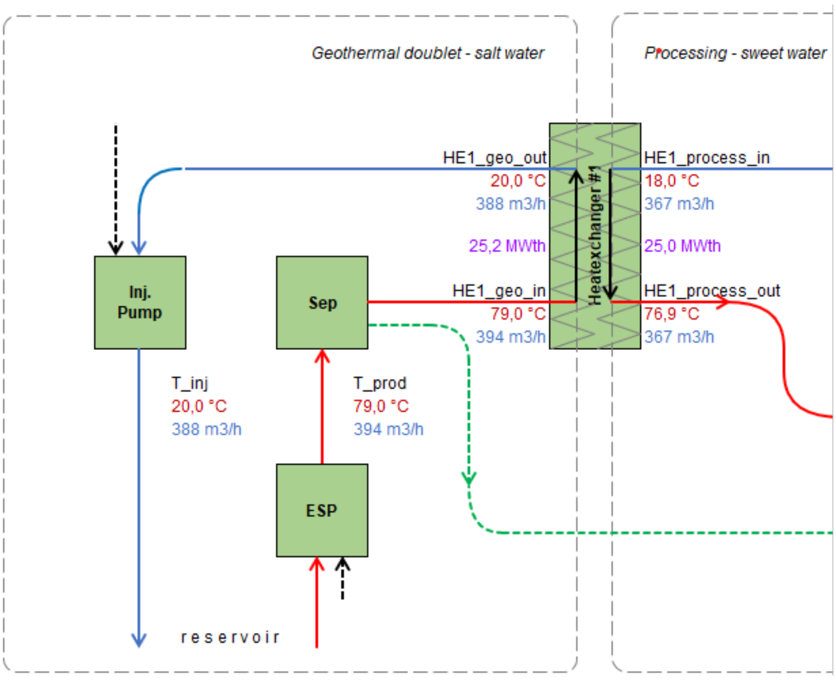

Figure 4.4: Process diagram - Geothermal doublet [23]

In the modeling framework, the geothermal well is implemented as a converter, where electricity input is transformed into thermal output. Constraints on minimum and maximum heat output are enforced to ensure realistic operational behavior. The system parameters of the geothermal well are summarized in Table 4.2.

Parameter	Value	Unit
Maximum capacity	$25,2$	MW_{th}
Minimum capacity	4.9	MW_{th}
Extraction temperature	79	°C
Maximum flow rate	367	m^3/h
COP of the geothermal source	51.15	$-$
Lifetime	30	$years$

Table 4.2: Parameters geothermal well

Heat pump

The heat pump is essential for temperature regulation within the district heating network. It ensures that the return flow is sufficiently cooled before reinjection into the geothermal well and that the supply temperatures meet the requirements of the district heating network. It operates as a converter, transforming electricity and cooled return water into heated water at the required temperature level. The heat pump utilizes geothermal heat and the returned water from the district heating network as its thermal input, increasing their temperature. By transferring heat from a low-temperature source (the cooled return water) to a higher-temperature output and to the low-temperature geothermal injection temperature. The heat pump operates as a water-to-water heat pump.

As illustrated in Figure 4.5, geothermal water first passes through a primary heat exchanger, transferring energy to a separate freshwater loop. This preheated loop then enters a second heat exchanger shared with the district heating system and the heat pump. In this stage, the geothermal water gives up additional thermal energy and is directed to the evaporator of the heat pump, where it is cooled to 18°C. After accounting for a 2°C loss in the reinjection heat exchanger, the final reinjection temperature reaches 20°C matching the reservoir requirements. Simultaneously, the heat extracted by the heat pump is transferred to the district heating network, increasing the temperature of the supply water to the required delivery level. In doing so, the heat pump serves two purposes: it maximizes the thermal efficiency of the geothermal source and ensures stable, high-quality heat delivery to end-users.

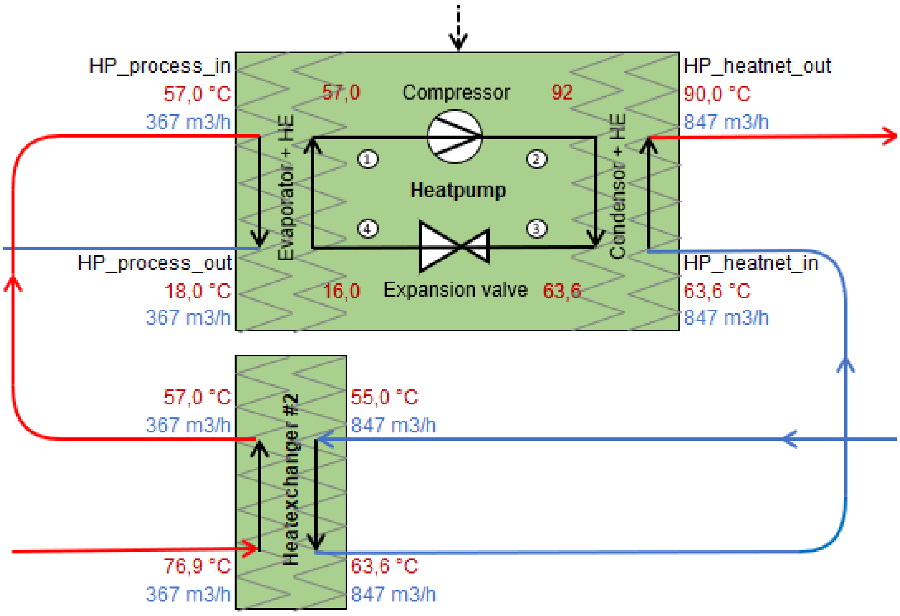

Figure 4.5: Process diagram - Heat pump [23]

To correctly model the two different district heating network flows, the system includes two separate heat pumps, which together represent a single physical unit. This differentiation allows for clear allocation of heat to either the OWD, TU Delft district heating networks or HT-ATES. A constraint is implemented to ensure that the combined output of the heat pumps does not exceed the installed maximum capacity.

The heat pump's COP is calculated dynamically at each timestep based on the return and supply water temperatures. The relationship between these temperatures influences the COP, where a smaller ΔT reflects a higher COP. The COP values are precalculated in Excel for the different operational scenarios. These values are then incorporated into the Python model to represent real-time system behavior accurately. Thereby is the system efficiency of the heat pump defined as COP/COP_Carnot, which is set at 0.6. The key design parameters of the heat pump are summarized in Table 4.3.

Parameter	Value	Unit
Maximum capacity	var	MW_e
output temperature	18	°C
Lifetime	15	$years$

Table 4.3: Parameters heat pump

4.2.3. Heat storage

HT-ATES system

The HT-ATES system is designed to enhance the flexibility and efficiency of geothermal energy projects by storing surplus heat. The HT-ATES system consists of seven wells: three hot wells operating at an initial temperature of 80°C and four warm wells at 50°C. These wells are located within an unconsolidated sedimentary aquifer at depths ranging from 160–200 meters. The system operates by controlling water flow between the hot and warm wells, ensuring efficient heat management. The maximum flow rate is 275 m^3/h, while the minimum operational flow is 10% of the maximum, equivalent to 27.5 m^3/h. These flow rates correspond to specific thermal power values, which dictates the maximum heat delivery at any given time.

During the storage period, heat losses occur, primarily as a result of temperature differences between the wells and the surrounding environment. As discharging progresses, the temperature in the hot well decreases, thereby reducing the available power output. A smaller temperature difference (ΔT) between the hot and warm wells results in a lower potential heat output. These dynamics are captured through a heat loss curve replicating realistic system performance. These heat losses arise due to the interaction between the stored heat and the surrounding groundwater and aquifer, which maintains a lower temperature of approximately 12°C. The loss rates applied in the model are derived from similar systems and calibrated to align with observed performance data. The HT-ATES system is connected through a heat exchanger with the network, where the heat exchanger delivers heat to the return flow of the district heating network. This configuration allows the HT-ATES system to operate until the stored water temperature reaches the cut-off temperature, which is five degrees above the return temperature of the network.

In the first few years, the injected heat is mainly used to heat the aquifer and groundwater to operational temperatures. The starting temperature of the groundwater is 12°C, and this must be raised to 80°C and 50°C for the hot and warm wells. To optimally use the HT-ATES this will take a few years until the groundwater and aquifers are at the supposed temperatures. In those first years, the maximum output of the the HT-ATES can be very high due to the large ΔT but this is only for a very short period before reaching the cut-off temperature.

For this study, a scenario is taken where the HT-ATES has reached a steady-state condition, where the where the surrounding aquifer has been heated to the target operational temperatures. In these conditions: the hot well has a temperature of 80°C, the maximum heat flow capacity can reach a value of 12.1 MW. However, as the delta T decreases the available heat output gradually declines. Reaching a maximum output of 1.5 MW at the end of the discharging period. During charging, the injected heat has a temperature of 80°C. The warm well temperature gradually decreases over time. As a result, the initial maximum charging rate is 10.6 MW, which subsequently increases to 12.1 MW as the ΔT slightly improves.

The energy transfer process is supported by the ESP, which maintains a stable electricity output to maintain the necessary flow rates. The efficiency of these pumps is related to the available flow rate, meaning that as the heat content diminishes, the COP also decreases. This reduction occurs because, while the flow rate remains constant, the energy contained in the water progressively decreases.

The efficiency of the HT-ATES system depends on the thermal conditions, particularly the shape and size of the thermal plume. The contact surface between the stored water and the surrounding groundwater influences heat losses [7]. Key parameters for simulating heat losses include:

- Thermal conductivity of the insulation layer (λ_iso): Determines the rate of heat transfer through the insulating layer.
- Thickness of the insulation layer (s iso): Impacts the overall thermal resistance of the storage
- Heat transfer coefficients (α inside, α outside): Define the heat transfer rates at the internal and external surfaces of the storage

To simplify the HT-ATES system and be able to design it in the current model a few assumptions are made:

- Heat losses are not dynamically calculated within the model. Instead, they are replicated using predefined loss rates based on performance data from similar systems.
- The nominal capacity is calculated using the storage volume, heat capacity, water density, and the temperature range (incoming temperature to cut-off temperature). Loss rates are applied to estimate the actual usable capacity over time.
- Charging and discharging operations are seasonally constrained to reflect realistic system behavior. Charging is only allowed between May 11th and October 14th, a period that corresponds with lower heat demand and the opportunity to store excess thermal energy. Discharging is permitted from October 28th to April 12th, aligning with the heating season when stored energy is required. During the intermediate periods, neither charging nor discharging is performed, as storage activity is typically not beneficial. Additionally, the system is constrained to prevent simultaneous charging and discharging, ensuring that these two processes do not occur at the same time.

The key design parameters of the HT-ATES system are summarized in Table 4.4.

Parameter	**Value**	**Unit**
Initial volume hot well	$-$	m^3
Maximum flow capacity	12	MW
Initial temperature hot well	80	$^\circ$C
Cut-off temperature	50	$^\circ$C
Groundwater temperature	12	$^\circ$C
Maximum flow rate	275	m^3/h

Table 4.4: Parameters HT-ATES

4.2.4. Cost overview

The economic feasibility of the district heating system is based on a given cost assessment. The costs of the system are divided between capital expenditure (CAPEX), fixed operating expense (fixed OPEX), and variable operating expense (variable OPEX). The CAPEX consists of the investment expenditures required to build infrastructure such as geothermal wells, heat pumps, and thermal storage systems. Fixed OPEX consists of reoccurring annual expenses, including maintenance, staff salaries, administration, and monitoring costs. Variable OPEX are costs that are a function of the heat or electricity produced and fuel costs for the different applications.

The cost assessment depends on a well-balanced combination of heat generation, storage, and flexibility technologies. HT-ATES and geothermal provide a reliable, cost-effective supply options but have high initial cost investments. Heat pumps and E-boilers can respond to demand-side flexibility while the electricity price and grid limitations determine their profitability. Gas boilers are still an available option and their cost-competitiveness is increasingly diminished by carbon pricing measures.

A key factor supporting the economic viability of new technologies is government subsidy programs. These subsidies help to reduce the cost gap between conventional and sustainable heating solutions. The subsidies are shown in the cost overview table, but in the calculated LCOH not included. All the main cost parameters for district heating technologies are outlined in Table 4.5. The cost values, except for HT-ATES and gas boilers, are primarily derived from the PBL Eindadvies Basisbedragen

SDE++ 2024 report, which provides government-guided cost estimates for renewable and emerging energy technologies, including applicable subsidies [42, 55]. The HT-ATES costs are derived from the WarmingUP report [39]. These costs are averages for different cases and are thus not specifically for the Delft region, there are a lot of uncertainties about these costs and are very region specific. The cost estimates are shown below:

Parameter	Value	Unit
HT-ATES		
Variable OPEX	–	€/MWh
Fixed OPEX	0.21	M€/year
CAPEX	3.4	M€
Subsidy	1.9	M€
Geothermal		
Variable OPEX	0.5	€/MWh
Fixed OPEX	0.093	M€/MW_{th}/year
CAPEX	1.119	M€/MW_{th}
Subsidy	52.5	M€/MW_{th}
Heat Pump		
Variable OPEX	0.77	€/MWh
Fixed OPEX	0.0809	M€/MW_{th}/year
CAPEX	1.152	M€/MW_{th}
Subsidy	61	M€/MW_{th}
E-boiler		
Variable OPEX	3.3	€/MWh
Fixed OPEX	0.195	M€/MW/year
CAPEX	0.257	M€/MW
Subsidy	135.9	M€/MW_{th}
Gas Boiler		
Variable OPEX	4	€/MWh
Fixed OPEX	0	M€/MW/year
Subsidy	0	–
Gas Price	24	€/MWh

Table 4.5: Cost specification per technology.

Network tariffs

Higher electricity demand necessitates upgrades to the grid infrastructure, which involves significant costs and spatial challenges. New users connected to the grid are required to pay a network tariff that partially covers reinforcement costs. For this analysis, it is assumed that any additional power demand will trigger the need for grid reinforcement. If spare capacity exists, reinforcement may not be immediately necessary. However, considering projections for 2050, electricity demand is expected to increase at such a rate that a grid expansion will almost certainly be required [62]. To calculate the costs for grid reinforcement, the basic principle is that the total investment costs are divided by the maximum amount of power connection for the technology. For example, a 1 MW connection of a technology (heat pump, solar farm) leads to a 10 MW grid reinforcement, the costs for the certain technology will be 1/10th of the total costs and will be calculated in the price and thus paid by the consumer [4]. The costs for a 1 MW grid reinforcement are calculated by CE Delft, at each grid level whereas for this project the costs are at the medium voltage grid which is 375,000 €/MW [62]. The reinforcement costs are really region specific, this number is an estimated average for reinforcement costs in the Netherlands. It is an approach to be able to calculate with a certain number and is in real-time very dependent on the case and time of the project.

CO_2 prices

CO_2 emissions and their associated costs form a critical component of the economic framework. The ETS defines the CO_2 price, which is market-based. The model incorporates CO_2 as both a constraint and a cost parameter, as summarized in Table 4.6. The ETS significantly impacts the economic performance of carbon-intensive technologies by imposing a cost on CO_2 emissions. The current price of 0.07417 €/kg CO_2 makes gas boilers less attractive due to their high emissions of 223 kg CO_2/MWh. On the other hand, electricity-based technologies, with an average lower emission factor of 23.98 kg CO_2/MWh, benefit as the electricity grid becomes more sustainable over time. For 2030, the expected CO_2 price will be 108 €/ton CO_2 (within the range 73-134 €/ton CO_2), where the expected emission factor for electricity will be 12.7 kg CO_2/MWh (range 9.4-19.7 kg CO_2/MWh). These numbers were obtained with the help of the KEV 2024 [55]. According to the Climate Agreement, district heating systems are not allowed to emit more than 18.9 kg CO_2/ GJ [18].

Technologies with higher emission factors, such as gas boilers, are faced with increasing costs by the ETS, reducing their economic viability in the long run. Low-emission and renewable technologies are made more competitive as their marginal costs are less responsive to CO_2 pricing. Dynamic interplay between CO_2 pricing, emission factors, and operational constraints calls for regular model updates to reflect evolving market and regulatory conditions.

Parameter	Value	Unit
CO_2 Price	0.108	€/kg CO_2
CO_2 limit	10,000	ton CO_2/year
Emission Factors		
Gas boiler	223	kg CO_2/MWh
Electricity	12.7	kg CO_2/MWh

Table 4.6: CO_2-related parameters and emission factors used in the model.

4.3. Verification and validation

This section evaluates whether the conceptual district heating network model has been correctly implemented. The evaluation consists of two primary processes: verification and validation. Verification ensures that the model operates logically, adheres to expected behaviors, and maintains computational stability within various conditions. Validation assesses whether the model serves its intended purpose, optimizing the heating network in different scenarios and providing reliable insights into system performance.

4.3.1. Verification

To confirm the reliability and accuracy of the Python model, continuous test runs were conducted throughout its development. These tests were aimed at identifying potential errors, validate the core functionalities of the model, and refine its behavior under different conditions. The verification process specifically focused on key elements such as the operational behavior of HT-ATES, and the distribution of heat sources. For verification purposes, the demand profile from the 2030 scenario was implemented. To reduce computational time, an aggregated model was utilized, where hourly time series were converted into 24-hour averages, resulting in a 365-time-step model for an entire year. This approach allowed for efficient verification of model behavior while preserving seasonal and daily variations.

HT-ATES behavior

The behavior of the HT-ATES system is evaluated by altering its variable costs, maximum inflow/outflow rates, and storage size.

- *variable operational costs HT-ATES: ∞ €/MWh*
  The first test examined how HT-ATES behaves when its variable operational costs are set to an artificially high value (∞ €/MWh). The hypothesis was that HT-ATES would become economically uncompetitive, meaning it would be used only at its minimum operational flow rate to meet the system's technical constraints. Also, because of thermal losses, the system might occasionally

increase its activity to maintain storage levels. The model's behavior aligns with expectations. The HT-ATES system remains at its minimum operational flow throughout the year, except for slight increases in August and September, where it compensates for storage losses to maintain the required minimum flow rate.

- *Maximum in- and outflow: ∞ MWh*
  The second test assessed the impact of removing limitations on HT-ATES inflow and outflow rates, allowing it to charge and discharge at a significantly higher rate. This test evaluated whether the system would leverage HT-ATES as a primary storage mechanism during periods of peak energy prices and increase its responsiveness to cost fluctuations. The results confirm that HT-ATES effectively adapts its operations when flow rate constraints are removed. The system now charges and discharges at significantly higher rates, particularly during electricity price peaks. This suggests that the model correctly prioritizes HT-ATES utilization when its operational flexibility is maximized.
- *Storage size: ∞ m^3*
  The final test explored the effects of an infinite storage volume. This allowed for a larger heat buffer, reducing the need for immediate heat production during high-cost periods. The objective was to determine whether a larger storage system would result in increased stored heat. It is expected that a larger storage system would lead to higher total outflows, with discharge events becoming more distributed over time. The results show that the discharge is more frequent and longer at its maximum discharge rate. However, the discharge does not always reach maximum flow rates, indicating that the system still operates according to a merit order. Heat losses in the storage also need to be taken into account.

Heat distribution

This section examines how heat distribution between system components responds to changes in electricity prices, CO_2 prices, and gas prices. The distribution is shown in Figure 4.6.

- *Fixed electricity price: ∞ & 0 €/MWh*
  When electricity prices are set to an extremely high value, the cost of operating electricity-driven technologies becomes endlessly high. As a result the gas boiler becomes the dominant heat source, increasing from 2% to 87% share. The gas share is not 100% because of the operating constraints for geothermal and HT-ATES. This outcome conforms the model's ability to correctly adapt extreme electricity cost increases, shifting towards gas production.

  Conversely, when electricity prices are set to zero, electricity-driven technologies become the most economical choice. The heat pump benefits the most from this pricing condition, as it can operate at full capacity without incurring additional costs. In this scenario, geothermal energy and HT-ATES also contribute significantly to the energy supply. This confirms that the model properly responds to economic incentives, leveraging cheap electricity to maximize the use of heat pumps.
- *CO_2 price: ∞ & 0 €/kg CO_2*
  CO_2 pricing directly influences the competitiveness of fossil fuel-based heating technologies, primarily the gas boiler. The first case were a prohibitively high CO_2 price was introduced to test whether the system would eliminate gas-based heating in favor of cleaner alternatives. The gas boiler's share drops from 2% to 0.5%, confirming that high CO_2 costs make gas heating less attractive. So, because the CO_2 price is not a really large share of the total costs it does not have a really big influence but as can be seen is the gas share decreased to only the point where there are no other technologies available and gas is needed to use.

  Setting the CO_2 price to zero had little impact on system behavior. Since gas was already more expensive than geothermal and electricity-driven heating in the base case, removing CO_2 costs did not significantly change the merit order of technologies. This indicates that even without carbon pricing, gas is already less economically competitive in the current conditions.
- *Gas price: 0*
  Finally, the model was tested with zero gas costs to observe whether cheaper fuel would increase the reliance on gas-based heating. The gas boiler use increases to 65% making it the dominant heat source, when only the electricity prices are cheap the geothermal source will be used next

to the minimal flow of the geothermal well. This scenario confirms that fuel pricing significantly impacts heat generation choices, with cheap gas reversing the transition to sustainable alternatives.

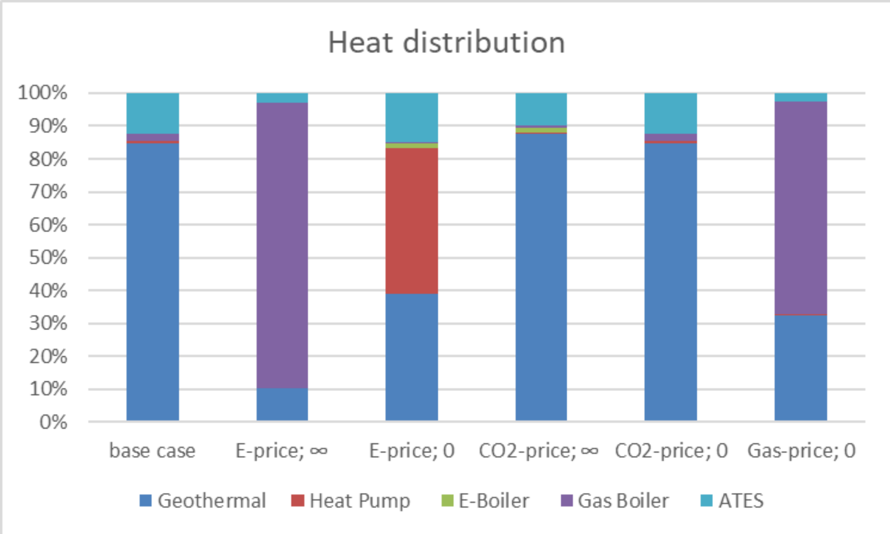

Figure 4.6: Verification runs: Heat distribution for different scenarios

4.3.2. Interaction geothermal well and heat pump

The interaction between the heat pump and geothermal well is an important factor in determining the system's operability. That is, during cold periods, the heat pump must raise the temperature of the geothermal heat in order to meet the supply temperature requirements of the district heating network. However, the capacity of the heat pump puts a restriction on how much can actually be utilized of the geothermal heat, especially in the presence of very low temperatures.

The geothermal well provides thermal energy at a constant extraction temperature of 75°C, this temperature is not sufficient to always supply the required supply temperatures. The heat pump plays a critical role in boosting this temperature. However, when its capacity is limited and there is a cold period a significant portion of the heat pump's available capacity is dedicated to temperature boosting and reducing. This reduces the fraction of geothermal heat that can be delivered directly to the district heating network.

This is captured in the load duration curve in Figure 4.7, which illustrates the distribution of the heat demand throughout the year. The times of peak heat demand correspond to the lowest external temperatures, at these moments the heat pump is focusing on boosting the geothermal flow. Which results in a lower possible geothermal outflow because the heat pump is fully utilized. To verify this dynamic, the outdoor temperature pattern is plotted against geothermal utilization, and the outcome is a strong correlation: the proportion of direct geothermal heat supply decreases as outdoor temperatures drop. Observe that the temperature curve in the figure is not a strictly monotonic function. This captures the fluctuation of heat demand both thermally driven and in daily and weekly usage cycles. For example, morning, evening, and weekday demands are greater. Such behavioral factors introduce a small deviation in the temperature-heat demand relationship.

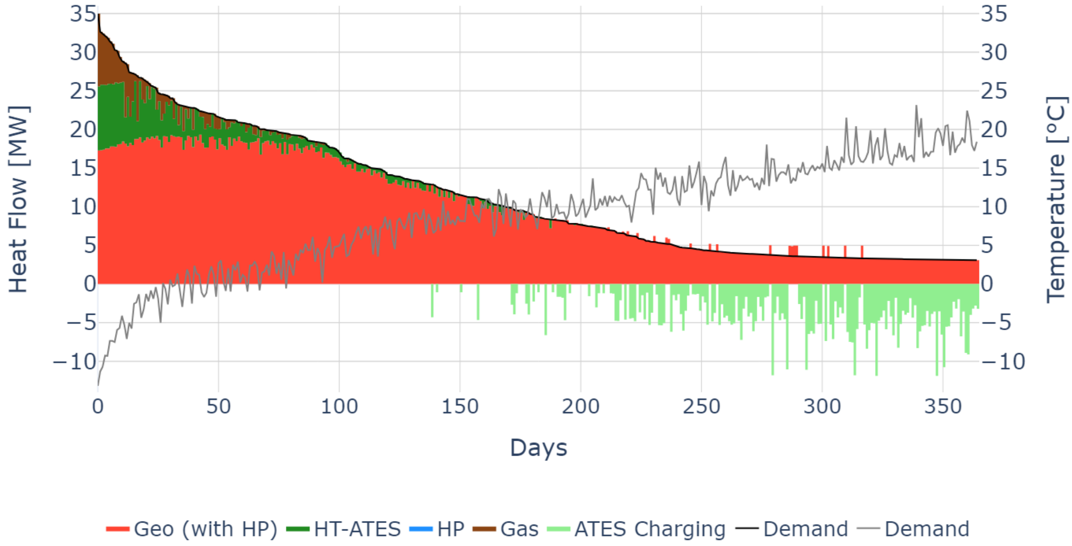

Figure 4.7: Load duration curve and outside temperature

In Figure 4.8, the heat pump capacity usage is plotted to verify this behavior. When the two lines in the graph overlap, it indicates that the heat pump is completely used by the geothermal flow. When these lines reach 3.5 MW, the full capacity is being used for geothermal heating. During a part of the month January this is clearly visible. No additional geothermal heat can be utilized unless an alternative method, such as gas-fired boosting is introduced at these peak moments.

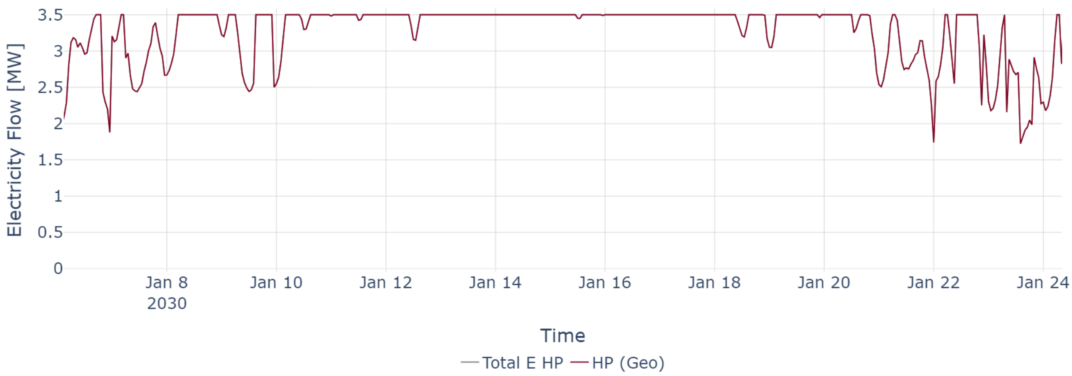

Figure 4.8: Heat pump usage for the geothermal flow

The verification process guarantees that the heat pump properly traces outdoor temperature changes, giving priority to temperature boosting when necessary. However, the results show inefficiencies in the model's execution of geothermal heat with heat pump interaction. Instead of concentrating on gas boiler heat generation, an arrangement facilitating gas-fired assistance for temperature boosting would enable utilization of geothermal power to the maximum degree.

From a broader system perspective, this limitation does not directly affect HT-ATES operation, as the thermal storage system remains governed by seasonal storage strategies rather than short-term heat pump constraints. However, it does introduce small variations in electricity consumption, depending on whether the system relies solely on the heat pump for temperature boosting or incorporates gas-fired assistance. Since the COP of the geothermal well remains the same and is relatively high, any added electricity use would not be affecting the system too much. Therefore, the additional electricity consumption is not significant enough to require major grid capacity changes.

4.3.3. Sensitivity analysis

To assess model robustness and address input uncertainty, a sensitivity analysis was conducted. This analysis tests how variations in key parameters affect the primary performance indicators (KPIs), including the levelized cost of heat (LCOH), total system costs, and CO_2 emissions. The sensitivity analysis also supports the experimental design by identifying which variables are most influential and thus worth exploring further. The sensitivity runs were performed using daily average values to reduce computational time. As a result, the values differ from those presented in more detailed analyses. Each parameter was varied by a 25% increase to evaluate its relative impact. It is important to acknowledge that the variable OPEX is approximately 15 % of the total costs. The sensitivity analysis is presented in appendix A, Table A.1.

The results indicate that the supply temperature of the district heating network is the most sensitive variable. Increasing this temperature leads to the largest rise in both operational costs and emissions, as the heat pump must work harder to boost the geothermal flow. Similarly, total heat demand has a major impact, particularly on emissions, since increased demand leads to greater reliance on gas-based backup heat. On the other hand, some variables show clear potential for improving system performance. Increasing the maximum discharge rate of the HT-ATES results in better coverage of peak demand, reducing the need for gas boilers. Likewise, increasing the capacity or efficiency of the heat pump has a strong positive effect, especially in lowering emissions. These improvements come with slightly higher investment or operational costs, but they contribute significantly to a more sustainable system.

4.3.4. Validation

Validation ensures that the developed Python model accurately represents the behavior of a district heating network in real-world conditions and aligns with established principles of heat system operation. To achieve a robust validation, the model's outcomes are compared with existing simulation studies and expected operational trends.

A primary validation step involves benchmarking the model's heat production and storage dynamics against the WarmingUP study (2023) [39]. This study simulates the performance of a geothermal-powered district heating network incorporating HT-ATES storage and serves as a relevant reference to validate the seasonal heat dispatch and energy flows. Since this study also focuses on the Delft case, there are many similarities in terms of external conditions and heating system configurations. The heat production profile from the WarmingUP study, shown in Figure 4.9, demonstrates a clear seasonal trend. Geothermal energy consistently serves as the primary heat source, covering the base load throughout the year. During the summer months, surplus heat is actively injected into HT-ATES storage, while during the winter, this stored heat is discharged to support peak demand.

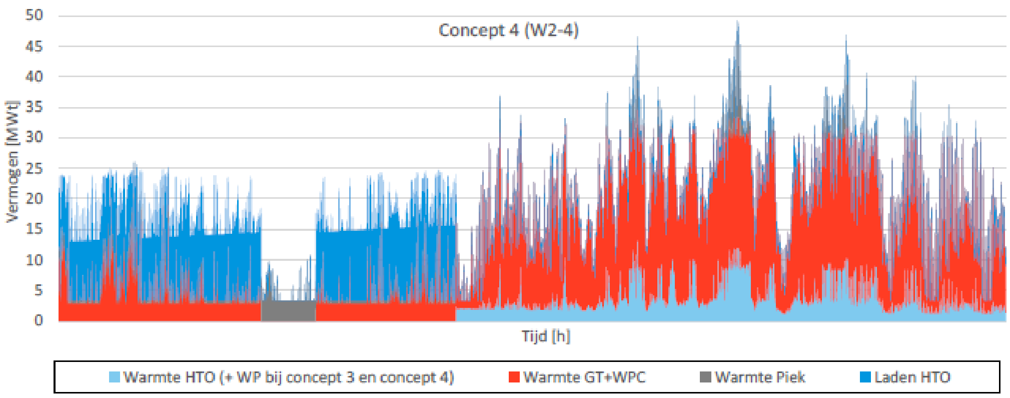

Figure 4.9: Heat production WarmingUP study for a year, from April till April

Another study that simulates a heating system and complies with a HT-ATES is a study from Kalavasta (2024) [72]. The Figure 4.10 shows a steady geothermal flow with a constant HT-ATES flow, and other demand is met with gas and a PTES/TTES storage. The ratio of the technologies used are quite different in this case but the principles are more or less the same, where in the Kalavasta study the storage is not used for peak demand but more as an additional source during the winter. These studies show a comparable heat generation mix with this study. The model displays also similar behavior during discharging, charging, and geothermal use.

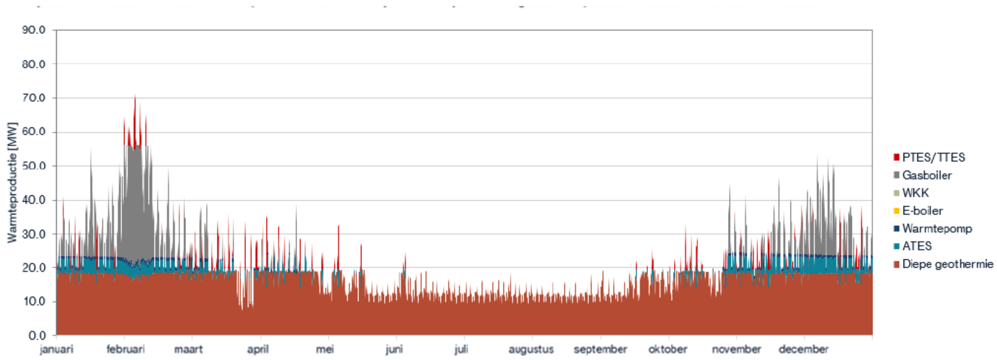

Figure 4.10: Heat generation Kalavasta

5 Experiment design

With the model parameters and outlines established in Chapter 4, the next step is experimentation. This phase aims to analyze system behavior in different conditions and test key parameters influencing the economic and operational feasibility of the heating system. This chapter outlines different experiments and scenarios that will be simulated to answer the sub-questions derived from the central research objective. The experiments are structured to progressively add layers of complexity from fixed electricity pricing to dynamic pricing, grid constraints, and economic incentives.

5.1. System designs

The setup of different system designs is based on insights from the sensitivity analysis, which identified two key variables that strongly influence system performance: the capacity of the heat pump and the volume of the HT-ATES. These variables were selected because they are both technically adjustable and have a significant impact on the economic and operational efficiency of the heating system. By varying these two parameters, a structured set of design configurations can be explored and compared.

Certain system elements are assumed to be fixed across all designs, based on known project specifications in the Delft case. For example, the geothermal well is considered a constant base-load source with a fixed output capacity. Other parameters, such as electricity prices, weather years, and tariff structures are treated as external conditions.

- HT-ATES storage volume: Determines the system's ability to balance heat demand and supply. If storage is too small, it may not effectively buffer demand fluctuations. Conversely, oversized storage can lead to under-utilization, increasing capital costs without significant benefits. Three storage sizes are therefore researched, which are realistic measurements and are being considered in the Delft case. The storage sizes are further indicated with the following abbreviations **SS** - small storage, **MS** - medium storage, and **LS** - large storage.
- Heat pump size: The heat pump capacity determines how much heat can be produced with the help of electricity. This influences the amount of geothermal energy that can be used during cold days and also the amount of heat directed to the network and to storage and is partly determined for the resilience of the system, the profiles will be indicated with the capacity that is implemented into that design. The range between the capacities that are tested are between the 3 MW and 5 MW.

By varying these parameters, a range of cost-effective configurations is explored. Table 5.1 provides an overview of the different system designs selected for experimentation. For the small and large storage, heat pump sizes are simulated for the two most extreme values. The MS is simulated for four different heat pump sizes. This is done to see more details between the differences into configurations on a basis of small differences in the size of the heat pump. Lastly, a base case (**BC**) profile is constructed which is a design without storage facility, to be able to compare a geothermal system without storage facilities and be able to see the difference in costs, flexibility, and emissions. The BC is simulated for different heat pump sizes to be able to compare this for configuration with and without storages.

Moreover, a distinction is made between system design choices (related to infrastructure, such as storage and heat pump sizing) and operational choices (which involve constraints and management decisions). For example, operational constraints such as HT-ATES discharge limits and gas and CO_2 price changes are analyzed separately in the additional experiment section.

System designs	**Storage volume** [m^3]	**HP size** [MW_e]
BC	0	-
SS-3.5	300.000	3.5
SS-5		5.0
MS-3	400.000	3.0
MS-3.5		3.5
MS-4		4.0
MS-5		5.0
LS-3.5	600.000	3.5
LS-5		5.0

Table 5.1: Profiles with corresponding storage volume and HP size

5.2. Experiment series

With all relevant input variables identified, the experimental setup is finalized. A total of four experiment series have been designed, each addressing a specific research sub-question. Not all scenarios and weather years are tested in every experiment to maintain computational efficiency while still capturing the most critical system behaviors. Additionally, from initial test runs, it became evident that the electric boiler did not provide added value for this design. As a result, it has been removed from most simulation runs.

Fixed electricity price (fixE)
This experiment investigates how a district heating system can be designed to optimize electricity usage and heat demand with a fixed electricity price. By maintaining a stable electricity price of 64.5 €/MWh, which represents the projected annual average for 2030 in default weather conditions, this scenario isolates the system performance of the network without interference from price fluctuations. This approach allows us to establish a baseline performance of the system, identify efficiencies and bottlenecks independent of electricity price variations, and evaluate how different system designs impact costs and performance.

Dynamic electricity price (dynE)
To examine the impact of real-time electricity prices on the optimal design of a heating system, this experiment introduces hourly fluctuations in electricity prices, reflecting real-world market conditions. This experiment evaluates whether price-responsive heat production and storage strategies can improve economic performance and system efficiency. The introduction of dynamic pricing creates opportunities to optimize heat pump operation, shifting electricity consumption to periods of low prices while minimizing costs during high-price peaks. For this experiment all the different system designs are tested for three different weather years (def, W1, W3).

Grid constraints (gridC)
This experiment explores how network capacity constraints on the electricity grid affect the heating system's ability to function optimally. In modern energy systems, grid congestion and capacity limitations can restrict electricity consumption for heat production, particularly for large-scale heat pumps. To simulate these constraints, peak-hour electricity limitations are introduced, restricting the available grid capacity during high-demand periods (06:00–09:00 and 16:00–21:00). These hours represent the peak loads in the network, where during these periods the largest possibility of congestion can occur. Different constraint levels are tested, where the electricity capacity is reduced to 80%, 60% of the max-

imum grid connection. The maximum grid connection is in the simulations a half MW point above the heat pump capacity, which is an indication for the total needed electricity input of the system, The NP scenario infuse a grid constraint just above the capacity for the heat pump. Therefore, the electricity use will be capped to reduce the maximum electricity use of the system.

By comparing system behavior with these different constraints, the experiment assesses how resilient the system is to grid limitations. Whether it is necessary to shift heat production and if alternative heat sources such as storage or gas boilers become a more dominant factor. The findings will inform future decisions on grid reinforcement costs, flexible demand strategies, and potential technological adaptations.

ID	Description
Grid constraint	
NP	No peak factor
P0.8	0.8 peak factor
P0.6	0.6 peak factor

Table 5.2: Grid constraint descriptions

Grid reinforcement (E-Invest)
Economic incentives play a key role in shaping the performance of a district heating system. This experiment evaluates how different electricity pricing structures influence system operation and whether they encourage more efficient and cost-effective heat production.

A simulation that will be encountered for the complete system is the implementation of electricity grid reinforcement costs. Grid reinforcement costs are applied at different dynamic electricity simulations. Grid reinforcement will be applied based on the maximum electricity use required by the simulation. Grid reinforcement will be applied based on the maximum electricity use required by the simulation. Two designs will be compared: the NP system from the grid constraint experiment and a simulation without grid limitations, taken from the second experiment (dynE). These systems will be adjusted with the necessary grid reinforcement and compared, the costs will be applied to the necessary MW of reinforcement that is needed to the grid. Therefore, a comparison between investments in grid reinforcement will be made between investments in what kind of design is it worth to invest. Are grid reinforcements a better investment or is it cheaper to just have limited grid capacity. Table 5.3 presents the experiments conducted to analyze differences in total system costs across various configurations. The ”restriction” cases represent scenarios with limited grid capacity, while the ”no-limit” cases reflect configurations where grid reinforcements have removed such constraints.

ID	System Design	Max available grid capacity
(restriction)-MS-3	MS-3	3.1
(no limit)-MS-3		3.6
(restriction)-MS-3.5	MS-3.5	3.6
(no limit)-MS-3.5		4.1
(restriction)-MS-4	MS-4	4.1
(no limit)-MS-4		4.6
(restriction)-MS-5	MS-5	4.1
(no limit)-MS-5		4.6

Table 5.3: E-Invest Scenarios for Grid Reinforcement with Available Capacities

Furthermore, the network tariff experiment explores how different tariff levels affect electricity use within the heating system. A fixed additional tariff will be applied on top of the regular electricity price, making electricity consistently more expensive throughout the year. Different tariff levels will be evaluated, ranging from €2/MWh up to €30/MWh. This setup allows the assessment of how increased electricity costs influence system performance and energy consumption.

In addition, another specific test introduces a peak electricity charge, where any electricity consumption above 2 or 3 MW incurs an additional cost of 20 €/MWh or 30 €/MWh. By implementing these scenarios, the experiment aims to determine whether financial mechanisms can enhance system flexibility by incentivizing optimized heat pump operation and storage utilization. This is a capacity-induced tariff, which should introduce a limitation at high peak use with a price incentive. This can be done by a contract with the operating electricity party where it is said that for the first 2 or 3 MW, normal prices will be paid, when allocating more input an extra tariff will be implemented.

Additional experiments
Beyond the four primary experiment series, additional simulations are conducted to explore other uncertainties in system design that could impact the feasibility and performance of the district heating network. These experiments are intended to test external factors and edge cases that may become relevant in future system development or for different boundary conditions.

From the earlier sensitivity analysis, it became clear that the availability of geothermal heat supply is a critical factor. To examine the effect of a different injection temperature in the geothermal well, a simulation is carried out in which the injection temperature is increased to 35°C. This will result in a thermal capacity of 18.8 MW. Also an experiment will be conducted where the injection temperature will be 45°C, this reduces the maximum capacity to 14.5 MW. While geothermal energy is typically seen as a stable base-load heat source, potential limitations need to be considered. This experiment investigates how the system compensates for increased use of the heat pump, greater reliance on thermal storage, or fallback to gas-fired backup capacity. It also provides insights into how similar systems may perform in other regions with other geothermal properties.

Another experiment tests the impact of higher CO_2 prices to evaluate whether rising fossil fuel costs could make alternative heat sources more economically attractive. This could influence the long-term viability of gas-fired components in future heating systems. In this experiment will be explored where the tipping point is located for different heat pump configurations. At what point will a larger heat pump worth the investment of higher investment and fixed OPEX costs. The tested values will be 0.4 and 0.8 €/kg CO_2.

From the sensitivity analysis it became clear that the network temperature is a important factor for the performance factors. By decreasing the supply and return network temperatures by 5 and 10 °C, the system will be tested on the effects of potential future network temperature reductions.

Scenario	Description
dynE	Base scenario without any adjustments.
E-CO_2	CO_2 price increased to 0.4 and 0.8 € / kg CO_2
E-Geo35/45	Geothermal injection temperature to 35/45 °C.
E-Tdhn	Temperature of the district heating network adjusted with 5/10 °C.

Table 5.4: Additional experiments

6 Results

This chapter presents the quantitative outcomes of the simulation experiments, focusing on cost, emissions, storage use, and system behavior in various configurations. Each scenario directly addresses one of the sub-research questions introduced earlier.

6.1. Fixed electricity price

The first experiment evaluates the impact of a fixed electricity price on the operation of a district heating network and electricity use. The results provide insights into the heat production mix, storage utilization, system performance, and financial implications.

Heat production

A distinct pattern emerges in the daily heat production data, where geothermal energy serves as the primary heat source throughout the year. The heat pump, while present in the system, does not directly contribute heat to the district heating network but is instead used to increase the temperature of geothermal heat and ensure the right injection temperature for the geothermal well. The HT-ATES system is designed to store excess energy during the summer. It charges when the network temperatures are the most favorable, thus when the COP for the district heating network is the highest. At these moments, the maximum capacity for charging is used to optimally use the best conditions for charging.

The hourly heat production graph in Figure 6.1 illustrates the operational behavior of the heating system. It shows the hourly heat output from each technology, with colors representing different sources: red indicates the geothermal flow, which is always accompanied by the heat pump because of the required cooling before reinjection into the geothermal well. The green area represents the discharging flow from the HT-ATES, while the brown area indicates gas boiler usage. The blue color shows heat production by the heat pump that is not linked to the geothermal flow and, in this case, only occurs during charging of the HT-ATES. The lighter red area corresponds to the portion of geothermal heat that is stored in the HT-ATES.

During mid-summer, the graph shows only charging from the geothermal well. This reflects the required minimum continuous flow from the geothermal source, even when demand is low. In this period, there is no charging from the heat pump. This is due to a lower return temperature in the district heating network, caused by the absence of TU Delft heat demand. Geothermal energy provides a stable and continuous heat supply, with its output varying slightly to match seasonal demand. During periods of peak demand, the HT-ATES discharges stored heat to supplement the geothermal source. When demand exceeds the combined output of geothermal energy and HT-ATES, the gas boiler is activated. This operation follows a strict merit order: geothermal energy is used first as the most cost-effective base-load source, followed by stored heat from HT-ATES, and finally the gas boiler as the last resort. This production hierarchy directly results from the fixed electricity price, as marginal costs remain constant throughout the year, removing incentives for dynamic operational adjustments.

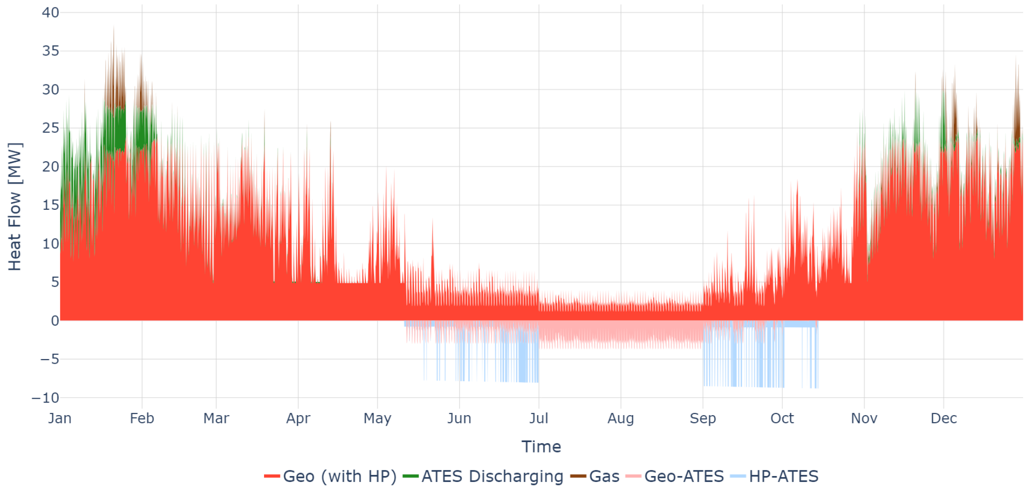

Figure 6.1: Daily average heat production [SS-3.5-(def)]

When examining HT-ATES utilization across different system configurations it becomes visible that in larger storage configurations, the HT-ATES utilization decreases. This occurs because when geothermal energy is abundant, storing heat for later use becomes less attractive due to the lack of demand for storage. Which is caused by the higher prices for the use of electricity and the efficiency losses in the HT-ATES. This effect is particularly noticeable in configurations featuring a large heat pump and expanded storage capacity, where flexibility allows the system to rely less on thermal storage and more on direct geothermal usage. This can directly be linked to the fixed electricity prices which ensure that storing heat is less interesting when there are no price incentives to use the thermal storage unless it can prevent the use of gas.

LCOH & emissions

The financial and sustainable performance factors of the system are analyzed based on LCOH and CO_2 emissions and are shown in Figure 6.2 and Figure 6.3. The results show that for the weather year W1 the variable OPEX of the system increases significantly, primarily due to the higher gas consumption. The cost impact is particularly evident in smaller configurations, where gas dependency results in a higher operational cost burden. While larger heat pumps and expanded storage help reduce gas consumption, they come at a higher capital cost, which make them economically less attractive. A notable trade-off emerges between cost-effectiveness and sustainability. Systems with smaller heat pumps and storage exhibit higher CO_2 emissions, reinforcing the reliance on fossil fuels. This dynamic suggests a critical decision point for policymakers and system designers in balancing affordability against sustainability.

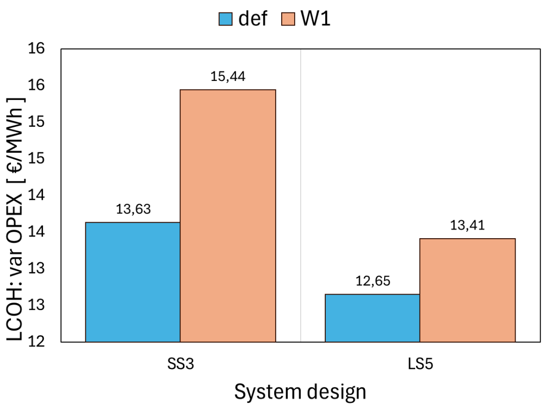

Figure 6.2: LCOH variable OPEX

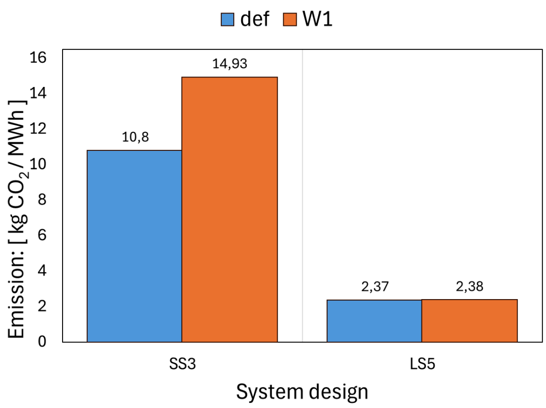

Figure 6.3: CO_2 emission

6.2. Dynamic electricity prices

The second experiment introduces dynamic electricity pricing, fundamentally altering the operation of the district heating system compared to the fixed electricity price scenario. Real-time electricity prices are implemented that correspond to outside temperature and the mix of renewable energies.

Heat production

The most notable difference is the increase of the direct contribution of the heat pump to the heating network and the fluctuating charging of the HT-ATES, as demonstrated in the heat production graph Figure 6.4. Unlike in the fixed-price scenario, the dynamic pricing model creates an economic incentive for the heat pump to deliver heat directly to the network whenever electricity prices are low. The marginal costs for the heat pump can now be lower then the geothermal marginal costs, which explains the heat pump use during some periods.

Similarly, HT-ATES utilization undergoes a significant transformation. For dynamic pricing, the flow of heat into the storage fluctuates significantly throughout the charging period. This shift is driven by varying electricity prices, which influence the merit order of heat production technologies. This enables the system to inject heat into storage when electricity prices are low and discharge in winter during peak demand when prices are often high, increasing its strategic role in balancing energy supply and demand. The charging is therefore compared to the fixed electricity price more infrequent, which is due to the price fluctuations.

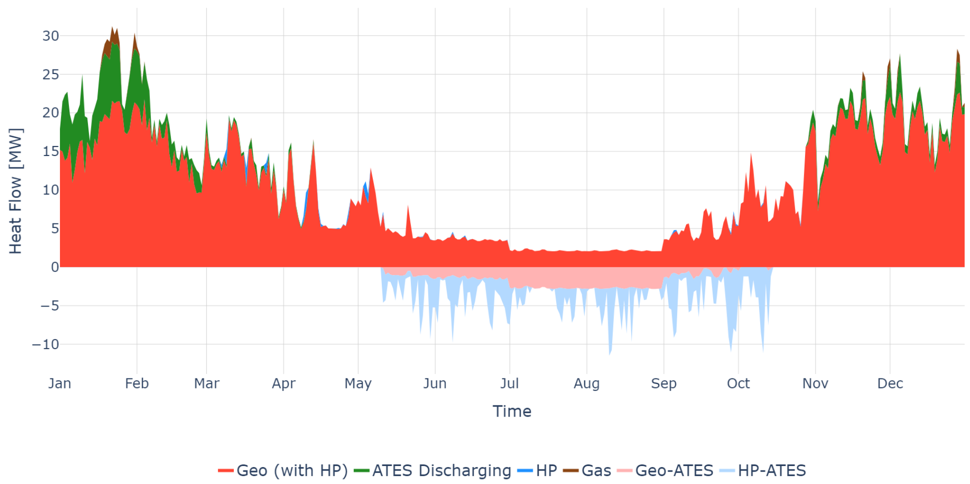

Figure 6.4: Daily heat production [dynE: MS-3.5 (def)]

Electricity

One of the most critical differences between the two scenarios is the total electricity consumption of the system. The introduction of dynamic pricing leads to a different use of electricity. The results indicate that electricity consumption increases with 1.5% when dynamic pricing is implemented. This is largely due to the system's ability to exploit low-cost electricity periods, increasing the electricity use in the summer. This results in a more variable heat production pattern. However, this increase in electricity use has a noticeable impact on the grid. In the fixed electricity price scenario, electricity usage was relatively stable, as the heat pump followed a predictable operating pattern. In contrast, in dynamic pricing, the system reacts to pricing signals, leading to frequent on/off cycling of the heat pump. This results in more volatile electricity peaks, which can possibly cause more strain on the electricity grid.

The average electricity price used during the whole year increases in the dynamic price scenario, the primary reason for this is the elevated electricity expenditure during peak demand periods, when the system is forced to operate within less favorable pricing conditions. Although the system takes advantage of low electricity prices, especially during summer these savings are offset by significantly higher costs during peak periods in winter. The average used electricity price over the year increases by 4.1%. This leads to an increase of 5.3% in the total electricity costs for the MS3.5 scenario.

HT-ATES
The storage does perform better compared to the in the fixed electricity price, especially the smaller storage configurations. The utilization of the storage configurations is dependent on the size of the storage, a smaller storage size will have a lower utilization due to more thermal losses at the surroundings. In the results for the default weather year the utilization for the large storage configurations are lower. The large storage is not completely utilized in the default weather scenario which can be explained by the fact that the needed heat can be delivered cheaper by the geothermal energy. In the more extreme weather year, the HT-ATES is utilized completely.

The total variable costs for the HT-ATES decrease for dynamic pricing, the storage now utilizes low-electricity prices. The total costs for the HT-ATES decrease for all the storage configurations. For the MS3.5 system design the total costs for the HT-ATES decrease with 34% compared to the fixed electricity price. This shows that the HT-ATES with dynamic electricity prices does improve its economical feasibility. Figure 6.5 presents the variable costs for the HT-ATES system in the fixed and dynamic electricity price scenarios. The use of dynamic pricing leads to a significant cost reduction, with the highest relative decrease observed in the MS3.5 configuration.

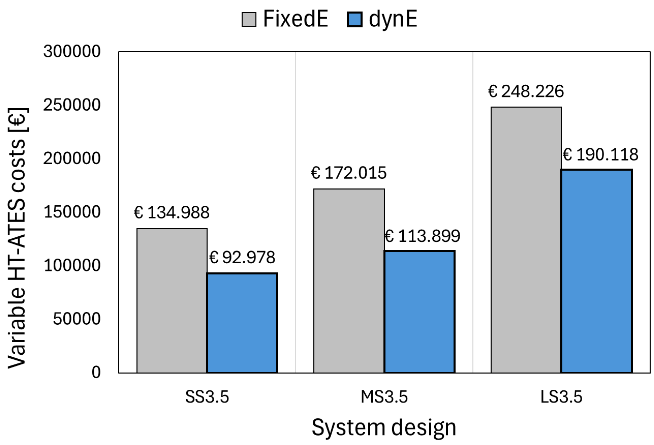

Figure 6.5: Variable HT-ATES costs for the fixed and dynamic electricity price scenario

LCOH
The introduction of dynamic electricity pricing does not result in overall lower variable costs compared to the fixed electricity price scenario. As a result, the LCOH is higher in dynamic pricing which can be explained by the increased total electricity costs. Although operational costs may decrease in the summer months, which is showed by the decreased HT-ATES costs. They increase notably during winter, leading to a higher yearly average prices. Additionally, gas usage increases slightly in dynamic pricing scenarios. This occurs during periods when gas-fired heating becomes temporarily more cost-competitive than electricity. The LCOH for the variable OPEX are presented in Figure 6.6 for the various configurations. The figure shows a clear variation in variable OPEX between different system configurations and weather conditions. The base case without an HT-ATES consistently has the highest variable OPEX. This highlights the added value of thermal storage for the variable OPEX, as the inclusion of HT-ATES reduces costs by approximately 11-16% in the default weather year and 14-23% in the extreme weather year compared to the 3.5 heat pump.

The configuration with the lowest variable OPEX in the default weather year is LS-5, the large-sized storage system combined with a 5 MW heat pump. This configuration is expected to produce the lowest variable costs because of the low dependence on back-up generators. In the default weather year, the difference between the LS-5 and MS-5 is minimal. This is due to the already large heat pump which ensures higher flexibility. Weather variability clearly impacts variable costs, with extreme weather leading to higher gas consumption. In the extreme weather year (W1), the LS-5 configuration featuring the largest heat pump and storage achieves the lowest variable OPEX. In this scenario, the benefits of scale does have effect on the system. The difference between the medium and large storage increase in the W1 scenario. This show the relevance of larger systems is more important in extreme weather years. In general, the differences in the W1 setting are larger than in the default setting, this suggests that the systems encounter more constraints. This is particularly evident in configurations with smaller heat pumps, where the LCOH shows that these values are significantly higher than those for larger heat pumps and the cost-efficient.

The increase for the LCOH in design SS3.5 and MS-3 are the largest between the default and extreme weather year. This can be attributed to the smaller heat pump capacities of the system. The system lacks therefore flexibility and is more sensitive to peak demand conditions, making it more dependent on expensive electricity and gas backup. This underlines the importance of system robustness. Configurations with larger heat pumps and greater storage capacity are better able to maintain performance in extreme conditions. In the default weather year, the differences in variable OPEX between the 3.5, 4, and 5 MW heat pump configurations (with medium storage) are relatively small. This suggests that a 3.5 MW heat pump is adequately sized for typical conditions. Increasing the capacity beyond that yields only marginal operational savings. However, in extreme conditions, larger heat pumps still provide significant benefits. This raises the key design question: do the reductions in variable costs achieved by larger systems justify the higher fixed OPEX and CAPEX? While the answer may vary by context, the results clearly show that in dynamic pricing and extreme weather, larger, more robust systems provide better resilience and lower operational risks.

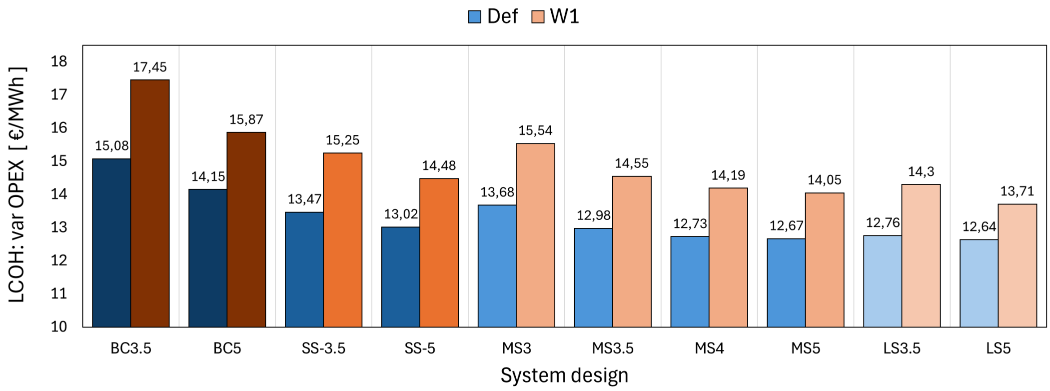

Figure 6.6: LCOH: Variable OPEX for different system designs [dynE]

The impact on total costs is shown in Figure 6.7. The influence of variable costs on overall expenses is relatively limited, as CAPEX and fixed OPEX together make up approximately 85% of the total annual costs. In contrast, variable OPEX accounts for only about 15%, depending on the system configuration. Across the different profiles, it becomes evident that configurations with the lowest operational costs often require the highest initial investments. This trade-off is even more pronounced in extreme weather conditions. For example, system design MS-3 has a 7.5% higher variable OPEX compared to MS-5, yet its total system costs are 15% lower due to significantly reduced capital expenditure. This highlights the importance of balancing investment costs with long-term operational performance when designing robust and cost-effective heating systems. Compared with and without storage, it shows that the base cases are more expensive than the corresponding SS and MS configurations. This indicates that HT-ATES does add enough value to the heating system to be economically viable.

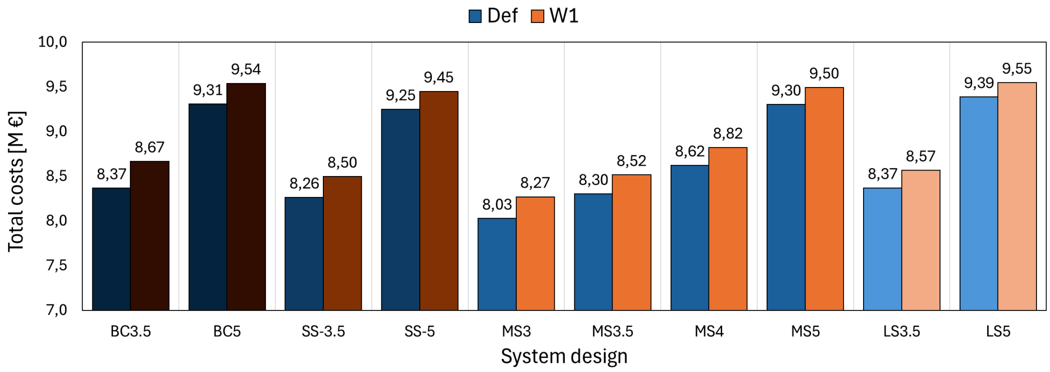

Figure 6.7: Total yearly system costs for different system designs [dynE]

Emissions

Figure 6.8 shows the average CO_2 emission in kg per MWh of heat produced for the different configurations in both weather scenarios. In general, CO_2 emissions are inversely correlated with total system costs except for the base case. Configurations with smaller heat pumps tend to have lower total costs, but also significantly higher emissions due to a greater reliance on gas-fired backup. The difference in emissions between the default and extreme weather years becomes exponentially larger for smaller heat pump configurations. For the 3.5 MW system, emissions increase with 19–45% in extreme conditions. In comparison, the increase for the 5 MW heat pump systems is more moderate, at 3–26%, indicating that larger heat pumps offer greater system robustness and better emissions performance during high-demand periods.

The storage size also influences system robustness, where the emission decrease is 31% for the SS-3.5 to MS-3.5 configuration. The decrease in emission for the MS to LS configuration is 14%. This shows that the impact in smaller systems is relatively much higher. When comparing the impact of the heat pump it can be seen that this has relatively more effect, a decrease of 54% is presented for the SS3.5 to SS5 configuration. The decrease for the LS configuration is 27%. This states that pump size is the dominant factor in determining both robustness and CO_2 performance. These results confirm that low-emission system designs require higher upfront investments. More cost-effective configurations, particularly those with smaller heat pumps and storage, continue to rely heavily on fossil fuels. Thus, there is a clear trade-off between economic performance and environmental impact. The lowest-cost configurations may appear attractive from a financial perspective, they are associated with significantly higher emissions, undermining long-term sustainability goals.

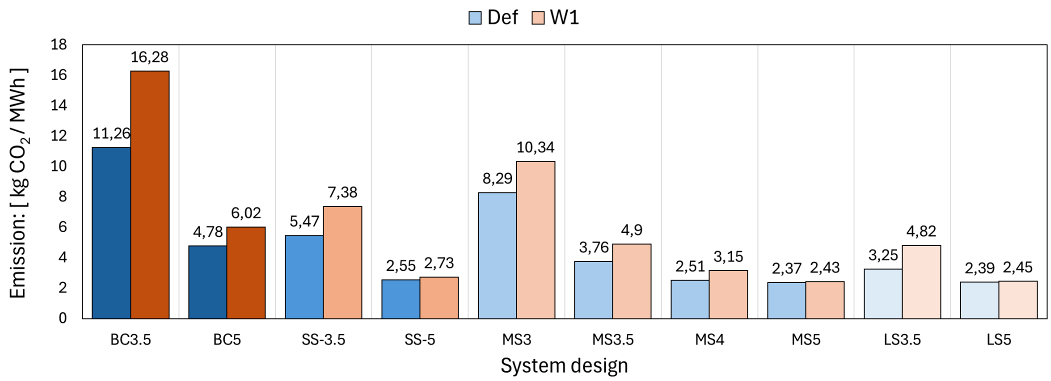

Figure 6.8: CO_2 emissions for different system designs [dynE]

6.2.1. Detailed system behavior

This section provides an in-depth analysis of a specific system configuration, focusing on system design with the medium storage and the 3.5 MW heat pump, comparing its performance for the default and extreme weather years. By zooming in on these two cases, a deeper understanding of how these systems adapt to varying weather conditions and explore the electricity use.

Heat production

The annual load duration curve profiles for both runs are illustrated in Figure 6.9 and Figure 6.10. A clear distinction is visible between the two scenarios, where the extreme weather year shows an increase in heat demand. The increase in gas use in the w1 scenario is due to the colder periods which can be seen with the temperature profiles in the Figure. The reliance on the gas boiler reflects the system's need for enough backup capacity. The load duration curve shows that when cold periods occur the supply temperature is higher which result in a lower amount of geothermal output due to the limited factor of the heat pump.

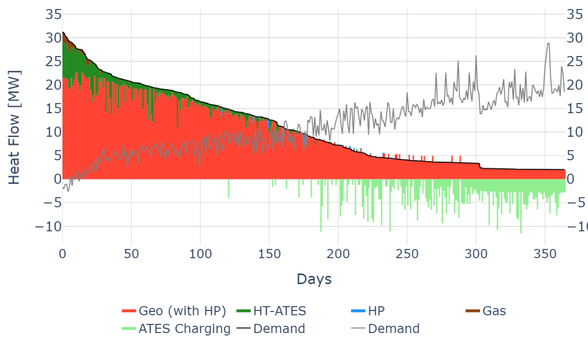

Figure 6.9: Load duration curve dynE-MS-3.5(def)

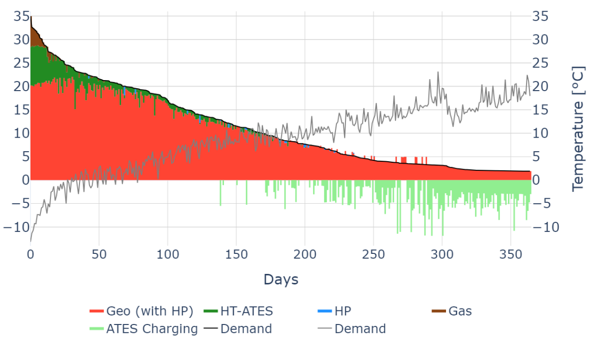

Figure 6.10: Load duration curve dynE-MS-3.5(W1)

Coldest week

A closer examination of the coldest week in both runs provides insight into the dynamics of the system. For the extreme weather scenario the coldest week occur from January 10 to January 17, with an average temperature of -9.9°C, while in the default weather year, the coldest period occur from January 18 to January 25, with an average temperature of -1.7°C. Figure 6.11 and Figure 6.12 show the hourly heat production during these coldest weeks. The system should reach maximum output levels for the HT-ATES and geothermal sources during this cold period, the heat demand is high in this period thus the electricity graphs should show a constrained electricity graph for the heat pump and a maximum output for the HT-ATES flow. In the default weather year, the HT-ATES is prioritized over direct geothermal use, reflecting its lower marginal operational costs. For the W1 profile the graph shows a lower maximum output of the geothermal well, which can be declared by the maximum reached output of the heat pump. The heat pump has reached their maximum capacity of boosting the geothermal heat, which is dependent of the outside temperature. In Figure 6.14 the electricity flows do confirm this. When the heat pump becomes larger this effect become less significant, in Appendix C the profiles for the coldest weak for larger heat pumps are visible, which shows that the geothermal output in these cases are larger and thus this effect is lower.

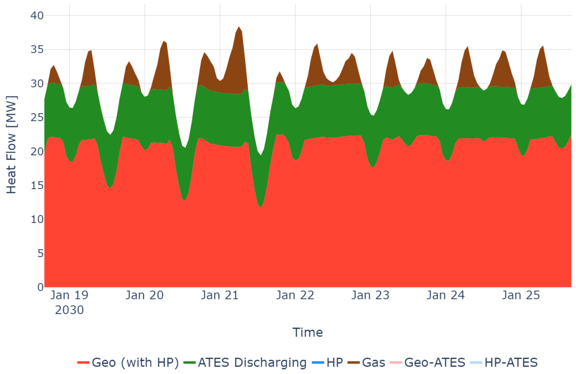

Figure 6.11: Heat distribution coldest week [dynE-MS3.5(def)]

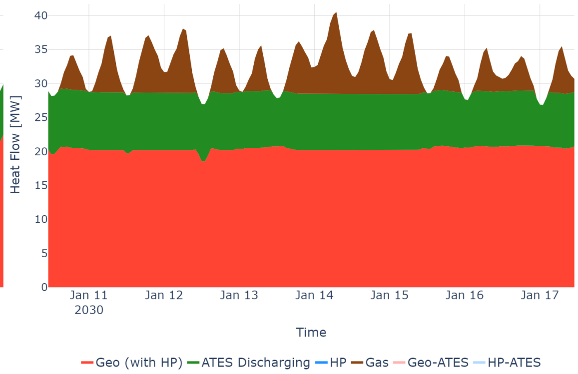

Figure 6.12: Heat distribution coldest week [dynE-MS3.5(W1)]

Electricity grid load

Electricity consumption patterns provide insight into the operational constraints of the system, particularly in extreme weather conditions. Figure 6.13 shows the electricity consumption profile during the coldest week for the default weather year. The different electricity flows indicate the various destinations of electricity within the heat system. The blue area represents electricity used by the heat pump to supply heat directly to the district heating network (HP to DH), where return water from the network is reheated without the involvement of geothermal flow. The “HP to ATES” flow corresponds with the electricity used to reheat district heating return flow and charge it into the HT-ATES. The “HP (Geo to ATES)” flow, which is zero during this cold week (and only appears in summer), represents the electricity required to raise the geothermal flow to the appropriate temperature for storage in the HT-ATES. The “HP (Geo)” flow refers to the electricity needed to raise the geothermal output to the supply temperature required by the district heating network. Additionally, the “ATES ESP” flow indicates the electricity consumption of the ESP during discharging and charging. The total electricity demand represents the sum of all these components within the heating system.

The figure shows that both the heat pump and HT-ATES operate at full capacity during several hours, suggesting that technical limitations for these components are reached during high-demand periods. In particular, the HT-ATES reaches its maximum discharge capacity, highlighting its critical role as a buffer during peak heating demand. For the extreme weather year, the electricity consumption profile becomes nearly constant, indicating that the system operates at its maximum allowable capacity for extended periods. The grid load during peak hours reaches approximately 4 MW, with the highest observed load peaking at 4.04 MW.

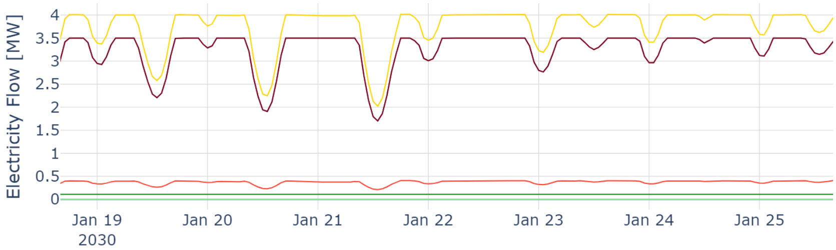

Figure 6.13: Electricity flows coldest week [dynE-MS-3.5(def)]

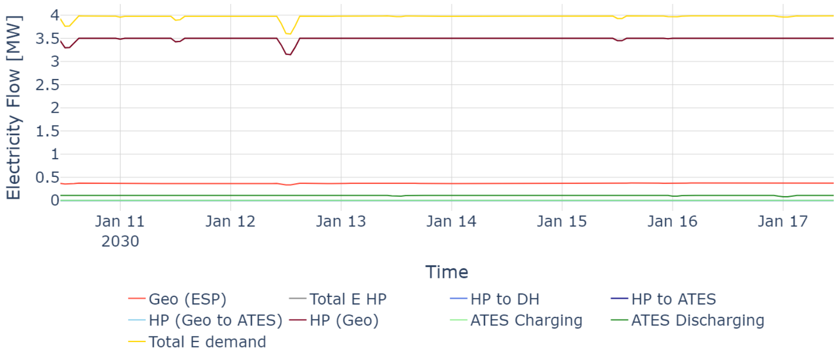

Figure 6.14: Electricity flows coldest week [dynE-MS-3.5(W1)]

The daily load duration curve for electricity consumption is presented in Figure 6.15. This graph is ordered according to the corresponding heat demand, with the electricity use corresponding to the highest heat demand on the left side. The right axis shows the heat demand, represented by the ascending black line, while the left axis indicates the various electricity flows within the system. The graph illustrates that during periods of high heat demand, nearly all of the heat pump’s capacity is allocated to upgrading the geothermal flow, indicated by the dark red segment labeled HP (Geo). As heat demand decreases, the geothermal flow also reduces, resulting in a decline in electricity use for HP (Geo). When heat demand becomes sufficiently low and electricity prices drop, the system shifts towards charging the HT-ATES. This is visible as an increase in electricity use by the heat pump for HT-ATES charging, shown in the corresponding color. Additionally, the electricity required for boosting geothermal flow specifically for HT-ATES charging, labeled HP (Geo to ATES), becomes more prominent during periods of lowest heat demand. This process ensures the cooling of the geothermal injection flow and enables temperature lifting up to 80°C for effective storage use. The red-colored flow represents the electricity required by the ESP for geothermal production and reinjection into the wells. Finally, the flows related to HT-ATES charging and discharging are also visible: discharging occurs during periods of high heat demand, while charging takes place primarily during low demand periods. This reflects the role of the storage system in balancing thermal supply and electricity consumption throughout the year.

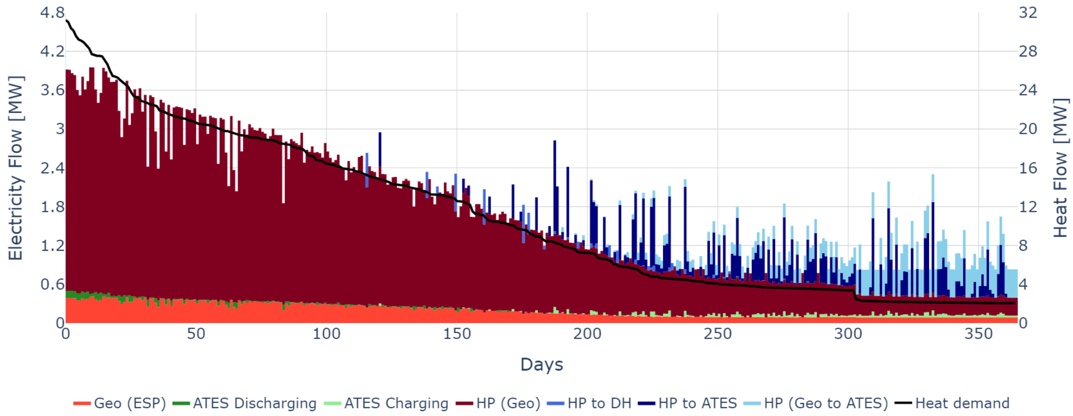

Figure 6.15: Heat demand duration curve with daily electricity usage [dynE-MS3.5(def)]

In Figure 6.16, electricity use is plotted against the corresponding electricity price. The graph reveals that the highest electricity prices align with increased use of the heat pump for boosting geothermal heat, indicated by the concentration of geothermal-related electricity use on the left side of the curve. As the electricity price decreases, the share of electricity used for charging the HT-ATES increases, with these flows primarily appearing on the right side of the figure. This pattern highlights the added value of an integrated system: low-priced electricity is strategically used to charge thermal storage, which can then be discharged during high-demand periods in winter. This illustrates how dynamic electricity pricing supports smart load shifting and enhances the overall efficiency and flexibility of the heating system.

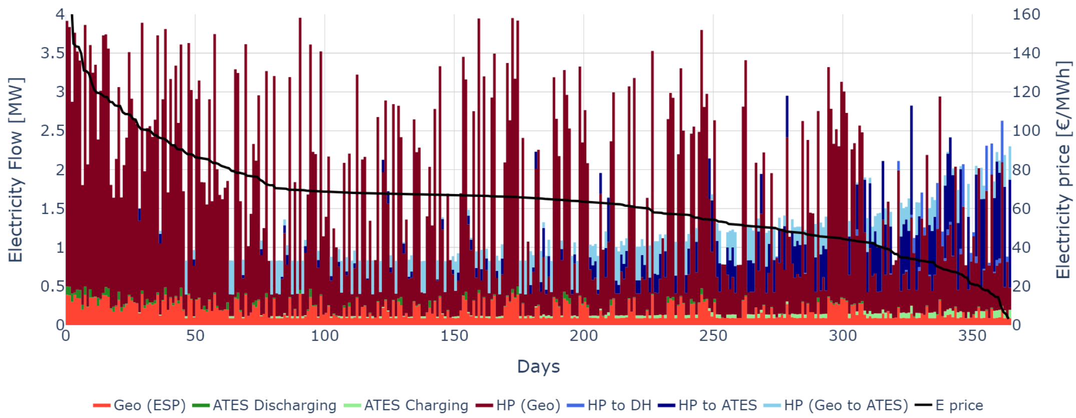

Figure 6.16: Electricity price duration curve with daily electricity usage [dynE-MS3.5(def)]

6.3. Grid constraints

The grid constraints experiment was designed to assess the impact of limitations in electricity supply on the operation of the district heating system, particularly on the heat pump, which represents the system's largest electricity consumer. Instead of analyzing all configurations in detail, a selection was made based on prior results. The MS configuration is investigated further due to its overall strong performance.

LCOH

The introduction of grid constraints imposes a significant limitation on the heat pump's ability to operate optimally. However, when grid capacity constraints are introduced, the system faces additional restrictions, forcing the heat pump to curtail operations during peak demand periods. This limitation increases the system's reliance on alternative heat sources, notably geothermal heat and gas boilers. As a result, variable operational costs (variable OPEX) increase as a result of less efficient heat generation and increased gas usage. Since the heat pump is the primary electrical consumption component, grid limitations directly affect the balance between geothermal output and HT-ATES charging or discharging.

The results indicate that the impact of grid constraints on variable OPEX is more severe in systems with smaller heat pumps. This is because smaller heat pumps tend to operate closer to their capacity limit and are more frequently constrained. As shown in Figure 6.17, the most substantial cost increase is observed in the smallest heat pump configuration (MS-3), where variable OPEX increases by 16% compared to the P0.6 scenarios. This increase is primarily driven by the transition from electricity-based heat generation to gas-fired backup, which is both more costly and less sustainable. In contrast, systems with larger heat pumps experience only a minor increase in variable OPEX, in the MS-5 configuration the increase is 3%. Larger heat pumps are typically underutilized and therefore less affected by short-term restrictions in grid capacity. This indicates that systems with larger heat pumps are more robust under grid constraints, maintaining operational efficiency more effectively than smaller systems. Therefore, grid constraints do become a relevant factor in future system design, particularly in cases where grid limitations coincide with critical heat demand periods or strict time-based electricity tariffs.

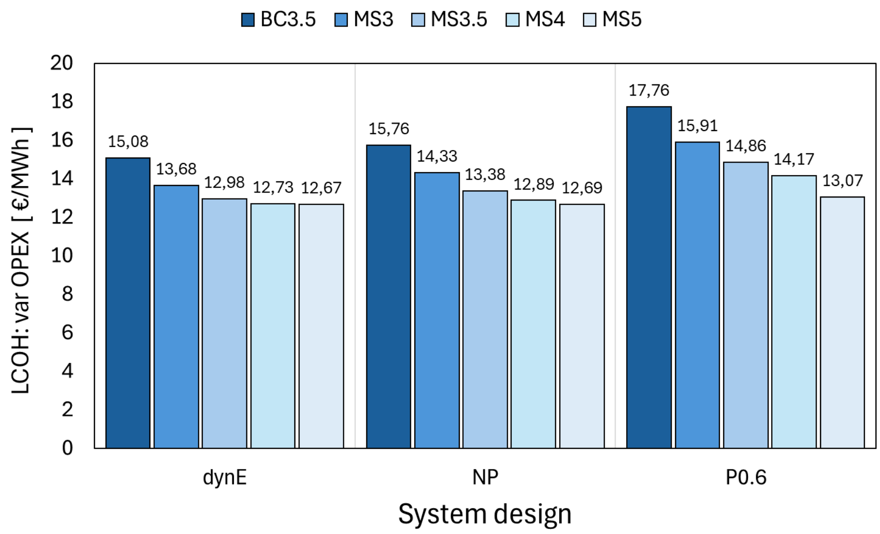

Figure 6.17: LCOH var OPEX for different grid constraints and configurations

CO_2 emission

The grid constraints do impact the CO_2 emissions in a specific way, as seen from Figure 6.18. There is a considerable increase in emissions when the grid capacity is limited, especially in the arrangements of smaller heat pumps and for the configuration without storage. These arrangements are less efficient in the use of electricity and must resort to more gas-fired backup when the heat pump is limited. The rise in emissions indicates a lower use of the heat pump, along with greater use of fossil fuels. This effect is most significant for low-capacity systems, which lack flexibility to reschedule operations or employ thermal storage effectively during periods of tight electricity supply.

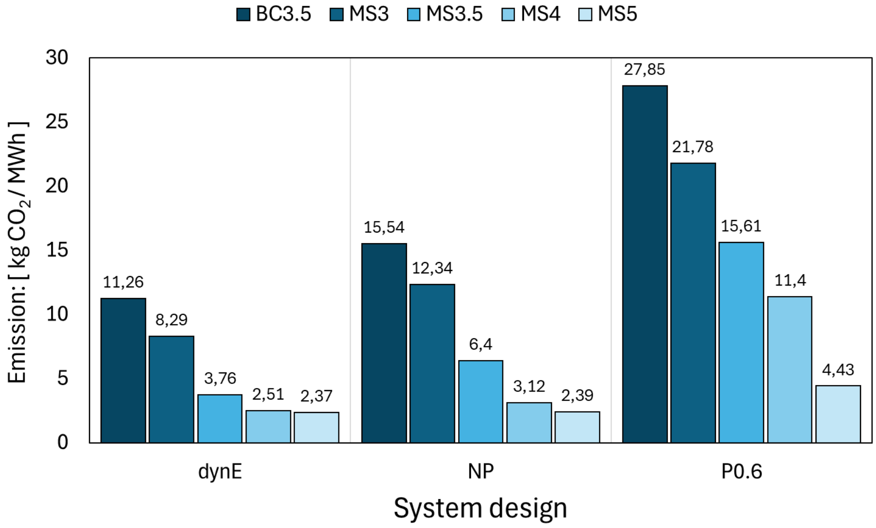

Figure 6.18: CO_2 emissions for different grid constraints and configurations

Electricity grid load

The impact of peak-hour restrictions is clearly visible in the electricity load duration curve shown in Figure 6.19.This figure illustrates the simulation results for the medium storage (MS) configuration with a 3.5 MW heat pump operating under a peak electricity constraint of 0.6. The graph presents the electricity load duration curve, where electricity use is sorted from highest to lowest. Different colors indicate the purpose of electricity consumption. The majority of electricity is used by the heat pump to boost the geothermal flow. The impact of the grid constraint is clearly visible: electricity consumption is capped at 2.4 MW_e during peak hours. This results in a flat section of the curve, where the peak load is reduced from 4.05 MW to 2.4 MW. In the P0.6 scenario, the reduced electricity usage during these high-demand hours is compensated by increased reliance on the gas boiler and HT-ATES.

To illustrate this, in the dynamic pricing case (dynE), the electricity consumption above 3.2 MW_e accounts for 4653 MWh. For the P0.6 constraint, this is reduced to 2577 MWh. This is a reduction of 2076 MWh in the peak periods, while the total electricity reduction is 'only' 1337 MWh. The difference suggests that electricity is more evenly spread across non-peak periods, and that grid constraints significantly reshape the load profile, particularly for smaller heat pump configurations, which face the tightest capacity limits.

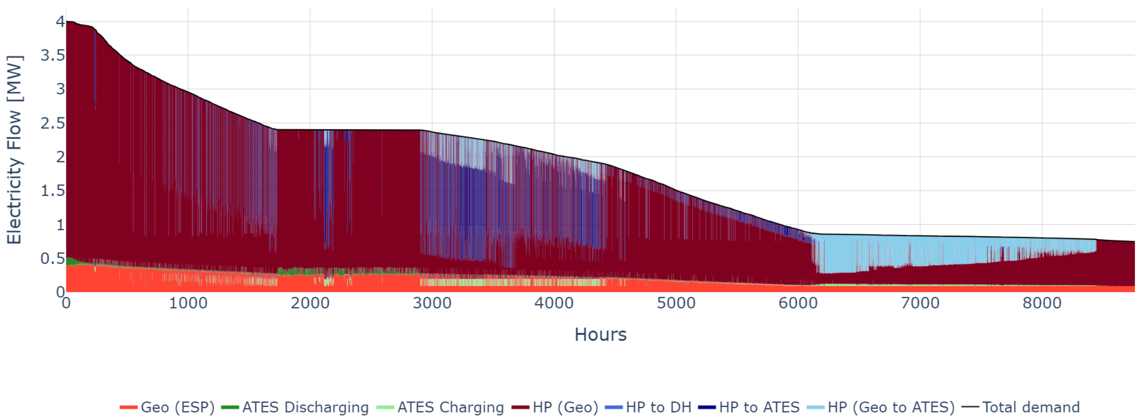

Figure 6.19: Electricity load duration curve [gridC-MS-3.5-P0.6(def)]

Storage capacity

Grid constraints restrict the ability of the heat pump to fully exploit periods of low electricity prices. However, since such constraints typically occur during short-duration peak periods, increasing storage capacity may offer a practical solution. By charging HT-ATES during low-price periods, the system can avoid peak-hour electricity use without sacrificing heat delivery. This is particularly relevant for configurations with smaller heat pumps, which are more affected by capacity constraints. In such cases, an increase in HT-ATES capacity could provide the flexibility needed to buffer against short-term electricity availability issues. This not only reduces reliance on gas but also improves operational stability and efficiency without the need for immediate grid reinforcement. In this way, storage becomes an essential part of a heating system for mitigating the impacts of grid limitations.

The economic advantage of integrating storage becomes increasingly evident in constrained conditions. In the MS3.5 scenario, the configuration with storage is €64,000 cheaper than the no-storage equivalent in an unconstrained setting. However, when grid constraints are introduced (P0.6), this cost difference more than doubles to €140,000. This highlights that storage plays a more critical role as grid limitations become more severe.While increasing storage capacity can further reduce variable operational costs, the marginal benefit diminishes beyond a certain point. For instance, the jump from medium to large storage (MS to LS) increases variable OPEX savings from €275,000 to €320,000. Yet, due to the significantly higher investment costs, the total system cost savings decline from €140,000 to €95,000. This indicates that the MS3.5 configuration offers the most economically balanced solution, even in grid-constrained conditions.

In Figure 6.20 the differences between the costs are showed for the BC3.5 and MS3.5 configurations in different experiment settings, here can be seen that the cost differences and therefore the value of the HT-ATES increase when grid constraints are implemented.

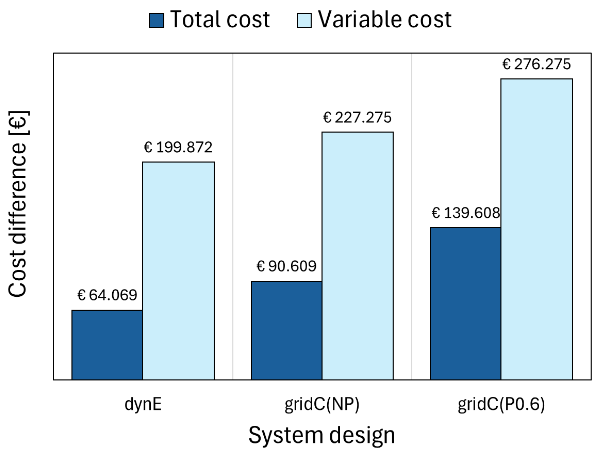

Figure 6.20: cost differences with and without storage (BC3.5 and MS3.5)

6.4. Grid reinforcement

Grid reinforcement

This experiment incorporates grid reinforcement costs into the analysis to reflect the larger societal investment required to increase electricity connection capacity. The focus lies on comparing medium storage system configurations in two scenarios: one where the electricity output of the heat pump is restricted to its nominal capacity, and one with unconstrained electricity use, assuming full grid reinforcement. These two cases are evaluated in both the default and extreme weather conditions, where 375,000 €/MW is taken as reference point for investment costs. The results are presented in Table 6.1, showing both absolute differences in annual costs and percentage changes.

In the default weather scenario, grid reinforcement proves economically beneficial for all configurations except the 5 MW heat pump. In that case, the additional reinforcement costs outweigh the potential operational savings. This is because these larger systems already operate with lower utilization, meaning the gains from removing the grid constraint are minimal. For extreme weather conditions (W1), the demand for heat increases substantially, making the ability to fully utilize the heat pump more valuable. As a result, smaller systems particularly the 3 MW and 3.5 MW configurations show considerable cost savings when grid constraints are removed. The 4 MW configuration also shows a slight net benefit. For the MS-5 configuration, however, grid reinforcement remains unjustified due to its limited marginal impact on system performance and cost. These findings suggest that grid investment becomes more cost-effective as system stress increases, such as during extreme weather events or in highly utilized system designs.

From a broader perspective, this experiment demonstrates that grid reinforcement and electricity pricing together incentivize more efficient system behavior. The electricity price serves as a real-time driver for cost optimization, while the network costs, fixed OPEX, and CAPEX determine long-term system feasibility. By comparing system designs with and without reinforcement, the trade-offs between infrastructure investment and operational flexibility can be analyzed. In particular, smaller heat pump systems benefit the most from grid reinforcement. These systems tend to operate closer to their capacity limits and are more affected by grid constraints. Enabling unrestricted operation allows these configurations to fully capitalize on low electricity prices and reduce their reliance on gas backup. In such cases, the costs of grid reinforcement are offset by operational savings, making the investment worthwhile.

Grid Reinforcement	**Def Scenario**			**W1 Scenario**		
ID [E-invest]	**Total Costs [M€]**	**Change**	**% Diff.**	**Total Costs [M€]**	**Change**	**% Diff.**
(restriction)-MS-3	8.158	-€62,219	-0.76%	8.439	-€99,305	-1.18%
(no limit)-MS-3	8.096			8.339		
(restriction)-MS-3.5	8.410	-€28,790	-0.34%	8.636	-€42,132	-0.49%
(no limit)-MS-3.5	8.381			8.594		
(restriction)-MS-4	8.715	-€5,504	-0.06%	8.926	-€15,999	-0.18%
(no limit)-MS-4	8.710			8.910		
(restriction)-MS-5	9.402	€8,212	0.09%	9.593	€7,135	0.07%
(no limit)-MS-5	9.410			9.600		

Table 6.1: Total cost comparison for grid reinforcement scenarios for Def and W1 assumptions.

HT-ATES

To assess the trade-off between short-term and long-term investments, it is essential to evaluate the added value of thermal storage. Short-term investments primarily concern the deployment of flexibility solution that can alleviate pressure on the electricity grid. In contrast, long-term investments are oriented toward structural grid reinforcement to accommodate future capacity needs. As shown in Figure 6.22, it is challenging for systems without storage to match the CO_2 emission profile of those with a HT-ATES. Storage enables the system to utilize and preserve low-emission heat typically sourced from electricity during off-peak periods when the grid is less carbon-intensive. In contrast, systems without storage often rely on real-time heat pump operation during high-demand periods, when electricity is not only more expensive but also more carbon-intensive, or fallback to gas boilers, which directly increases emissions.

Without storage, maintaining robustness in the system would require either a significantly oversized heat pump or substantial grid upgrades, both of which entail considerably higher capital costs than investing in a well-sized thermal storage unit. The figures show that the operational costs of the configurations decrease when a HT-ATES is added. The HT-ATES offers therefore a dual benefit: it enables economic load shifting and strengthens the system's compatibility with grid limitations. Its importance becomes especially evident during winter peaks, when demand is highest and grid availability is lowest. In these conditions, storage mitigates the system's exposure to high electricity costs and emissions, offering a more efficient and environmentally friendly alternative. In comparison to the base case without storage, the integration of HT-ATES adds significant value not just in operational savings, but also in enhancing system resilience and supporting decarbonization objectives.

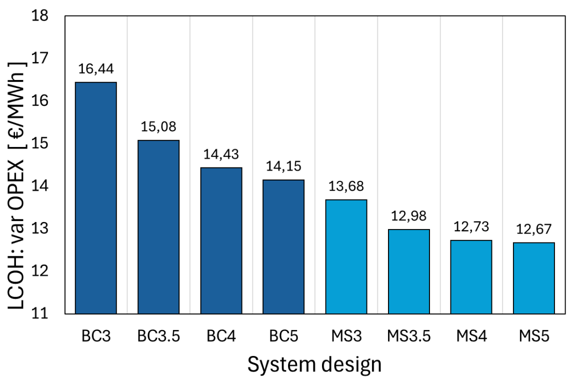

Figure 6.21: LCOH var OPEX with and without HT-ATES

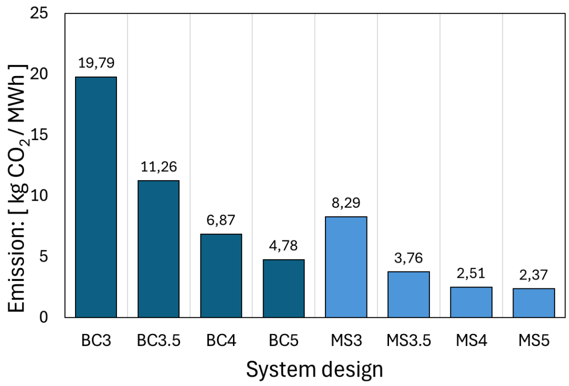

Figure 6.22: CO_2-emission with and without HT-ATES

Network tariffs

This experiment analyzes the impact of general increases in electricity network tariffs on system costs. Unlike the level tariff, this tariff is applied uniformly across all electricity use throughout the year, irrespective of peak usage. As shown in Figure 6.23, the results show that increasing network tariffs leads to higher variable costs, which is a logical outcome given the higher electricity prices. These network tariffs can be seen as indicative of the price signals that may be necessary to help fund future grid reinforcements. The impact is relatively larger for configurations that involve storage, such as HT-ATES, due to their higher electricity consumption.

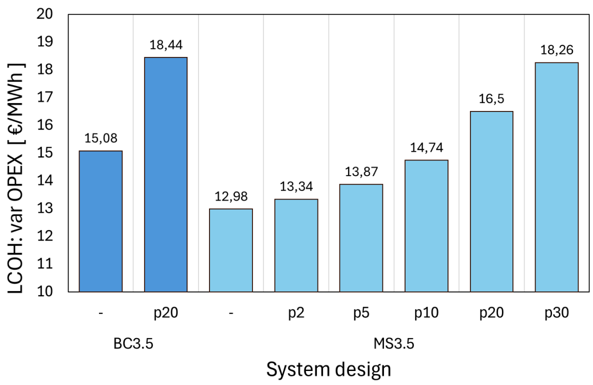

Figure 6.23: Vaiable costs network tariffs

Levels tariff

This experiment investigates how varying electricity tariffs during peak load periods affect the operational behavior of the heating system. The tariffs were implemented for electricity consumption exceeding 2 MW or 3 MW, with added price levels of €20/MWh or €30/MWh. The results are summarized in Appendix B (Table B.6). These tariffs aim to discourage electricity use during high electricity demand by introducing an extra electricity tariff on top of the electricity price.

The main outcome is that these level tariffs lead to a slight increase in variable operational costs. the variable OPEX rises by approximately 5–8%, depending on the threshold and tariff level. This increase is primarily linked to the more expensive electricity consumption of the heat pump during periods of geothermal boosting. However, despite the additional tariff, the operational behavior of the heating system does not significantly change. During colder periods, when heat demand rises, the heat pump continues to operate at high loads despite the price signal, as immediate heat delivery is required. As illustrated in Figure 6.24, the current tariff structure has limited impact on electricity usage. A small plateau forms around the 2 MW threshold, indicating some response to the higher price. Nonetheless, this effect remains limited, and the heat pump still processes a substantial volume of geothermal energy requiring boosting. Consequently, while operational costs rise modestly, the behavioral impact of the level tariff remains marginal.

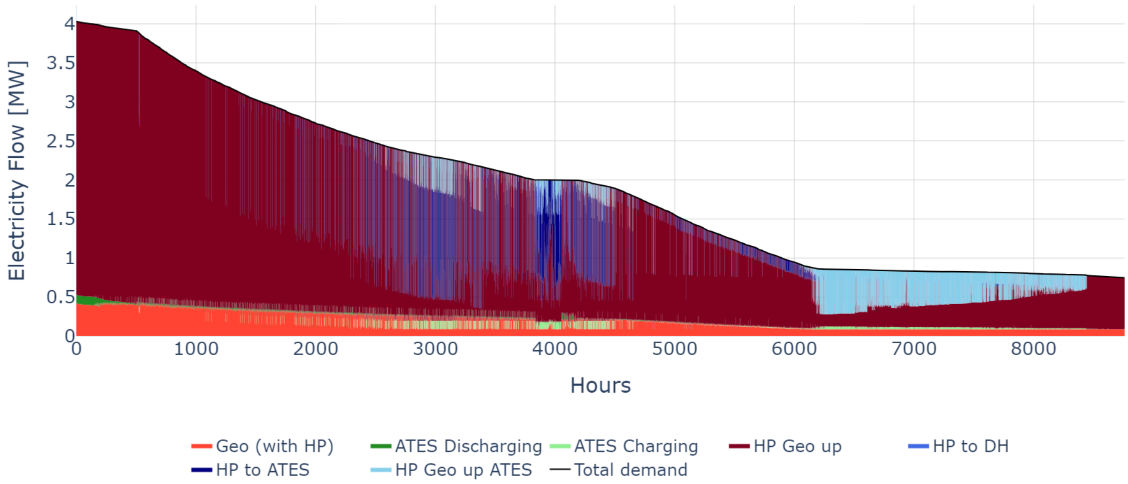

Figure 6.24: Electricity load duration curve (PT(2MW-p30)-MS3.5-def)

6.5. Additional experiments

This section presents a series of additional experiments conducted to broaden the understanding of system performance for alternative design choices and boundary conditions. These analyses aim to provide insights not only for the Delft case but also for other potential applications of similar district heating systems. Specifically, the experiments explore constraints related to grid reinforcements, variations in geothermal injection temperature, network temperature, and CO_2 pricing.

Geothermal output

This experiment investigates the effects of reducing the temperature difference (ΔT) between the production and injection wells in the geothermal system. In this case, the injection temperature is increased to 35°C, resulting in a lower maximum output capacity of 18.8 MW. A smaller ΔT leads to reduced geothermal heat extraction, but it also lowers the electricity demand for cooling the injection water.

As shown in Figure 6.25 and Figure 6.26, this configuration results in lower variable OPEX, primarily due to reduced electricity consumption throughout the year. The total annual electricity use decreases significantly in the Geo35 scenario (13,859 MWh) compared to the base scenario (16,846 MWh). This decline in electricity use is due to the reduced need to boost the geothermal temperature, as less energy is required to reinject at lower temperatures. Despite the lower geothermal capacity, gas consumption remains stable. Overall, emissions also decline as a result of the improved system efficiency and reduced electricity use, while gas use remains relatively constant.

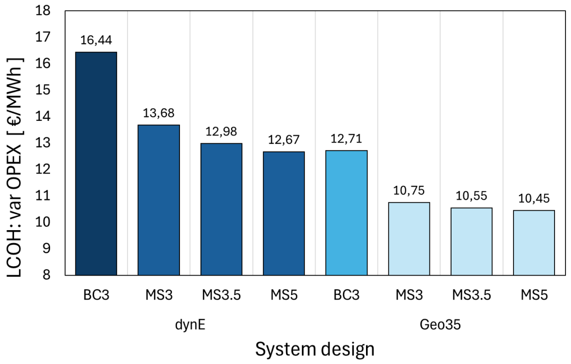

Figure 6.25: Variable OPEX comparison dynE and Geo35

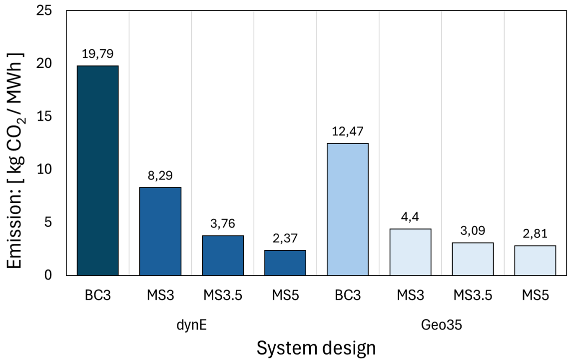

Figure 6.26: CO_2-emission comparison dynE and Geo35

In Figure 6.27, it becomes evident that the heat pump compensates for the reduced geothermal capacity by providing more direct heat to the district heating network. This compensation leads to increased heat pump utilization. However, due to the more efficient operation and reduced load for boosting geothermal flow, total electricity demand is still lower. The load duration curve highlights a shift: it shows a clear, flat output limit for geothermal production, which contrasts with the less-defined upper limit in the 18 °C injection scenario due to high electricity use.

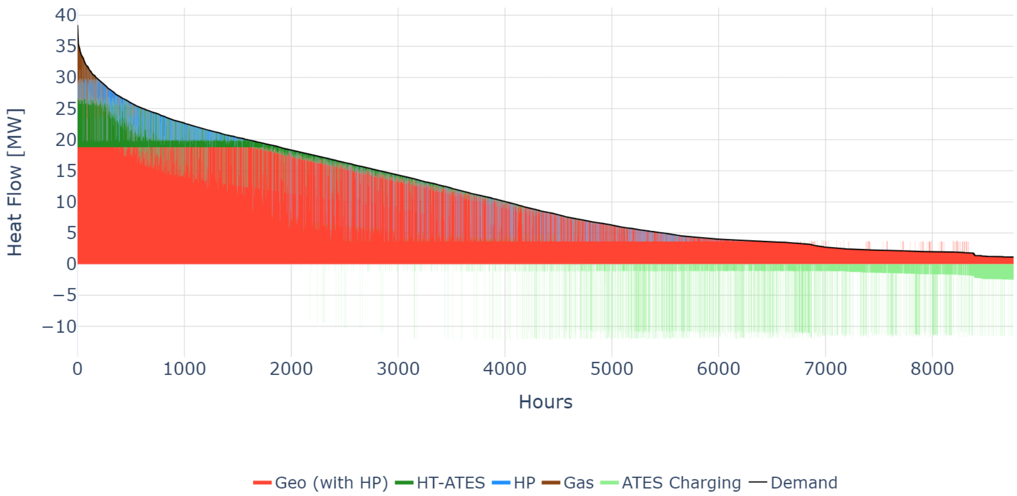

Figure 6.27: Hourly load duration curve for geothermal injection T(35 C) [Geo35-MS3-def]

When the injection temperature is further increased to 45°C, the geothermal capacity drops to 14.5 MW. Consequently, the heat pump takes on a larger role in supplying heat. In the MS3 configuration, 74.4% of the heat comes from geothermal energy (including heat pump-boosted output), while 15% is delivered by the heat pump directly as a supplementary source. Interestingly, gas use further decreases in this scenario. The gas share drops from 1.1% in the Geo35 case to just 0.3% in the Geo45 case. As a result, the variable operational costs also decrease, reaching 9.83 €/MWh. This reflects the improved efficiency of the heat pump and the system's ability to rely more heavily on electricity, even at reduced geothermal output, without increasing emissions or gas consumption.

Supply temperature

Reducing the network supply temperature improves the economic viability of the system by lowering the variable OPEX. However, the cost savings are relatively modest. This can be attributed to the fact that the cooling requirement for the geothermal reinjection remains unchanged, meaning the electricity demand for this process is unaffected. Although a 5°C reduction in the network temperature does influence system performance, it does not result in substantial changes to overall system costs.

Interestingly, the cost reduction in the base case (without storage) for standard temperature conditions is more pronounced than in the reduced-temperature scenario as shown in Figure 6.28. This is due to the higher coefficient of performance (COP) of the heat pump at lower supply temperatures, which enables the system to generate more heat using less electricity. As a result, the system benefits from a lower variable OPEX, even though the overall economic impact remains moderate.

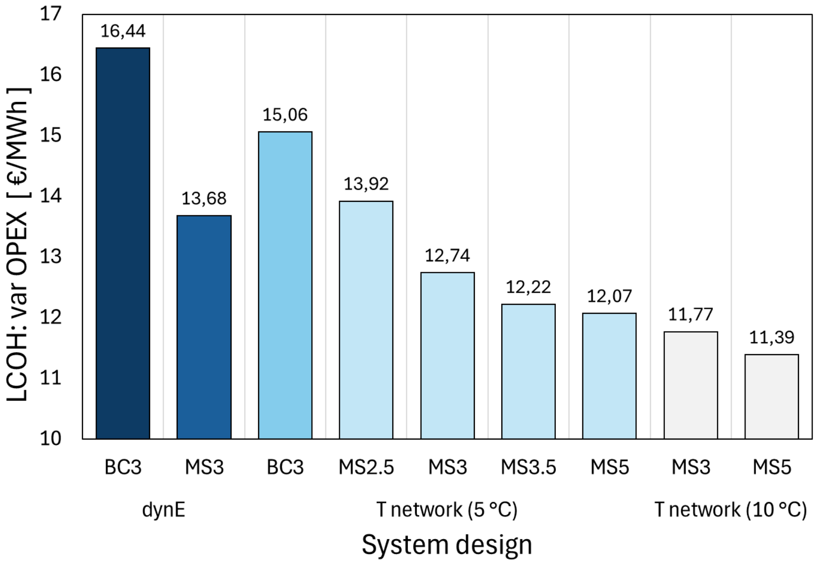

Figure 6.28: LCOH variable OPEX network temperature experiment

CO_2 price

The CO_2 price has a significant impact on the variable OPEX of the system configurations. This additional experiment investigates the effect of CO_2 pricing by identifying the tipping points at which larger, more electrified systems become economically preferable due to reduced emissions. In this analysis, two CO_2 price levels are tested: €0.40/kg and €0.80/kg CO_2, compared to the standard assumed value of €0.108/kg CO_2.

At a CO_2 price of €0.40/kg, the tipping point occurs at the 3 MW heat pump configuration with medium-sized (MS) storage. From this point onward, the total system costs for the 3 MW system are lower than those of the 2.5 MW system. This is primarily due to the increased reliance on gas in the smaller system, which becomes more expensive as CO_2 prices rise.

For a higher CO_2 price of €0.80/kg, the tipping point shifts to the 3.5 MW configuration. This indicates that as carbon pricing becomes more stringent, systems with higher electrification and lower gas dependency become more cost-effective. In Figure 6.29, the resulting LCOH total costs curves clearly illustrate these tipping points, highlighting how the choice of system configuration is increasingly influenced by CO_2 pricing policy.

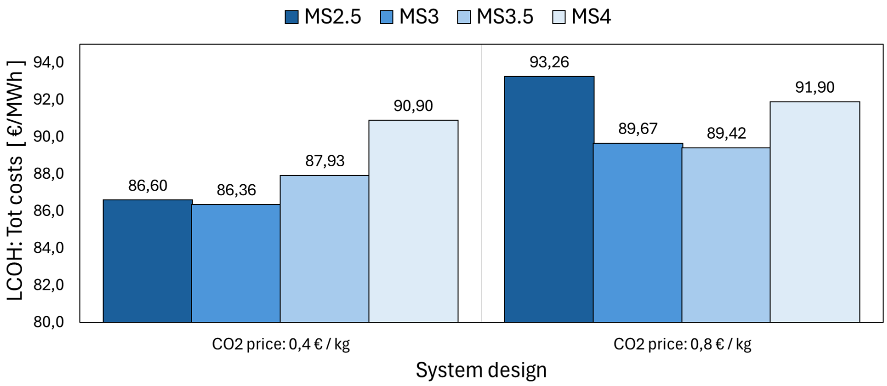

Figure 6.29: CO_2 comparison for different system designs

7 Discussion

Based on the simulation results, this chapter critically reflects on the findings by linking them back to the research questions and interpreting them in a broader technical and societal context. It also addresses model limitations and provides policy and academic reflections.

7.1. Interpretation of results

This section interprets the results of the experiments, focusing on key aspects such as heat production dynamics, electricity grid interactions, storage behavior, and cost implications. The findings provide insights into how different configurations of the district heating system respond to varying electricity price structures, grid limitations, and external conditions such as extreme weather events.

7.1.1. Fixed electricity price

SQ1: *How can a heating system be designed to optimize electricity usage and heat demand with a fixed electricity price?*

An important initial observation is the system's heat production hierarchy. The strict merit order demonstrates that the system dynamically responds to variations in heat demand, driven by outdoor temperature. The fixed price eliminates short-term fluctuations and is focused on following a certain production order. In this order, geothermal energy is prioritized as the base load due to its low marginal cost. HT-ATES is utilized during peak loads, followed by the heat pump if capacity is available, while the gas boiler functions as a last-resort backup. This static operational structure helps minimize costs but inherently limits system flexibility. Another observation is the underutilization of HT-ATES during average weather years. This prompts a critical question: is the storage system over-dimensioned for typical conditions, or is its potential simply underexploited due to a lack of dynamic charging incentives? The fixed electricity price structure provides no economic signal to charge storage when electricity is cheap or to discharge it when it is expensive. As a result, HT-ATES operates more as a passive seasonal buffer rather than as an active balancing tool. This suggests that, while HT-ATES adds resilience to the system, it is not exploited to its full potential without the right incentives.

The results show that the size of the heat pump plays a crucial role in the resilience of the system. When the heat pump increases in size, utilization decreases, which has a positive effect on the CO_2 emission and variable costs. This highlights a fundamental design trade-off: a smaller heat pump minimizes total costs but increases dependency on gas during peak demand. Conversely, a larger heat pump ensures greater robustness, but the risks of underutilization for most of the year make the investment economically less attractive. If the goal is to minimize reliance on gas, the system would require a larger heat pump, even if it remains underutilized in normal conditions. However, this increases capital costs, potentially leading to over investment in electrification when a backup gas boiler could provide the same flexibility at a lower cost. Thus, the decision to size a heat pump must balance capital expenditure, variable costs, and CO_2 emissions.

7.1.2. Dynamic electricity price

SQ2: What is the impact of electricity prices in real time on the optimal heating system design?

The introduction of dynamic electricity pricing fundamentally reshapes the operation of the district heating network, demonstrating both opportunities and challenges. The results indicate that real-time pricing increases system flexibility. A notable outcome of this experiment is the increase in heat pump utilization. During dynamic pricing scenarios, the heat pump shifts from primarily a geothermal heat booster to a more active heat supplier to the district heating network. The results also show that HT-ATES utilization increases with dynamic pricing, where it actively follows the market conditions. This behavior increases the economic value of thermal storage and strengthens the coupling between the electricity and heating systems. The storage acts as a buffer, enabling load shifting and reducing reliance on fossil fuels during peak heat demand.

A key consequence of dynamic pricing is an increase in total electricity consumption, with a 1.5% rise in electricity use. This increase is primarily due to the greater role of the heat pump, which takes advantage of low electricity prices which replaces a part of the geothermal energy. The results show that electricity usage is higher during summer, with frequent on/off cycling according to price signals. The higher electricity peaks could put additional strain on the electricity grid which causes grid congestion.

Configuration for Delft

Applying these results to the Delft case, a balanced trade-off must be made between investment costs, operational expenses, and sustainability performance. Among the configurations analyzed, the MS3.5 configuration is presented as the most well-rounded option. It achieves substantial CO_2 emission reduction, approximately 60% lower than the MS3 configuration while maintaining moderate capital and fixed operational costs. Although larger systems (MS4 and MS5) further decrease variable operational expenses and emissions, these improvements are marginal compared to the higher capital investments required. The MS3.5 configuration thus provides a strong balance: it is large enough to offer operational flexibility and robustness during extreme weather events, yet small enough to remain economically feasible.

Although dynamic electricity pricing improves operational flexibility but does not significantly reduce overall system costs. This is primarily due to the dominance of CAPEX and fixed OPEX, which account for approximately 85% of the annual costs. Therefore, while dynamic pricing reduces variable OPEX, it alone does not provide a sufficient economic rationale for major infrastructure investments. Incorporating system improvements that ensure future-proof systems could strengthen the case. This highlights the ongoing trade-off between economic feasibility and environmental sustainability. Moving toward a low-carbon system requires substantial investment in heat pumps and storage, whereas a more cost-effective approach continues to rely more on fossil fuel-based backup systems.

Additional experiments adjusting geothermal injection temperatures demonstrate that increasing the injection temperature (35°C or 45°C instead of 18°C) significantly improves system performance. By reducing the cooling requirement of the geothermal source, the COP of the heat pump increases. This causes a reduction in electricity consumption for the heat pump and a decreasing variable OPEX. As a consequence of higher injection temperature there is a reduction in geothermal output capacity.l This limitation occurs only during peak demand periods and can be effectively compensated by the heat pump without increasing gas usage. Simulations confirm that even with reduced geothermal contribution, total emissions do not rise, as the heat pump is able to absorb the additional load efficiently.

These results suggest that higher injection temperatures can lead to more cost-effective and energy-efficient systems without compromising robustness or sustainability. Nevertheless, the majority of simulations in this thesis were conducted with lower injection temperatures, and thus most conclusions are based on these configurations. However, the findings from the geothermal design experiments present a compelling direction for future system design improvements.

Broader implications

One of the clearest indications of system synergy is the improved utilization and economic performance of the HT-ATES system in dynamic electricity pricing. Compared to the fixed electricity price scenario, the value of thermal storage increases significantly when the system can respond to real-time market signals. HT-ATES is able to charge strategically during periods of low electricity prices, which often coincide with high renewable electricity generation. This reduces reliance on fossil backup during peak demand periods. The simulation results show that the variable OPEX associated with HT-ATES can decrease by up to 30% under dynamic pricing compared to fixed pricing, making storage more economically attractive and shortening its payback period.

The trade-offs between robustness, cost-efficiency, and carbon performance become more apparent during dynamic pricing. Smaller-sized systems may be cost-effective in mild weather scenarios, but during extreme weather years the performance declines significantly. These systems lack the flexibility to meet peak demand efficiently and become heavily reliant on gas, leading to increased CO_2 emissions and higher operational costs. In contrast, larger systems demonstrate greater resilience and have consistently lower emissions, which partly justify their higher capital investments. This reveals a clear and critical trade-off: achieving low emissions and high resilience comes at the expense of higher upfront costs.

These findings highlight the complex relationship between electricity market dynamics, system design choices, and long-term sustainability objectives. This emphasizes the need for integrated policy and investment strategies. The optimal system is not necessarily the one with the lowest operational cost or highest short-term efficiency, but the one that best balances long-term robustness, emissions reduction, and investment viability. To best realize the benefits of dynamic pricing, supportive policy instruments such as carbon pricing, capacity-based incentives, or network tariff structures may be necessary. These mechanisms can help bridge the gap between economic and environmental performance. Policymakers and planners must decide whether to prioritize short-term cost savings or long-term sustainability, as these objectives do not always align in current system configurations.

7.1.3. Grid constraints

SQ3 How do network capacity constraints on the electricity grid affect the optimal layout of the heating system?

The results demonstrate that electricity grid limitations significantly affect the performance, cost effectiveness, and sustainability of electrified district heating systems. Specifically, constrained grid capacity reduces the operational flexibility of heat pumps, leading to higher operational costs and increased CO_2 emissions. These findings highlight important considerations for the design of heating systems in areas facing grid congestion or limited connection capacity.

This impact is especially pronounced in configurations with smaller heat pumps. Since these systems already operate close to their maximum capacity, any limitation in electricity availability more frequently leads to curtailment of electricity-based technologies. However, these smaller systems also require less connection capacity, thereby reducing the overall likelihood of encountering grid congestion. If constraints occur, the system is forced to rely more heavily on gas, which increases both emissions and operational costs. Larger heat pump configurations demonstrate better resilience to grid limitations. Their higher installed capacity enables better adaptation by shifting production over time or utilizing HT-ATES for buffering. As a result, these systems experience smaller reductions in electricity use and are less dependent on fossil fuels. This illustrates that larger heat pump systems offer increased robustness in constrained grid conditions.

HT-ATES as a congestion mitigation strategy
An effective tool to mitigate the effects of grid constraints is an HT-ATES. The simulation results show that in the P0.6 scenario, a configuration equipped with HT-ATES uses 4.2% more electricity compared to a system without storage, resulting in a gas reduction from 11% to 6%. From a financial perspective, the difference in total system costs between storage and no-storage systems without grid limitations is €64,000. This already highlights the added value of storage. In the P0.6 constrained scenario, the total system costs further decrease to €140,000 lower, demonstrating the enhanced financial benefit of storage during grid stress. The HT-ATES system compensates for limited electricity availability by supplying heat during restricted periods, thereby reducing reliance on gas.

The financial analysis further shows that the impact of grid constraints on variable operational costs is more severe for smaller heat pump systems. These systems are less flexible and more susceptible to electricity supply disruptions, which negatively affects both their economic performance and emissions. Although total system costs increase only modestly, the cost-effectiveness of less robust systems is disproportionately reduced during constraints. Storage enables more flexible operation by decoupling heat production from demand. Larger heat pumps and integrated thermal storage amplify this benefit, allowing systems to shift electricity consumption to off-peak hours or take advantage of low-cost electricity when available. Without these measures, the system is forced to revert to gas, compromising decarbonization objectives.

System design, policy implications
The findings have important implications for both system design and policy development. First, they emphasize that the electrification of heating systems must go hand-in-hand with sufficient grid capacity. Without adequate electricity infrastructure, the operational potential of heat pumps cannot be realized and leading to increased reliance on gas-based alternatives. This undermines both economic and environmental goals. Increasing the size of the heat pump improves the robustness and reduces variable costs under grid constraints, it also raises fixed costs. Therefore, the optimal system layout requires a careful balance. Oversizing causes underutilization and inefficiency, while undersizing compromises resilience and increases dependency on gas. Proper heat pump sizing is crucial to ensure compatibility with electricity grid limitations while retaining enough flexibility to respond to market price signals.

Grid expansion and reinforcement must be prioritized in regions aiming for widespread electrification of district heating. Policymakers should align infrastructure investments with heating system rollouts, ensuring that sufficient grid capacity is available to support future electricity loads. At the same time, complementary strategies such as demand-side response programs, local energy storage integration, and peak shaving incentives should be supported to enhance flexibility during transitional phases.Future-ready heating systems must account not only for thermal demand but also for the constraints and opportunities of the electricity system. Only through coordinated co-optimization of heat and electricity infrastructure can the full benefits of multi-energy systems be realized.

7.1.4. Grid reinforcements

SQ 4: How do economic incentives need to be designed to influence the heating system for optimal performance?

Grid reinforcement costs represent a societal investment, these are not just costs by individual system owners but reflect broader infrastructure requirements needed to accommodate high electricity demand technologies. The results show that when the utilization of heat pumps is low, which occurs in large heat pump configurations, grid reinforcement are economically not justified. In these cases, the heat pumps are underused, therefore the additional investment cannot be recovered through operational savings. The benefits of more grid capacity become economically justifiable for most configurations, except for the 5 MW heat pump. In extreme weather conditions, heat pump utilization increases, meaning that the benefits of grid reinforcement become more pronounced. This is particularly evident in smaller heat pump configurations, where reinforcement unlock the full value of the heat pump. This highlights that the economic value of grid expansion is closely linked to both system stress levels and operational flexibility. Specifically, grid reinforcement is clearly worthwhile for the 3 MW, 3.5 MW, and 4 MW systems.

Tariffs
Network tariffs are designed to send the economic signal for electricity grid usage. However, the simulation results raise questions about their current effectiveness. In the peak tariff experiments, minor shifts in behavior were observed. The system continued to operate the heat pump during peak hours when it was necessary to increase geothermal power, indicating that operational necessity overrides price signals. Tariffs triggered at a 2 MW threshold led to small reductions in electricity use but increase system costs as well. Similarly, applying general network tariffs resulted in a rise in variable operational costs, yet the system's heat production behavior changed only marginally.

These findings suggest that these network tariffs are not designed to accurately reflect true grid scarcity or to provide strong enough incentives for system-wide optimization. Their static structure, which lacks alignment with real-time congestion or capacity planning, limits their effectiveness in guiding investment decisions or encouraging load shifting. To better support optimal system behavior, tariffs should be more closely aligned with actual local grid congestion patterns, reflect time-varying capacity constraints, and incentivize flexible system operation where it provides broader societal benefits.

System integration

This analysis presents a critical strategic dilemma for heat system developers: should they invest today in local flexibility to overcome short-term grid constraints, or wait until grid capacity expansions materialize? When grid congestion is introduced, the added value of storage becomes more pronounced compared to a system without. However, this benefit is time-sensitive. If grid reinforcements are realized within 5–10 years, the economic value of storage investments diminishes over time.

Thus, the business case for flexibility investments depends on the expected duration and severity of congestion at a specific location. It becomes a question of weighing the upfront capital costs of installing storage or larger heat pumps against the potential operational savings that can be achieved during periods of restricted grid access. Importantly, the simulations demonstrate that storage adds value even in large heat pump configurations; therefore, the operational savings achieved do outweigh the additional investment costs across a wide range of conditions.

In scenarios where no additional grid capacity is available, developers can consider increasing thermal storage to enable load shifting: charging during unconstrained periods (at night or during weekends) and discharging during peak hours. Alternatively, hybrid systems that combine electrification with seasonal gas backup for covering peak loads may be implemented. These approaches enable continued system operation during constraints while minimizing gas dependency, which is key to meeting district heating sustainability targets.The effectiveness of these strategies ultimately hinges on a coordinated design approach that matches electricity availability, thermal demand profiles, and system flexibility. Without this alignment, even well-intentioned flexibility investments could underperform.

From a broader perspective, economic incentives should be designed to reflect the system-wide benefits of flexibility, not just the gains within the heating sector itself. Avoiding grid congestion and improving operational efficiency provide value at the societal level. Assessing the necessity of local grid reinforcements should therefore be done on a case-by-case basis, ensuring that public investment is matched with systemic need. In essence, storage functions as a dynamic buffer that protects the grid from additional strain and reduces fallback to gas during critical hours. The HT-ATES not only lowers the frequency and severity of constrained periods, but also expands the amount of energy that can be delivered within existing grid limits. Although, it must be acknowledged that any electric heating system with a large heat pump inherently increases base electricity demand, coupling it with thermal storage significantly improves its grid compatibility and system flexibility. This integrated approach offers a pathway to sustainable, robust, and cost-effective district heating in the face of growing electrification and intermittent renewable energy supply.

7.2. Recommendations for policy-makers and project developers

Based on the results of this study, several policy recommendations can be made for the effective implementation of a district heating network integrated with the electricity system. These recommendations focus on improving system flexibility, ensuring long-term resilience, and creating the necessary economic and regulatory conditions to maintain an operating electricity network.

A central recommendation is the need for policies that support flexible energy production within district heating networks. Simulation results consistently demonstrate that thermal energy storage plays a central role in reducing operational costs, limiting peak electricity demand, and lowering CO_2 emissions. Given these system-wide benefits, policymakers should actively support the deployment of storage through direct subsidies or favorable financing mechanisms. Another approach is to further tighten the emission limit for district heating networks, which would incentivize greater integration of sustainable energy sources. Thermal storage can play a key role in meeting stricter decarbonization targets. Storage systems should therefore be formally recognized as essential infrastructure for resilient, electrified heat networks. Flexible operation should be financially rewarded when it demonstrably reduces pressure on the electricity grid and enhances overall system sustainability.

The electrification choices of heating developers are based on thermal demand which imposes a significant load on local grids. This can be without synchronized investment planning from DSOs or TSOs. This lack of coordination can lead to mismatches, congestion risks, or costly delays in grid reinforcement. To resolve this, formalized coordination mechanisms must be established. Regional energy strategies (RES) should include integrated planning tables in which municipalities, grid operators, and heating developers co-design system layouts and timelines. Connection decisions for heat networks should be conditional on the availability of grid capacity or the inclusion of compensatory flexibility measures. Policymakers should institutionalize early coordination and shared infrastructure forecasting. Long-term planning strategies should be encouraged to ensure that infrastructure investments made today remain viable under future market conditions.

The trade-off between short-term flexibility and long-term infrastructure reinforcement was highlighted in the results. Grid reinforcements are essential in areas with persistent congestion. However, storage can provide a cost-effective alternative or interim solution in areas awaiting reinforcement. Policymakers should support a phased investment strategy. In the short term, modular and scalable storage solutions should be encouraged to bridge capacity shortages. In parallel, national and regional governments must accelerate investment in electric grid expansion, with a focus on heat-dense urban areas where electrification will add substantial load. At the same time, investment schemes like SDE++ and infrastructural subsidies should be adapted to reflect these dual needs. Systems that combine moderate heat pump sizing with flexible storage should be prioritized for funding, especially in regions identified as congestion hotspots.

Finally, while this study focuses primarily on optimizing the supply side of the district heating system, it is essential to recognize that reducing heat demand at the consumer level can substantially enhance overall system efficiency and affordability. Policymakers should therefore promote building insulation and energy efficiency incentives to help lower heating demand. Improved insulation reduces overall heating requirements, making low-temperature district heating systems more viable and cost-effective. In such cases, the need for additional heat pump boosting capacity may be eliminated altogether. Future policies should prioritize incentives for energy-efficient construction and renovation and introduce stricter minimum energy performance standards for both new and existing buildings.

7.3. limitations

This section critically evaluates the methodological limitations of this study, addressing potential areas of uncertainty that may have influenced the results. Model assumptions, scenario design, and technical constraints all introduce inherent simplifications that, while necessary for computational feasibility, may impact the real-world applicability of the findings. By identifying these limitations, this section provides context for interpreting the results and offers guidance for future research improvements.

7.3.1. model setup

The district heating system model used in this research is based on a simplified representation of real-world heating dynamics, making certain assumptions that may not fully capture the complex interactions between geothermal heat, heat pumps, and storage systems.

One limitation is that the model assumes that geothermal heat must always pass through the heat pump when the required supply temperature is higher than the well's output. In extreme cold conditions, this setup limits the system's ability to fully use the geothermal capacity. The heat pump can reach its maximum capacity and prevent additional heat extraction from the well. In practice, an alternative approach could assume that the geothermal well always operates at full output, with a gas boiler supplementing the remaining heat requirement. This would reflect a more realistic operational strategy, where the heat pump is not the sole means of increasing the temperature. The impact of this assumption on overall efficiency is uncertain. In both cases, some gas use remains necessary, but differences in system efficiency and fuel dependence require further analysis to determine whether an alternative configuration would yield better results.

The second limitation is that the model operates with perfect foresight, meaning it anticipates future demand and therefore optimizes the storage dispatch accordingly its foresight. In real-world conditions, storage management is reactive rather than predictive, leading to greater reliance on backup heating sources during unforeseen demand spikes. This means that in practical applications, storage utilization could be lower than what the model predicts.Consequently, the model may overestimate the effectiveness of HT-ATES in real-world applications, particularly in handling extreme weather events. In real, these peaks are largely unpredictable and therefore perfect storage deployment is not realistic. A more realistic approach would involve uncertainty modeling or stochastic optimization, where storage dispatch is adjusted based on real-time conditions rather than perfect foresight or with a certain reserve at a certain moment in the year. Similarly, electricity prices are also fully anticipated in the model. This makes it harder to always utilize the lowest-cost electricity optimally.

The model assumes that HT-ATES directly supplies heat to the district heating network. However, in practice, stored heat is often used to preheat return flows rather than to supply heat directly to the main network. This simplification may not fully reflect real-world operational efficiency and could lead to slightly different system behavior in terms of dispatch priorities and storage cycling patterns. A more refined model could integrate a return-flow heating approach, improving alignment with actual district heating practices.

The model assumes some simplified heat transfer modeling, where a constant COP's for the ESP's is taken. In reality, the COP are based on certain pressure value and injection rates. Although these variations are relatively small and the model assumptions remain valid for system-level analysis, incorporating dynamic COP values could improve accuracy in operating conditions.

7.3.2. Scenarios

The model assumes a fixed average emissions factor for electricity consumption, regardless of the hourly variations in the grid mix. In reality, electricity emissions fluctuate significantly: emissions are lower during periods of high renewable energy generation and higher when fossil-based generation dominates. CO_2 emissions are not directly tied to electricity prices, but certain price levels often reflect the marginal generation technologies in use. When electricity prices are low, it typically indicates a surplus of renewable energy. Conversely, high electricity prices resulting in high emissions. Without incorporating real-time emissions modeling, the model may overestimate CO_2 emissions during low-price periods and underestimate emissions during peak-price periods. Consequently, it does not represent the right emission reduction potential of the storage systems. Storage systems allow electricity consumption to be shifted toward periods of low emissions, but this advantage is not fully captured when using a static emissions factor.

In addition, the model does not account for the occurrence of negative electricity prices, which arise occasionally in real-world energy markets during periods of renewable electricity oversupply. Excluding negative prices may limit the model's ability to fully evaluate the potential benefits of dynamic electricity pricing. In real applications, negative pricing periods could create strong incentives for flexible load and storage operation, further enhancing system efficiency and sustainability.

7.4. Academic reflection

7.4.1. Societal implications

The process by which this research was developed began with the question: Are there synergies between a heating system and the electricity system, and what are they? Guided by my academic and professional supervisors, I developed a model simulating the structure of a district heating network, progressively incorporating the dynamics of the electricity market.

This thesis contributes to the growing body of literature on integrated energy systems, specifically focusing on district heating-electricity grid interaction. By analyzing operational, economic, and environmental trade-offs across multiple system configurations, the findings offer valuable insights for policymakers, industry stakeholders, and energy planners. In particular, this study contributes to a deeper understanding of the complex trade-offs involved in the electrification of the heating system. While investment costs dominate the total system expenditure, system configuration plays a defining role in emissions performance, grid interaction, and overall flexibility. In doing so, this thesis helps shift public and policy discussions toward recognizing the broader role of heating networks within future energy systems. It demonstrates that technologies like HT-ATES can significantly support a more sustainable energy system, particularly by enabling lower electricity demand while enhancing system resilience. This research fits within the larger conversation about energy system integration, infrastructure planning, and climate policy alignment.

From a societal perspective, this study adds value in several areas. First, it provides insight into how heating and electricity systems interact and identifies integration opportunities that enhance efficiency and sustainability. The analysis of CO_2emissions across different scenarios shows that system design can directly impact national climate performance. For the public sector and municipal energy planners, this research can support decision-making on heating system design, investment timing, and infrastructure planning.

One of the key contributions of this research is its holistic approach to analyzing both above-ground district heating infrastructure and underground heat storage and geothermal systems. In contrast, many studies focus on either heat production technologies or underground storage performance. This study demonstrates that both aspects must be considered together, as the performance of underground resources directly influences the broader energy system.

It is important to note that this research remains case-specific. The Delft case has been extensively analyzed, but the generalization of the conclusions to other contexts remains uncertain. Smaller towns or regions with different characteristics may require different system designs. In particular, cost parameters used here are derived from generalized sources and are not specifically tailored to Delft. As a result, while the cost-related KPIs offer useful reference points for comparative purposes, they should not be interpreted as exact predictions for real-world project outcomes.

For EBN, this thesis has provided concrete insights into the synergies between heat pumps, storage systems, and the electricity grid. It addresses strategic questions such as: Under which conditions do heat pumps provide the most value? When does grid reinforcement become economically viable? What are the trade-offs between minimizing total system cost and reducing emissions? It also raises broader questions, such as whether heating systems should be more explicitly designed with electricity system interactions in mind. More broadly, the project demonstrated the necessity of integrated, cross-sectoral thinking. For an organization like EBN, which operates across multiple energy domains, this research offers a valuable lens for evaluating not only individual technologies but also their contribution to overall system performance and resilience.

7.4.2. Suggestions for further research

While this study provides valuable insights into the integration and optimization of district heating networks within electricity systems, several areas remain either unexplored or simplified. Further research could enhance the real-world implication, scalability, and policy/regulation relevance of future modeling efforts.

One key area for further exploration is detailed electricity grid modeling. In this study, the electricity grid was represented in a simplified form to keep the focus on the heating system. However, a more detailed representation of electricity transmission, distribution, and network congestion would provide a more accurate picture of how heat pumps interact with electricity systems. This is particularly relevant in future scenarios with high renewable penetration, where grid bottlenecks could affect both electricity prices and the feasibility of large-scale heat pump deployment.Future models should also incorporate negative electricity prices, which are increasingly common during periods of excess renewable generation and can significantly impact system optimization strategies.

Beyond technical improvements, future studies should also assess the impact of policy and market mechanisms on district heating system investment and operations. Different carbon pricing levels, renewable energy incentives, and regulatory mandates shape the economic feasibility of electrified heating systems. Investigating how alternative policy scenarios influence heating system design choices would provide valuable insights for decision-makers. In addition, comparing market-based approaches with centralized control strategies would help identify the most effective governance models for future district heating networks.

Another important area for future research concerns the interaction between demand-side flexibility and thermal storage. Consumer behavior and the adoption of smart control technologies can significantly influence the responsiveness of heating systems to dynamic electricity prices. Research into how demand-side management could be integrated into heating system design could further enhance operational flexibility and system efficiency.

This study is based on the Delft case and is case-specific. Future studies should explore comparative modeling across multiple regions for example, comparing urban, semi-urban, and rural heating systems to test the scalability and transferability of the findings. Furthermore, extending the model to integrate cross-sector interactions (with mobility, industry, cooling) could reveal broader system-level trade-offs and synergies, aligning more closely with future energy system integration goals.

8 Conclusion

In the transition to a low-carbon energy system, district heating systems must evolve to become more sustainable, flexible, and integrated with the electricity grid. This thesis explored how such integration can be designed to minimize operational costs while improving system performance, with a particular focus on the case of Delft.

The central research question guiding this work was: ***What are the potential synergies of integrating and optimizing a heating system with an electricity system to minimize operational costs and improve system performance?***

The findings confirm that coupling heat production with the electricity system, particularly through the integration of heat pumps and thermal storage, can improve system efficiency and resilience. However, the full benefits of integration depend on smart system design, supportive market conditions, and coordinated infrastructure development.

Design layout for Delft
The analysis of the Delft case study reveals that the optimal heating system depends on the chosen trade-off between cost-efficiency and sustainability. The MS3 configuration emerges as the most economical offering the lowest total costs due to the smallest capital expenditures. However, this system remains highly dependent on gas during high-demand periods, resulting in significantly higher CO_2 emissions. From a long-term sustainability perspective, this makes it a less attractive option. A more balanced solution is offered by the MS3.5 configuration. It offers considerably lower emissions, while keeping investment and operating costs within a reasonable range. Larger systems such as MS4 and MS5 further reduce emissions and variable costs but at a disproportionately higher investment cost, making them less economically viable for a case like Delft. Moreover, the impact of variable operational costs remains relatively limited across all systems, as variable expenditures account for approximately 15% of total system costs. In contrast, capital expenditure and fixed operational expenses dominate the cost structure.

The added value of operational flexibility becomes particularly evident in grid congestion scenarios. HT-ATES not only reduces variable operational costs but also mitigates emissions by enabling the system to shift electricity demand to off-peak periods. Especially during times of limited grid capacity, HT-ATES can help reduce fallback to gas. This is done by storing energy during low-demand, low-price windows and dispatching it when electricity supply is limited.

Moreover, the simulations show that as the size of the heat pump increases, the effect of the grid constraint becomes smaller. Larger heat pumps offer greater operational flexibility, making the system more robust against electricity supply limitations. In this context, the integration of thermal storage significantly enhances the system's performance and supports both grid stability and sustainability goals. Based on these findings, the MS3.5 system configuration integrated with HT-ATES represents the optimal balance between robustness, emissions performance, and long-term economic viability for the Delft district heating system.

The role and influence of network tariffs
The network tariffs used in the experiments have limited ability to influence operational behavior. For network tariffs to effectively support the integration of heating and electricity sectors, they must better reflect real-time grid congestion levels and local capacity limitations. This raises a broader strategic trade-off between short and long-term investment strategies. In the short term,tariffs could be introduced to encourage demand shifting and to incentivize investments in flexibility measures which help reduce grid stress. In the long term, grid reinforcements will still be essential to accommodate the increasing load from electrified heating systems and to ensure sufficient capacity for future demand growth. Static tariffs alone cannot substitute for physical grid upgrades. Instead, an effective combination of smarter, dynamic pricing mechanisms alongside targeted infrastructure investments is necessary to build a resilient and sustainable heating system.

Limitations
The model used in this study is based on several simplifications that influence its real-world applicability. It assumes perfect foresight in both heat demand and electricity pricing, which may lead to an overestimation of HT-ATES utilization. Furthermore, the model applies constant electricity emission factors across all scenarios. In reality, electricity sector emissions fluctuate depending on the marginal generation technology operating at any given time. By not linking emissions to electricity price variations or the actual grid mix, the model may underestimate the environmental benefits of flexible system operations. Additionally, the exclusion of negative electricity prices limits the model's ability to fully capture the opportunities offered by surplus renewable energy in future electricity systems.

General conclusions and broader lessons
This thesis provides several broader takeaways for the design of integrated heating systems:

- This research confirms that integrating a district heating system with the electricity network can significantly enhance system flexibility, reduce fossil fuel reliance, and improve long-term sustainability. However, the high share of fixed expenditures (CAPEX and fixed OPEX) limits the impact that operational savings from optimized electricity use can have on total system costs.
- Larger heat pumps improve system resilience and sustainability. However, they entail higher CAPEX and the risk of underutilization becomes larger. Their economic and operational effectiveness improves substantially when combined with thermal storage systems.
- One of the most important synergies lies in the strategic role of thermal storage. HT-ATES becomes an valuable economic asset when integrated into a system with dynamic electricity pricing. It enables the use of low-cost electricity in off-peak periods and stores it for use during high-demand moments. In doing so, it increases the value of both geothermal heat and power-to-heat applications.
- The electricity sector also stands to gain from this integration. Heating systems equipped with thermal storage act as controllable, long-duration energy consumers. They can absorb surplus renewable energy during periods of overproduction and shift their consumption away from peak demand hours, contributing to grid stability. As a result, power-to-heat technologies become dispatchable loads that reduce the need for additional grid-scale electrical storage investment
- The trade-off between cost-efficiency and CO_2 reduction is unavoidable. Smaller system configurations offer lower capital costs but result in higher emissions due to greater gas reliance. In contrast, larger systems deliver lower emissions but require higher upfront investments. Smart sizing strategies and the incorporation of flexibility measures are essential for navigating this tension and achieving both economic and environmental objectives.

Recommendations for policymakers and developers
To unlock the full potential of integrated heating systems, the following recommendations are proposed:

- Incentivize storage and flexible system design: Treat storage as critical infrastructure. Support it with investment subsidies or operational incentives.
- Coordinate early between grid and heat developers: Integrated planning is essential to avoid costly mismatches. Connection approvals should depend on grid capacity or compensatory flexibility.

- Support near-term flexibility while preparing for long-term grid expansion: Storage provides an immediate bridge to electrification. It should be prioritized in areas facing grid congestion
- Integrate more smart system designs by implementing more supportive market conditions. Market mechanisms should value systems that reduce emissions, minimize peak demand, and support grid stability.

This thesis illustrates that system integration offers meaningful opportunities to improve the flexibility, sustainability, and efficiency of future heating networks. While HT-ATES has proven to be a highly valuable asset in this case, it is not the only solution. The broader lesson is that flexibility whether through storage, smart controls, or hybrid designs will be critical for building resilient energy systems. Achieving optimal system performance will require not only technical innovation, but also coordinated planning, supportive policies, and context-specific design choices.

9 Personal reflection

Before starting my thesis project, I had very little knowledge about district heating systems or heating networks. I was eager to learn more about these things, and I became interested in the various technologies and technical matters related to heating systems. Choosing the right modeling method was one of the most difficult parts of the process. Through trial and error, I eventually found an approach that worked for me. The literature and internet research provide many different ways to model energy systems, and I experimented with various tools. Some tools initially appeared to be reliable methods but ultimately proved unsuitable for this specific project. In retrospect, I realize that I should have consulted more on this step sooner, especially on the relative strengths and weaknesses of different modeling frameworks. Although I am comfortable working in Python, I am not yet an expert who can immediately determine which tool is best for what use.

Despite these challenges, I enjoyed building the model and gradually making it more complex and realistic. The time went really quick during the process of programming, and I found genuine satisfaction in constructing a working system step by step. Being in a company environment also helped, where there were always people at the office, and this made the overall experience more pleasant and motivating. At times, the modeling process could be frustrating, especially when debugging errors that weren't directly related to the actual logic of the code but instead came from mismatches or small mistakes in data handling. For example, I only discovered later in the process that the electricity prices were not correctly matched with the appropriate weather years. This error stemmed from a mistake in the Excel file I was using and ended up taking significant time to fix something that could have been avoided by more thoroughly checking data earlier on.

Another area where I struggled was in the design of my experiments. Throughout the project, I used different naming conventions for simulations, which became quite messy. It would have been much better to define a clear and consistent experiment ID system from the start. That would have helped me keep better track of simulations and allowed for a more organized and efficient workflow. I also found the process of simulating system behavior across different designs really interesting, but I sometimes conducted too many experiments, some of which turned out to be unnecessary. I've learned that it's valuable to clearly define your experimental scope early on and avoid adding new simulations unless they are clearly justified.

Starting the writing phase was also a personal challenge. I didn't maintain a consistent writing rhythm, and I often left parts as short drafts or rough outlines instead of fully finishing them. This meant that I had to revisit and rewrite large sections later in the process, which was time-consuming. In retrospect, I should have started the writing earlier and kept it more regularly updated alongside the modeling work. I also spent quite a lot of time improving smaller aspects of the model toward the end—time that probably would have been better spent writing and refining the report.

In the end, it was very satisfying to build a working model and to analyze the results. Although, some conclusions were not as impactful as I had initially hoped. For example, integration with the electricity grid did not significantly reduce overall system costs, but the process still provided valuable insights.

The results on grid reinforcement were particularly interesting and added value to the research topic. What this project showed me is the enormous complexity involved in designing heating systems. There are so many variables to consider, and this thesis only scratched the surface by focusing on the technical and production aspects. I did not explore regulatory or policy dimensions, which I realize are as well really important in real-world implementation.

Looking back, I am proud of what I have accomplished. I gained valuable experience in modeling complex systems, structuring experiments, and working within a company environment. I have developed a deeper understanding of district heating systems and their integration into the broader energy system. The results contribute meaningful insights to the ongoing dialogue about sustainable heating solutions and grid integration. Overall, this thesis has been an enriching period of my student time. I leave the project with a lot of enthusiasm for the challenges that lie ahead in my professional career.

References

[1] Hans van 't Spijker et al. *Definition of Electrosubmersible pump (ESP) design and selection workflow*. Tech. rep. June 2016. URL: https://geothermie.nl/images/Onderzoeken-en-rapporten/01_07_16_Definitie_ESP/20031_Definition_of_ESP_design-_final_version_20160919-public.pdf.

[2] Jos van 't Westende, Dorien Dinkelman, and TNO. *Feasibility study for combined geothermal and HT-ATES systems*. Tech. rep. 2023. URL: https://www.warmingup.info/documenten/feasibility-study-for-combined-geothermal-and-ht-ates-systems.pdf.

[3] International Energy Agency. *Power systems in transition*. 2020. URL: https://iea.blob.core.windows.net/assets/cd69028a-da78-4b47-b1bf-7520cdb20d70/Power_systems_in_transition.pdf.

[4] Pete Aston. *What is a Cost Apportionment Factor?* July 2023. URL: https://roadnighttaylor.co.uk/connectology/what-is-cost-apportionment-factor/.

[5] Getnet Tadesse Ayele et al. "Optimal heat and electric power flows in the presence of intermittent renewable source, heat storage and variable grid electricity tariff". In: *Energy Conversion and Management* 243 (June 2021), p. 114430. DOI: 10.1016/j.enconman.2021.114430. URL: https://doi.org/10.1016/j.enconman.2021.114430.

[6] Daniel Bakker and Els van der Roest. *Flexibele warmtesystemen en hun rol in het elektriciteitssysteem*. Tech. rep. June 2023. URL: https://api.kwrwater.nl//uploads/2023/12/KWR-2023.042-Flexibele-warmtesystemen-en-hun-rol-in-het-elektriciteitssysteem-(OPENBAAR).pdf.

[7] Stijn Beernink et al. "Heat losses in ATES systems: The impact of processes, storage geometry and temperature". In: *Geothermics* 117 (Dec. 2023), p. 102889. DOI: 10.1016/j.geothermics.2023.102889. URL: https://doi.org/10.1016/j.geothermics.2023.102889.

[8] M. Bloemendal et al. *HT-ATES at the TU Delft campus*. Tech. rep. Oct. 2020. URL: https://www.warmingup.info/documenten/window-fase-1---a1---verkenning-hto-tud---feasibility ht_ates_tudelft.pdf.

[9] Andreas Bloess, Wolf-Peter Schill, and Alexander Zerrahn. "Power-to-heat for renewable energy integration: A review of technologies, modeling approaches, and flexibility potentials". In: *Applied Energy* 212 (2018), pp. 1611–1626. ISSN: 0306-2619. DOI: https://doi.org/10.1016/j.apenergy.2017.12.073. URL: https://www.sciencedirect.com/science/article/pii/S0306261917317889.

[10] Maaike Braat et al. "Cost-Effective increase of Photovoltaic Electricity Feed-In on congested transmission lines: a case study of the Netherlands". In: *Energies* 14.10 (May 2021), p. 2868. DOI: 10.3390/en14102868. URL: https://doi.org/10.3390/en14102868.

[11] Gert Brunekreeft, Autoriteit Consument en Markt (ACM), and Constructor University Bremen. *Improving regulatory incentives for electricity grid reinforcement*. Tech. rep. June 2023. URL: https://www.acm.nl/system/files/documents/brunekreeft-acm-report-incentives-grid-reinforcement.pdf.

[12] Martina Capone, Elisa Guelpa, and Vittorio Verda. "Multi-objective optimization of district energy systems with demand response". In: *Energy* 227 (Mar. 2021), p. 120472. DOI: 10.1016/j.energy.2021.120472. URL: https://doi.org/10.1016/j.energy.2021.120472.

[13] Deniz Cetinkaya and Alexander Verbraeck. "MDD4MS: A model driven development framework for modeling and simulation". In: June 2011, pp. 113–121.

[14] Hongzhong Cheng et al. "Optimal planning of Multi-Energy system considering thermal storage capacity of heating network and heat load". In: *IEEE Access* 7 (Jan. 2019), pp. 13364–13372. DOI: 10.1109/access.2019.2893910. URL: https://doi.org/10.1109/access.2019.2893910.

[15] Alexandros Daniilidis et al. “Techno-economic assessment and operational CO2 emissions of High-Temperature Aquifer Thermal Energy Storage (HT-ATES) using demand-driven and subsurface-constrained dimensioning”. In: *Energy* 249 (Mar. 2022), p. 123682. DOI: 10.1016/j.energy.2022.123682. URL: https://doi.org/10.1016/j.energy.2022.123682.

[16] *Delft – PUSH-IT*. URL: https://www.push-it-thermalstorage.eu/pilots/delft/.

[17] Thibaut Desguers and Daniel Friedrich. “Design of a high-temperature, power-constrained electrified district heating network with thermal storage and curtailed wind integration”. In: *Sustainable Energy Technologies and Assessments* 67 (2024), p. 103815. ISSN: 2213-1388. DOI: https://doi.org/10.1016/j.seta.2024.103815. URL: https://www.sciencedirect.com/science/article/pii/S221313882400211X.

[18] Hester Dijkstra et al. *DUURZAAMHEID VAN GEOTHERMIE IN WARMTENETTEN*. Tech. rep. 2020. URL: https://www.installatie.nl/wp-content/uploads/2020/12/TNO-2020-duurzaamheid.pdf.

[19] Dorien Dinkelman and Frank Bergen. “Evaluation of the country-wide potential for High-Temperature Aquifer Thermal Energy Storage (HT-ATES) in the Netherlands”. In: Oct. 2022.

[20] Benno Drijver, Martijn Aarssen, and Bas Zwart. “High-temperature aquifer thermal energy storage (HT-ATES) - sustainable and multi-usable”. In: May 2012.

[21] Benno Drijver, Guido Bakema, and Peter Oerlemans. “State of the art of HT-ATES in The Netherlands”. In: Mar. 2019.

[22] EBN. *INFOGRAPHIC: Energie in Cijfers*. 2024. URL: https://www.ebn.nl/wp-content/uploads/2024/01/EBN-Infographic-2024.pdf.

[23] EBN. *Process diagram - Delft*.

[24] *Elektriciteitsnet Zuid-Holland bereikt maximale capaciteit voor grootverbruikers van elektriciteit*. URL: https://www.tennet.eu/nl/nieuws/elektriciteitsnet-zuid-holland-bereikt-maximale-capaciteit-voor-grootverbruikers-van.

[25] *Energy Transition model*. URL: https://energytransitionmodel.com/.

[26] Joshua M. Epstein. “Why Model?” In: *Journal of Artificial Societies and Social Simulation* 11.4 (2008), p. 12. ISSN: 1460-7425. URL: https://www.jasss.org/11/4/12.html.

[27] Paul Fleuchaus et al. “Risk analysis of High-Temperature Aquifer Thermal Energy Storage (HT-ATES)”. In: *Renewable and Sustainable Energy Reviews* 133 (2020), p. 110153. ISSN: 1364-0321. DOI: https://doi.org/10.1016/j.rser.2020.110153. URL: https://www.sciencedirect.com/science/article/pii/S1364032120304445.

[28] *Geothermie Delft*. URL: https://geothermiedelft.nl/.

[29] *Getting started — oemof.thermal documentation*. URL: https://oemof-thermal.readthedocs.io/en/latest/getting_started.html.

[30] Yuexuan Gong et al. “Research progress on the fifth-generation district heating system based on heat pump technology”. In: *Journal of Building Engineering* 71 (2023), p. 106533. ISSN: 2352-7102. DOI: https://doi.org/10.1016/j.jobe.2023.106533. URL: https://www.sciencedirect.com/science/article/pii/S235271022300712X.

[31] Warming UP GOO. *WARMINGUP WINDOW AFSLUITINGS- WARMINGUP GOO CONSORTIUMBIJEENKOMST*. URL: https://www.warmingup.info/documenten/presentatie-window-afsluitings--warmingup-goo-consortiumbijeenkomst-8-februari-2024_hto.pdf.

[32] L. Gustavsson et al. “Primary energy implications of end-use energy efficiency measures in district heated buildings”. In: *Energy and Buildings* 43.1 (2011), pp. 38–48. ISSN: 0378-7788. DOI: https://doi.org/10.1016/j.enbuild.2010.07.029. URL: https://www.sciencedirect.com/science/article/pii/S0378778810002598.

[33] Niels Hartog et al. *Duurzame warmte gaat ondergronds*. Tech. rep. 2017. URL: https://api.kwrwater.nl/uploads/2017/02/Duurzame-warmte-gaat-ondergronds.-Warmteopslag-heeft-meerwaarde-voor-warmtenetten-Hartog-Bloemendal-Slingerland-van-Wijk-KWR-Greenvis-(2016).pdf.

[34] Stefan Heldt, Christof Beyer, and Sebastian Bauer. "Uncertainty assessment of thermal recovery and subsurface temperature changes induced by high-temperature aquifer thermal energy storage (HT-ATES): A case study". In: *Geothermics* 122 (2024), p. 103086. ISSN: 0375-6505. DOI: https://doi.org/10.1016/j.geothermics.2024.103086. URL: https://www.sciencedirect.com/science/article/pii/S0375650524001755.

[35] S. Hilpert et al. "The Open Energy Modelling Framework (oemof) - A new approach to facilitate open science in energy system modelling". In: *Energy Strategy Reviews* 22 (July 2018), pp. 16–25. DOI: 10.1016/j.esr.2018.07.001. URL: https://doi.org/10.1016/j.esr.2018.07.001.

[36] Nico Hoogervorst and PBL Planbureau voor de Leefomgeving. *Toekomstbeeld klimaatneutrale warmtenetten in Nederland*. PBL Planbureau voor de Leefomgeving, 2017. URL: https://www.pbl.nl/sites/default/files/downloads/pbl-2017-toekomstbeeld-klimaatneutrale-warmtenetten-in-nederland-1926_1.pdf.

[37] IPCC. *IPCC, 2023: Climate Change 2023: Synthesis Report, Summary for Policymakers.* Tech. rep. July 2023, pp. 1–34. DOI: 10.59327/ipcc/ar6-9789291691647.001. URL: https://doi.org/10.59327/ipcc/ar6-9789291691647.001.

[38] Nima Javanshir et al. "Operation of district heat network in electricity and balancing markets with the power-to-heat sector coupling". In: *Energy* 266 (Dec. 2022), p. 126423. DOI: 10.1016/j.energy.2022.126423. URL: https://doi.org/10.1016/j.energy.2022.126423.

[39] R. Kleinlugtenbelt et al. *Haalbaarheid en uitwerking systeemconcept HTO TU Delft*. Tech. rep. 2023, pp. 1–66. URL: https://www.warmingup.info/documenten/haalbaarheid-en-uitwerking-systeemconcept-hto-tu-delft.pdf.

[40] Uwe Krien et al. "oemof.solph—A model generator for linear and mixed-integer linear optimisation of energy systems". In: *Software Impacts* 6 (Aug. 2020), p. 100028. DOI: 10.1016/j.simpa.2020.100028. URL: https://doi.org/10.1016/j.simpa.2020.100028.

[41] J.J. Laan. *Electricity grid congestion and application of a novel tariff in the Netherlands*. Tech. rep. Oct. 2023. URL: https://essay.utwente.nl/97435/1/Laan_MA_EEMCS.pdf.

[42] Sander Lensink et al. *Eindadvies basisbedragen SDE++ 2024*. Tech. rep. Jan. 2024.

[43] Wen LIU. "THE POTENTIAL OF HIGH-TEMPEATURE AQUIFER THERMAL ENERGY STORAGE (HT-ATES) TO ENHANCE THE TECHNO-ECONOMIC PERFORMACE OF DUTCH DISTRICT HEATING SYSTEMS". In: 2019, pp. 2–3. URL: http://www.energy-proceedings.org/wp-content/uploads/2020/02/887_Paper_0530113719.pdf.

[44] Wen Liu, Faye Best, and Wina Crijns-Graus. "Exploring the pathways towards a sustainable heating system – A case study of Utrecht in the Netherlands". In: *Journal of Cleaner Production* 280 (Nov. 2020), p. 125036. DOI: 10.1016/j.jclepro.2020.125036. URL: https://doi.org/10.1016/j.jclepro.2020.125036.

[45] Xuezhi Liu et al. "Combined analysis of electricity and heat networks". In: *Applied Energy* 162 (Mar. 2015), pp. 1238–1250. DOI: 10.1016/j.apenergy.2015.01.102. URL: https://doi.org/10.1016/j.apenergy.2015.01.102.

[46] Shuai Lu et al. "Dispatch of Integrated Energy Systems Considering Thermal Dynamics of Thermal Energy Storage". In: *IEEE* (Aug. 2020), pp. 1–5. DOI: 10.1109/pesgm41954.2020.9281951. URL: https://doi.org/10.1109/pesgm41954.2020.9281951.

[47] H. Lund et al. "The role of district heating in future renewable energy systems". In: *Energy* 35.3 (2010), pp. 1381–1390. ISSN: 0360-5442. DOI: https://doi.org/10.1016/j.energy.2009.11.023. URL: https://www.sciencedirect.com/science/article/pii/S036054420900512X.

[48] Henrik Lund et al. "4th Generation District Heating (4GDH)". In: *Energy* 68 (Mar. 2014), pp. 1–11. DOI: 10.1016/j.energy.2014.02.089. URL: https://doi.org/10.1016/j.energy.2014.02.089.

[49] Nicolas Marx et al. "Risk assessment in district heating: Evaluating the economic risks of interregional heat transfer networks with regards to uncertainties of energy prices and waste heat availability using Monte Carlo simulations". In: *Smart Energy* 12 (Sept. 2023), p. 100119. DOI: 10.1016/j.segy.2023.100119. URL: https://doi.org/10.1016/j.segy.2023.100119.

[50] Folckert van der Molen et al. *Overzicht Transitievisies Warmte: Signalen, obstakels potentieel*. Tech. rep. 2023. URL: https://www.pbl.nl/uploads/default/downloads/pbl-2023-overzicht-transitievisies-warmte-signalen-obstakels-potentieel_5051.pdf.

[51] *oemof community*. URL: https://github.com/oemof.

[52] *oemof.solph — oemof.solph 0.5.6 documentation*. URL: https://oemof-solph.readthedocs.io/en/stable/readme.html.

[53] P. Oerlemans et al. *Hoge Temperatuur Opslag van warmte: Stand der techniek en bodempotentie*. Tech. rep. Nov. 2023. URL: https://www.ebn.nl/wp-content/uploads/2023/05/1jun2023_Potentieonderzoek_HTO_EBN_IF_Technology_-Rotterdam_Den_Haag_-Leidse_Regio.pdf.pdf.

[54] *Open Warmtenet Delft - Stichting Warmtenetwerk*. Dec. 2024. URL: https://warmtenetwerk.nl/warmteproject/open-warmtenet-delft/.

[55] PBL. *Klimaat- en energieverkenning 2024*. Tech. rep. 2024. URL: https://www.pbl.nl/system/files/document/2025-01/pbl-2024-klimaat-en-energieverkenning-2024-5490.pdf.

[56] Steven van Polen et al. *Informatieblad netverzwaring en netcongestie*. Tech. rep. 2025, PBL | 2 –PBL | 5. URL: https://www.pbl.nl/system/files/document/2025-03/pbl-2025-informatieblad-netverzwaring-en-netcongestie-5667.pdf.

[57] Reiner-Lemoine-Institut. *oemof – Reiner-Lemoine-Institut*. URL: https://reiner-lemoine-institut.de/en/project/oemof/.

[58] Robin Renoth et al. "Social acceptance of geothermal technology on a global view: a systematic review". In: *Energy Sustainability and Society* 13.1 (Dec. 2023). DOI: 10.1186/s13705-023-00432-1. URL: https://doi.org/10.1186/s13705-023-00432-1.

[59] Stewart Robinson and Warwick Business School. *Simulation: the practice of model development and use*. John Wiley Sons Ltd, 2004. URL: https://lmsspada.kemdikbud.go.id/pluginfile.php/123916/mod_label/intro/simulation-the-practice-of-model-development-and-use.9780470847725.21800.pdf.

[60] Els van der Roest et al. "Towards Sustainable Heat Supply with Decentralized Multi-Energy Systems by Integration of Subsurface Seasonal Heat Storage". In: *Energies* 14.23 (2021). ISSN: 1996-1073. DOI: 10.3390/en14237958. URL: https://www.mdpi.com/1996-1073/14/23/7958.

[61] sayyed Mohammad Sanaei and Toshihiko Nakata. "Optimum design of district heating: Application of a novel methodology for improved design of community scale integrated energy systems". In: *Energy* 38 (Feb. 2012), pp. 190–204. DOI: 10.1016/j.energy.2011.12.016.

[62] Thijs Scholten et al. *Impact van de warmtetransitie op het lokale elektriciteitsnet*. Tech. rep. 23.220430.070. May 2023. URL: https://vng.nl/sites/default/files/2023-07/onderzoek_impact_warmtetransitie_elektriciteit_buurten.pdf.

[63] Peter Sorknæs. "Hybrid energy networks and electrification of district heating under different energy system conditions". In: *Energy Reports* 7 (Oct. 2021), pp. 222–236. DOI: 10.1016/j.egyr.2021.08.152.

[64] Centraal Bureau voor de Statistiek. "92 procent woningen op aardgas begin 2019". In: (Feb. 2021). URL: https://www.cbs.nl/nl-nl/nieuws/2021/07/92-procent-woningen-op-aardgas-begin-2019#:~:text=Voor%203%20procent%20van%20alle,heeft%20een%20all%2Delectric%20hoofdverwarmingsinstallatie..

[65] John Sterman. "Business Dynamics, System Thinking and Modeling for a Complex World". In: *http://lst-iiep.iiep-unesco.org/cgi-bin/wwwi32.exe/[in=epidoc1.in]/?t2000=013598/(100)* 19 (Jan. 2000).

[66] Sebastian Stinner, Kristian Huchtemann, and Dirk Müller. "Quantifying the operational flexibility of building energy systems with thermal energy storages". In: *Applied Energy* 181 (Aug. 2016), pp. 140–154. DOI: 10.1016/j.apenergy.2016.08.055. URL: https://doi.org/10.1016/j.apenergy.2016.08.055.

[67] *Tarieven Stedin | Stedin*. URL: https://www.stedin.net/zakelijk/betalingen-en-facturen/tarieven.

[68] Francis Tuffner. *Grid Capacity – What is it, what determines it, does one number work, and how does it relate to electric vehicles?* Tech. rep. Nov. 2023. DOI: 10.2172/2221804. URL: https://doi.org/10.2172/2221804.

[69] Unknown. *Aardgasvrije gebouwde omgeving: de realisatie en beïnvloedende factoren*. Tech. rep. URL: https://www.rvo.nl/sites/default/files/2022-11/74812_RVO_Aardgasvrij_2022_PDF_UA.pdf.

[70] Els Van Der Roest et al. "Introducing Power-to-H3: Combining renewable electricity with heat, water and hydrogen production and storage in a neighbourhood". In: *Applied Energy* 257 (Nov. 2019), p. 114024. DOI: 10.1016/j.apenergy.2019.114024. URL: https://doi.org/10.1016/j.apenergy.2019.114024.

[71] Philip Vardon et al. *High-Temperature Aquifer Thermal Energy Storage (HT-ATES) system for research development and demonstration on the TU Delft campus*. Tech. rep. Mar. 2024. DOI: 10.5194/egusphere-egu24-14989. URL: https://doi.org/10.5194/egusphere-egu24-14989.

[72] B. Visser and R. Terwel. *De kosten en baten van warmteopslag in warmtenetten*. Tech. rep. Nov. 2024. URL: https://kalavasta.com/projects/warmteopslag.

[73] Lena Vorspel and Jens Bücker. "District-Heating-Grid Simulation in Python: DiGriPy". In: *Computation* 9.6 (2021). ISSN: 2079-3197. DOI: 10.3390/computation9060072. URL: https://www.mdpi.com/2079-3197/9/6/72.

[74] D. Voskov et al. "A research and production geothermal project on the TU Delft campus: initial modeling and establishment of a digital twin". In: *PROCEEDINGS, 49th Workshop on Geothermal Reservoir Engineering Stanford University*. 2024. URL: https://pangea.stanford.edu/ERE/db/GeoConf/papers/SGW/2024/Voskov.pdf.

[75] Greg Wilson et al. "Best practices for scientific computing". In: *PLoS Biology* 12.1 (Jan. 2014), e1001745. DOI: 10.1371/journal.pbio.1001745. URL: https://doi.org/10.1371/journal.pbio.1001745.

[76] Weiye Zheng et al. "Participation of strategic district heating networks in electricity markets: An arbitrage mechanism and its equilibrium analysis". In: *Applied Energy* 350 (Aug. 2023), p. 121732. DOI: 10.1016/j.apenergy.2023.121732. URL: https://doi.org/10.1016/j.apenergy.2023.121732.

[77] Marette Zwamborn et al. "HT-ATES systems in district heating networks, a Dutch benchmark study". In: Oct. 2022.

A
Input variables

A.1. Input values 2030

This appendix presents the key input assumptions and datasets used in the simulation model. These values reflect expected conditions for the year 2030, based on projections from the *Klimaat- en Energieverkenning (KEV)* and related national energy outlooks. The aim is to capture realistic boundary conditions under which future district heating systems are likely to operate. The sections below outline electricity price profiles, network temperature settings, and ambient weather conditions that together define the energy and thermal demand environment for the simulations.

The chosen 2030 scenario represents a mid-term outlook where electrification and sustainability targets are gaining momentum, but certain infrastructure and cost barriers remain. This year was selected to evaluate the performance and feasibility of system configurations under plausible near-future market and policy conditions.

A.1.1. Electricity price profiles

Electricity price data for three representative years was used to simulate different market and weather conditions. These profiles represent hourly prices across the full year and reflect fluctuations due to weather, renewable generation, and overall electricity system behavior.

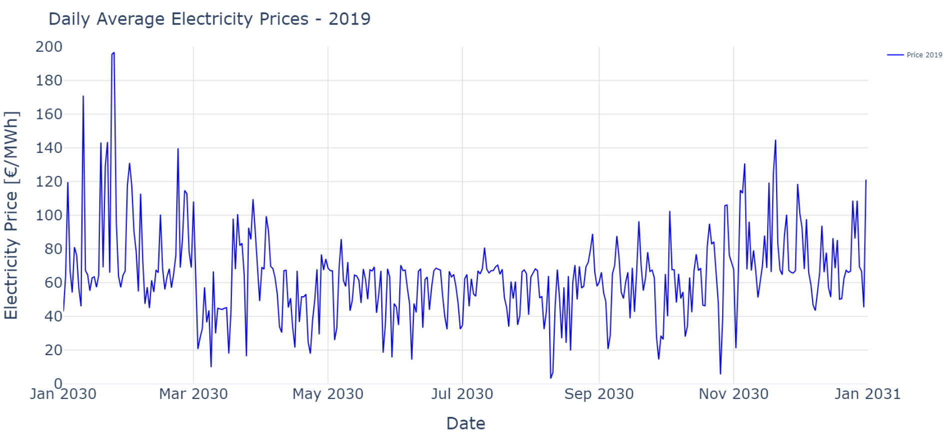

Figure A.1: Electricity price profile for default year (2019)

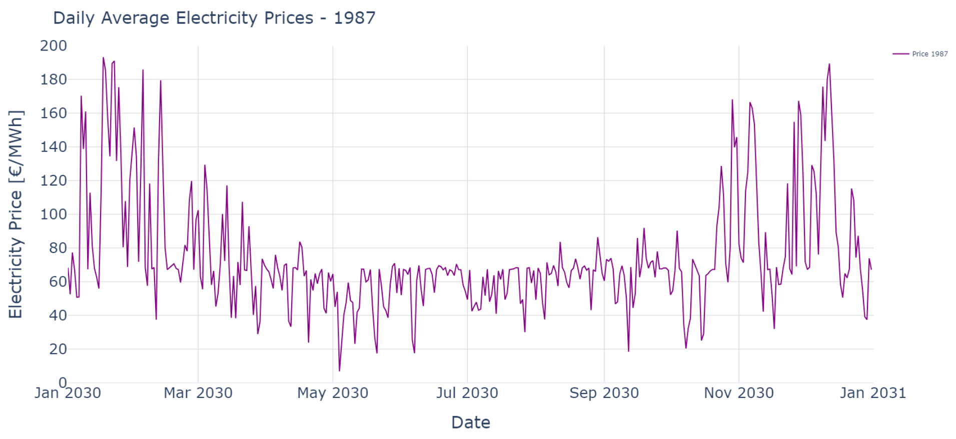

Figure A.2: Electricity price profile for weather year W1 (1987)

A.1.2. District heating temperatures

The district heating supply and return temperature profiles depend strongly on outdoor temperature and thus differ by weather year. The figures below show the modeled network temperatures for both the default (2019) and extreme (1987) years. These profiles determine the required supply temperature from generation technologies and directly affect the load on the heat pump.

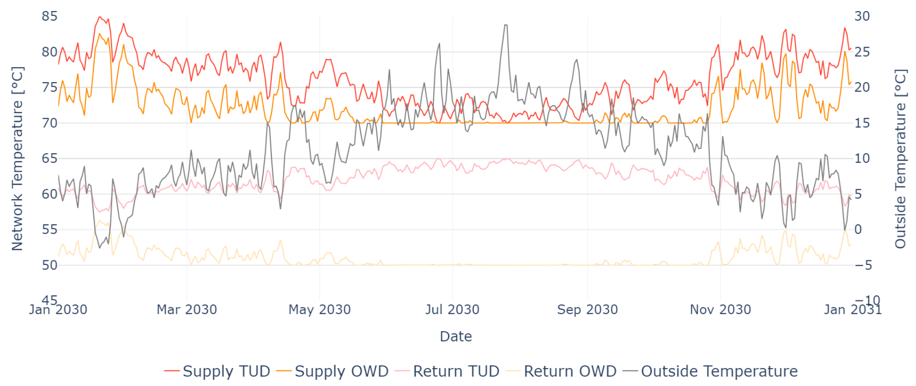

Figure A.3: Network temperatures during default year (2019)

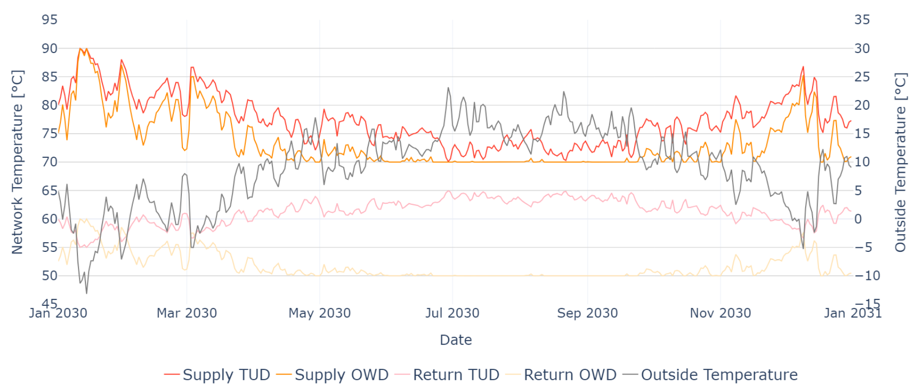

Figure A.4: Network temperatures during weather year W1 (1987)

A.1.3. Temperatures and demand

A critical input to the model is the heat demand profile, which is derived from the relationship between ambient outdoor temperature and required heating energy. The figures below demonstrate this correlation. As expected, colder conditions result in higher heat demand. These demand curves are used to simulate hourly thermal load requirements for the district heating network.

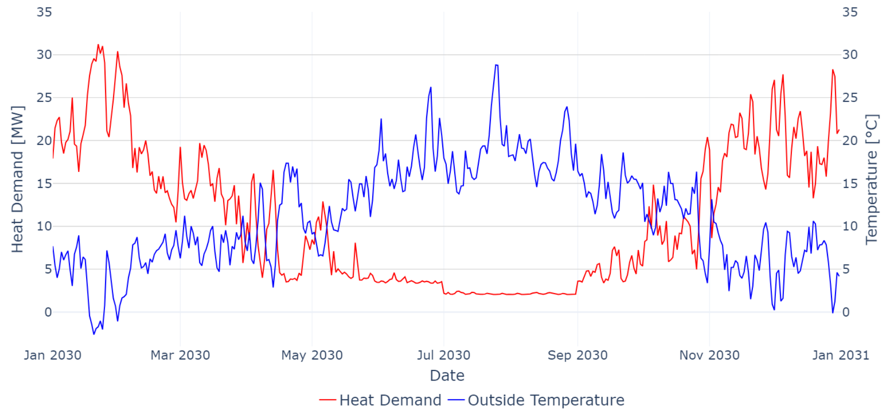

Figure A.5: Temperature and demand def(2019)

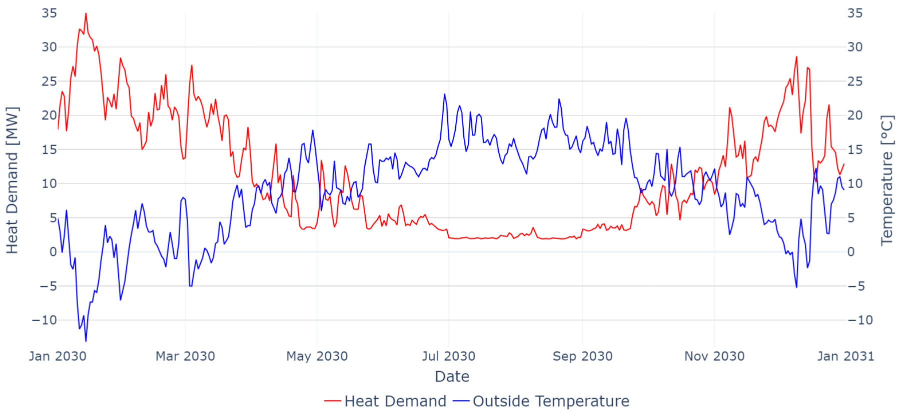

Figure A.6: Temperature and demand W1(1987)

Together, these input datasets form the foundation for the scenario modeling performed in this thesis. By combining realistic electricity price fluctuations, ambient temperature profiles, and network demand characteristics, the model reflects diverse operational contexts, ranging from average to extreme years. This allows a robust evaluation of heating system configurations under future conditions.

A.2. Sensitivity analysis

The sensitivity analysis show the results for varying each parameter with an increase of 25%. The test is conducted with daily averages which result in difficult results.

	LCOH var OPEX	Total Costs	CO_2 Emission
	€/MWh	*M€*	*kg/MWh*
Base Scenario	9.36	5.937	5.65
Total heat demand	25.7%	8.3%	176.1%
Electricity price	17.9%	2.6%	0.0%
Electricity CO_2 emission	0.4%	0.1%	5.1%
CO_2 price	1.6%	0.2%	0.0%
Supply T network	36.0%	11.8%	156.5%
HT-ATES			
Volume	0.0%	0.0%	0.2%
Max charge/discharge rate	-2.7%	-0.4%	-21.6%
Min charge/discharge rate	0.1%	0.0%	0.0%
COP of the ESP	-0.4%	-0.1%	0.0%
Geothermal			
Capacity	-1.3%	13.9%	-6.0%
COP of the ESP	-2.6%	-0.4%	-0.7%
Other variable OPEX	5.4%	0.8%	0.0%
Heat Pump			
Capacity	-3.8%	5.2%	-43.4%
COP of the heat pump	-13.6%	-2.0%	-46.0%
Other variable OPEX	0.1%	0.0%	0.0%
Gas Boiler			
Efficiency rate	-0.6%	-0.1%	5.1%
Emission factor	1.6%	0.3%	25.1%
Other variable OPEX	0.3%	0.1%	0.0%
Gas price	1.4%	0.2%	0.0%

Table A.1: Sensitivity analysis for 25% variation in input parameters. Highest increases are shown in red, largest decreases in blue.

B

Results overview

In this appendix, the detailed outputs of the simulations are presented. The results include tables of heat generation shares, component utilization, electricity consumption, emissions, and cost indicators (KPIs) for various configurations and weather years. These tables allow for a more granular inspection of the model performance and system behavior under different experimental settings. Some of the result tables are not fully completed due to a recent change in the model, which left insufficient time to finish running all simulations for every experiment and scenario.

B.1. Fixed electricity price

The first experiment evaluates system performance under a fixed electricity price, comparing various system configurations across both default and extreme (W1) weather years. The results are presented in Table B.1. This table provides an overview of the heat source distribution, the efficiency of the HT-ATES system, and the total annual electricity use per configuration.

The heat distribution columns show the share of heat delivered by geothermal energy (Geo), HT-ATES, heat pump (HP), and gas boiler (Gas). The HT-ATES efficiency, expressed as a percentage, indicates the ratio of heat discharged versus heat charged into the storage system. As storage size increases, so does the system efficiency rise from about 52% in small storage systems (SS) to over 60% in large storage systems (LS). This increase is primarily due to reduced relative thermal losses: larger systems experience proportionally less heat loss to the surrounding environment. Lastly, the electricity use (E-use) column shows the total annual electricity consumption for each configuration.

Table B.2 presents key performance indicators (KPIs) for the fixed electricity price scenario. The table compares several system configurations in terms of levelized cost of heat (LCOH), robustness, and CO_2 emissions. Two types of LCOH values are reported: the variable OPEX LCOH, representing operational cost per MWh when excluding investment and fixed costs, and the total cost LCOH, which includes CAPEX, fixed OPEX, and variable OPEX. The robustness column expresses the percentage increase in variable OPEX LCOH when moving from the default (Def) to the extreme weather (W1) scenario. This metric indicates how sensitive the system is to more extreme conditions. A lower percentage suggests greater resilience. Finally, CO_2 emissions per MWh are shown for both weather scenarios.

fixed-E	Heat Distribution [%]				Efficiency	E-use
Design	**Geo**	**HT-ATES**	**HP**	**Gas**	**HT-ATES [%]**	[MWh]
			Def scenario			
BC3.5	96.17	-	0.00	3.83	-	16076
SS3	89.56	6.58	0.00	3.87	51.8	16039
SS3.5	91.96	6.58	0.00	1.46	51.9	16448
MS3.5	90.04	9.29	0.00	0.07	55.6	16657
LS3.5	84.87	14.68	0.00	0.44	60.1	16895
LS5	85.23	14.68	0.00	0.01	60.1	16981
			W1 scenario			
SS3	87.99	6.29	0.00	5.72	52.0	16638
MS3.5	89,75	9,06	0.00	1.19	55.9	17363
LS5	85.79	14.06	0.11	0.05	60.1	17905

Table B.1: heat distribution, HT-ATES utilization and electricity use per design (dynE)

Fixed-E	LCOH [€/MWh]				Robustness	CO_2-Emission	
Design	**def**		**W1**		**Cost Increase**	**def**	**W1**
	var OPEX	tot costs	var OPEX	tot costs	[%]	[kg CO_2/MWh]	
BC3.5	13.74	86.17				11.26	
SS3	13.63	82.97	15.44	81.85	13.28	10.80	14.93
SS3.5	12.64	85.58				5.45	
MS3.5	12.39	86.24	13.84	86.79	11.70	3.72	4.92
LS3.5	12.47	88.05				3.24	
LS5	12.30	97.82	13.41	95.31	9.02	2.28	2.38

Table B.2: Fixed-E: LCOH, robustness, and CO_2-emission values under def and W1 assumptions

B.2. Dynamic electricity price

The second experiment evaluates system performance under dynamic electricity pricing. Two different weather years are considered: a default year (def - 2019), an extreme cold year (W1 - 1987).

B.2.1. KPIs

The table in Table B.12 summarizes the main KPIs. The LCOH, robustness, and CO_2 emissions for all system designs across the two weather scenarios are showed.

The total LCOH values are lower in the extreme weather scenario (W1) compared to the default case. This outcome can be attributed to the higher heat demand in the W1 scenario. While absolute system costs are higher because of increased variable OPEX. The total LCOH metric is calculated by dividing the total costs over a larger amount of delivered heat. This increased denominator leads to a lower €/MWh value for the system designs, despite the actual rise in system expenditure.

dynE	LCOH [€/MWh]				Robustness [%]	CO_2-Emission [kg/MWh]	
Design	def		W1		Cost Increase	def	W1
	var OPEX	tot costs	var OPEX	tot costs			
BC3.5	15.08	87.50	17.45	86.80	15.72	11.26	16.28
BC5	14.15	97.33	15.87	95.53	12.16	4.78	6.02
SS-3.5	13.47	86.41	15.25	85.09	13.21	5.47	7.38
SS-5	13.02	96.72	14.48	94.63	11.21	2.55	2.73
MS2.5	15.06	81.73	17.56	81.40	16.60	16.66	23.35
MS3	13.68	83.94	15.54	82.82	13.60	8.29	10.34
MS3.5	12.98	86.83	14.55	85.27	12.10	3.76	4.90
MS4	12.73	90.17	14.19	88.35	11.47	2.51	3.15
MS5	12.67	97.29	14.05	95.07	10.89	2.37	2.43
LS3.5	12.76	87.52	14.20	85.58	11.29	3.25	4.82
LS5	12.64	98.16	13.71	95.61	8.47	2.39	2.45

Table B.3: dynE: LCOH, CO_2-emissions, and cost robustness for def and W1 scenarios.

B.3. Grid constraints

This section presents the results of the GridC experiment, which explores the influence of electricity grid constraints on the performance of different heating system configurations. Two grid connection scenarios are considered: an unconstrained (NP – no peak limit) and a constrained (P0.6 – 0.6 MW peak limit) grid. Table B.4 summarizes key performance indicators.

GridC		LCOH [€/MWh]				Robustness [%]	CO_2-Emission	
Profile	design	def		W1		Cost Increase	def	W1
		var OPEX	tot costs	var OPEX	tot costs		[kg/MWh]	
BC3.5	NP	15.76	88.18				15.54	
	P0.6	17.76	90.18				27.85	
MS3	NP	14.33	84.59				12.34	
	P0.6	15.91	86.17				21.78	
MS3.5	NP	13.38	87.23	15.07	85.79	12.63	6.40	7.81
	P0.6	14.86	88.72				15.61	
MS4	NP	12.89	90.32	14.44	89.60	12.02	3.12	4.34
	P0.6	14.17	91.61				11.40	
MS5	NP	12.69	97.30	14.07	95.10	10.87	2.39	2.55
	P0.6	13.07	98.48				4.43	
LS3.5	NP							
	P0.6	14.42	89.18				12.39	

Table B.4: GridC experiment: LCOH and CO_2-emissions for def and W1 scenarios across designs and grid constraint levels.

Table B.5 provides a comparison of electricity-related indicators across various system configurations featuring a 3.5 MW heat pump. The table includes values for total annual electricity consumption (E-use), total electricity expenditures (E-costs), and the resulting average electricity price in €/MWh derived from these values. Additionally, the table shows the variable annual costs associated with operating the HT-ATES system (ATES costs).

Comparison E	E-use	E-costs	Average E-price	ATES costs
Design	[MWh]	[€]	[€/MWh]	[€]
FixedE				
BC3.5				0
SS3.5	16448	1060445	64.5	134988
MS3.5	16657	1073922	64.47	172015
LS3.5	16895	1089317	64.5	248226
dynE				
BC3.5	16076	1164129	72.4	0
SS3.5	16441	1140763	68.6	92978
MS3.5	16846	1130810	67.13	113899
LS3.5	17147	1188110	65.2	190118
grid C-NP				
BC3.5	15750	1132482	71.9	0
SS3.5				
MS3.5	16729	1109671	66.3	113366
LS3.5				
gridC-P0.6				
BC3.5	14884	1046215	70.3	0
SS3.5				
MS3.5	15509	1043273	65.3	114962
LS3.5	16368	1069790	65.4	190684

Table B.5: Electricity use, costs, average prices and ATES costs per design under various scenarios

Table B.6 presents the variable operational expenditures (LCOH – variable OPEX) for the MS3.5 configuration under dynamic electricity pricing and two peak tariff (PT) scenarios. In these PT scenarios, an additional electricity cost is applied for consumption above a specified threshold—either 2 MW (PT(2)) or 3 MW (PT(3)). The values are given in €/MWh and reflect how sensitivity to tariff thresholds affects operational economics. The first row shows the reference case under dynamic pricing without peak tariffs. The subsequent rows show the impact of two penalty levels: p20 (20 €/MWh surcharge) and p30 (30 €/MWh surcharge). These penalties are only triggered when consumption exceeds the defined peak limit.

The comparable value for the dynamic electricity price scenario for MS3.5 is 12.98.

Design MS3.5	PT(3MW)	PT(2Mw)
price €20	13.15	13.67
price €30	13.24	14.04

Table B.6: Variable OPEX values for different design scenarios

B.4. Grid reinforcement

B.4.1. Network tariffs

Table B.7 shows the results of the network tariff (NT) experiment, in which different electricity tariff levels are applied to evaluate their impact on system economics and performance. The profiles BC3.5 and

MS3.5 are tested under increasing tariff prices, where an extra tariff represents an additional cost per MWh for electricity use.

NT		LCOH [€/MWh]		CO_2-Emission	E-use
Profile MS3.5	Tariff Price	var OPEX	Total Costs	[kg/MWh]	[MWh]
BC3.5	-	15.08	87.50	11.26	16183
	p20	18.44	90.86	11.26	16076
MS3.5	-	12.98	86.83	3.75	16846
	p2	13.34	87.19	3.75	16846
	p5	13.87	87.71	3.74	16799
	p10	14.74	88.59	3.74	167999
	p20	16.50	90.35	3.74	16798
	p30	18.26	93.01	3.78	16794

Table B.7: NT-3.5 experiment: LCOH, CO_2-emissions, and electricity use for varying tariff levels.

Table B.8 provides data from Stedin on connection and annual usage fees for various grid capacities. These real-world tariffs highlight the step changes in infrastructure cost associated with different connection sizes. [67].

Network connection (MW)	Connection costs [€]	Yearly tariff [€/year]
> 1 & < 1.75	€ 45,252.62	€ 1,137.96
> 1.75 & < 5	€ 255,592.58	€ 2,762.05
> 5 & < 10	€ 341,986.09	€ 13,653.31

Table B.8: Network tariffs Stedin

B.4.2. Grid reinforcement costs

This section presents the input assumptions used to estimate the costs associated with electricity grid reinforcement and connection upgrades. It is important to note that these values are highly context-dependent—varying significantly by location, time, and local market conditions. Figure B.1 provides a reference cost estimate from CE Delft, which outlines the indicative investment needed for grid reinforcement per additional MW of connection capacity [62]. While these figures serve as a general benchmark, they are not universally applicable and should be adapted to the specific project context for accurate system planning and cost evaluation.

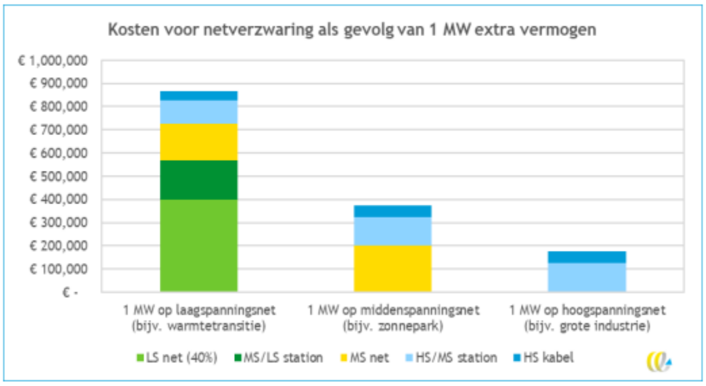

Figure B.1: Costs grid reinforcements

B.4.3. Cost overview
Table B.9 shows the full annual cost overview for the MS-3.5 design in the default weather year. The breakdown includes energy expenditures, emissions costs, fixed OPEX, CAPEX for each component, and grid-related investments.

Energie en kosten	**MWh/year**	**€/MWh**	**€/year**
Gas	649	24.7	€16,044
Electricity	16846	67.1	€1,130,810
Other	–	–	€56,729
Emissies	**kg CO_2/jaar**	**kg CO_2/MWh**	**€/year**
Direct gas	144,669	–	€15,608
Indirect electricity	213,946	–	€23,122
Emission intensity	–	3.75	–
Capex and fixed OPEX	**MW**	**Full load hours**	**€/year**
Geothermal [MW_{th}]	25.2	3,665	€4,224,156
Heat pump [MW_e]	3.5	4,254	€2,402,225
HT-ATES	–	–	€436,667
Gas boiler	–	–	300,000
Other costs			**€/year**
Network tariffs	–	–	–
Electricity grid reinforcements	–	–	€78,675
Total			**€8,384,037**

Table B.9: Cost overview for MS-3 with grid reinforcement

B.5. Extra experiments
B.5.1. Geothermal injection temperature
Table B.10 displays results for different geothermal injection temperatures (35°C and 45°C). The total LCOH values shown in this table may not fully represent real system costs. In this model, geothermal investment costs are scaled based on output capacity. However, changes in injection temperature affect this output value without necessarily reflecting changes in actual capital expenditures. Since the physical capacity of the well remains nearly the same, the associated cost reductions are not representable for real-life case.

GeoT	LCOH [€/MWh]				Robustness [%]	CO_2-Emission [kg/MWh]	
Design	35°C		45°C		Cost Increase	35°C	45°C
	var OPEX	tot costs	var OPEX	tot costs			
BC3.5	12.23	73.43	11.40	61.52	-6.79	9.48	8.60
MS2	11.99	63.85				12.00	
MS2.5	11.13	66.57				6.78	
MS3	10.75	69.79	9.78	61.32	-9.02	4.40	2.37
MS3.5	10.55	73.17	9.63	64.77	-8.72	3.09	1.91
MS4	10.49	76.69				2.88	
MS5	10.45	84.74				2.81	

Table B.10: dynE: LCOH, CO_2-emissions, and cost robustness for geothermal return temperatures of 35°C and 45°C.

B.5.2. Network temperature

Table B.11 provides the system outcomes for simulations with altered district heating supply temperatures of 5°C and 10°C.

T network	LCOH [€/MWh]				Robustness [%]	CO_2-Emission [kg/MWh]	
Design	5°C		10°C		Cost Increase	5°C	10°C
	var OPEX	tot costs	var OPEX	tot costs			
BC3	15.06	51.59				15.61	
MS2.5	13.92	80.59				13.09	
MS3	12.74	83.00	11.77	82.03	-7.61	5.99	3.97
MS3.5	12.22	86.07				2.72	
MS5	12.07	96.68	11.39	96.00	-6.79	2.26	2.15

Table B.11: dynE: LCOH, CO_2-emissions, and cost robustness for supply network temperature levels of 5°C and 10°C.

B.5.3. CO_2-price

Table B.12 summarizes the LCOH, CO_2 emissions, and robustness for various designs under increased CO_2 prices. Results are presented for two price levels: €0.40 and €0.80 per kg CO_2.

CO_2-price	LCOH [€/MWh]				Robustness [%]	CO_2-Emission [kg/MWh]	
Design	0.4		0.8		Cost Increase	0.4	0.8
	var OPEX	tot costs	var OPEX	tot costs			
MS2.5	19.92	86.60	18.11	85.72	33.43	16.66	15.01
MS3	16.10	86.36	14.74	85.97	20.56	8.28	6.23
MS3.5	14.08	87.93	13.56	87.36	10.58	3.75	3.01
MS4	13.46	90.90	13.08	90.35	7.43	2.50	2.14

Table B.12: dynE: LCOH, CO_2-emissions, and cost robustness for scenarios with CO_2 price at 0.4 and 0.8 €/kg.

C

Visualisation of Results

This appendix presents graphical outputs from key simulation scenarios, providing visual insights into the performance of different system configurations. The figures include load duration curves, daily heat generation profiles, and heat production during extreme conditions. These visualizations adds extra support to the quantitative results. It also provides more visual representation of different scenarios.

C.1. FixE: Fixed Electricity Price

SS-3.5

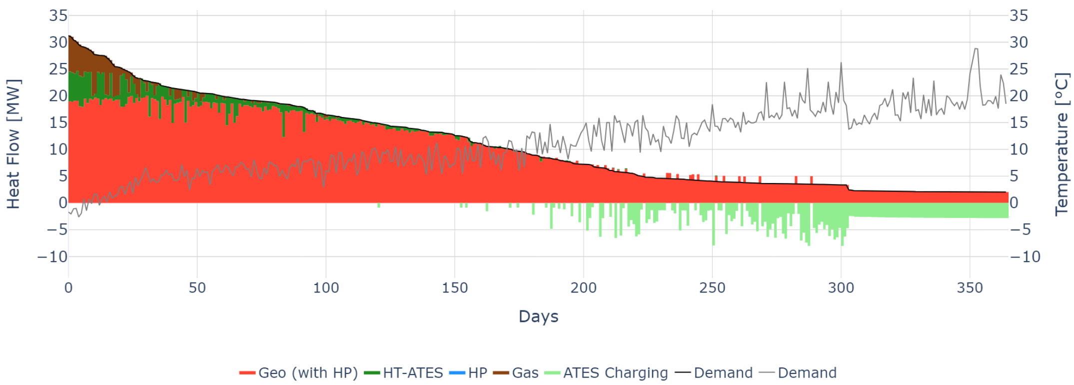

Figure C.1: Load duration curve [FixedE-SS-3.5 (def)]

MS-3.5

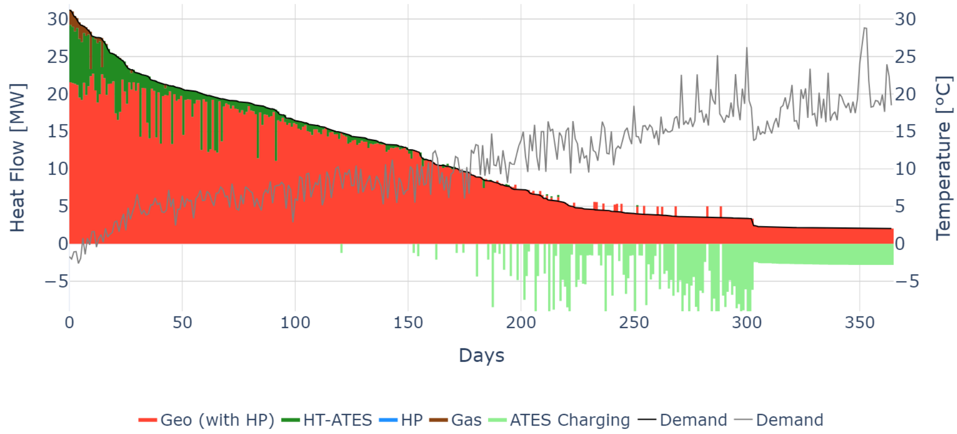

Figure C.2: Load duration curve [FixedE-MS-3.5 (def)]

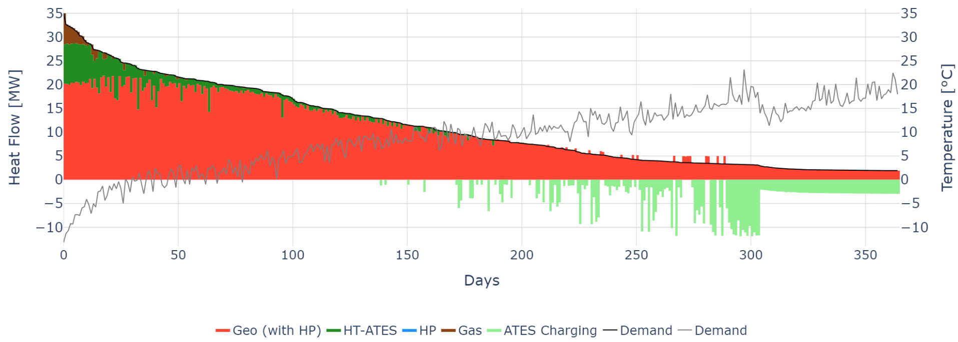

Figure C.3: Load duration curve [FixedE-MS-3.5 (w1)]

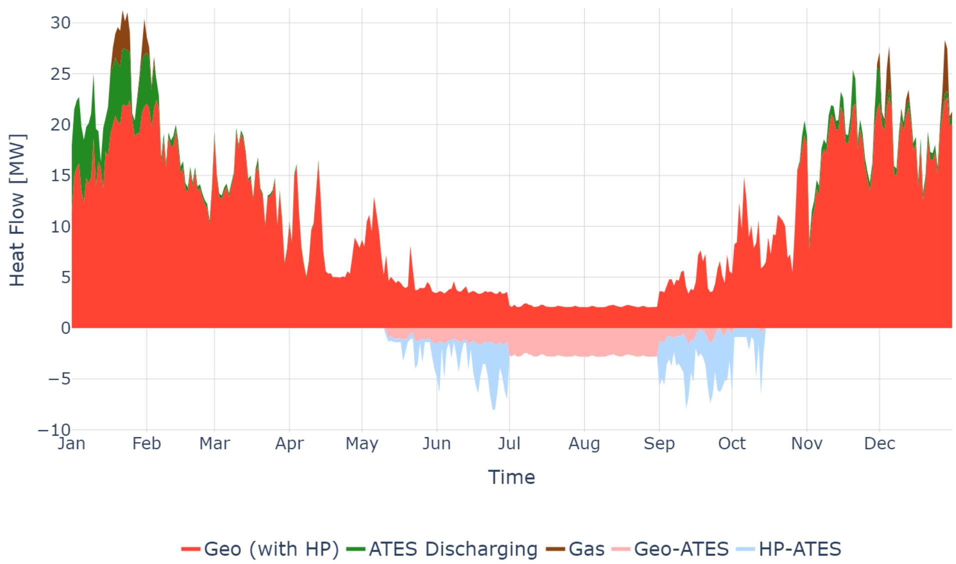

Figure C.4: Daily heat generation [FixedE-MS3.5 (def)]

C.2. dynE: Dynamic Electricity Price

Base Case MS3.5

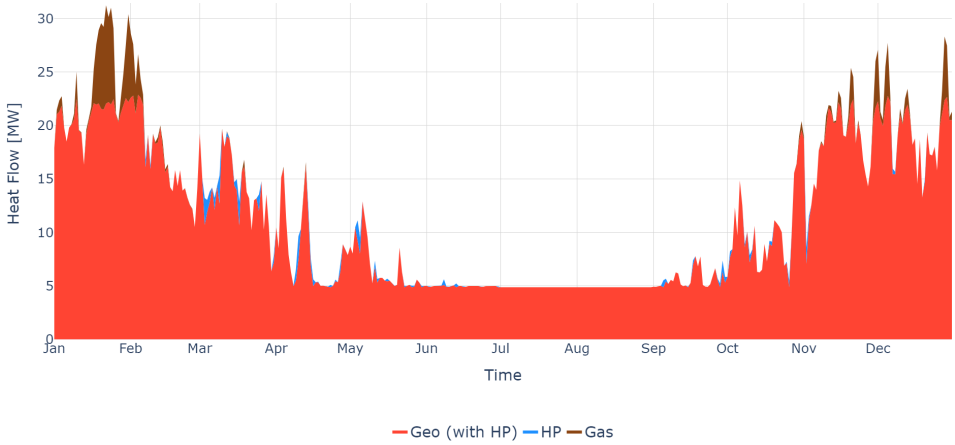

Figure C.5: Daily heat generation [dynE-BC3.5 (def)]

MS-3.5

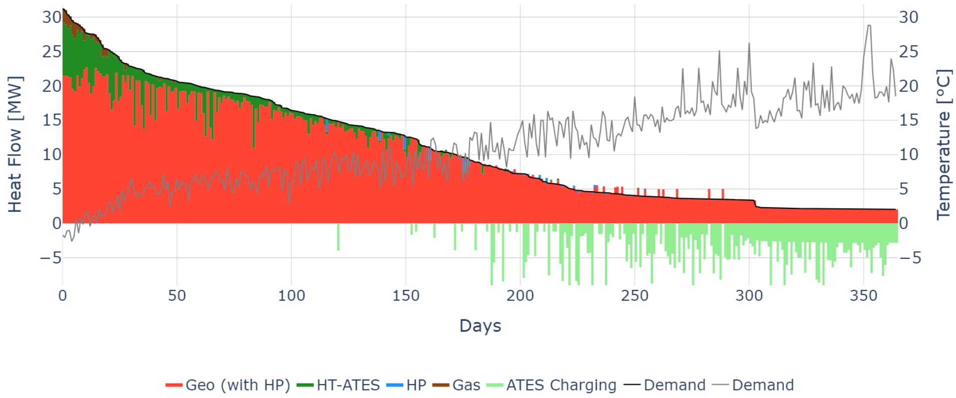

Figure C.6: Load duration curve [dynE-MS-3.5 (def)]

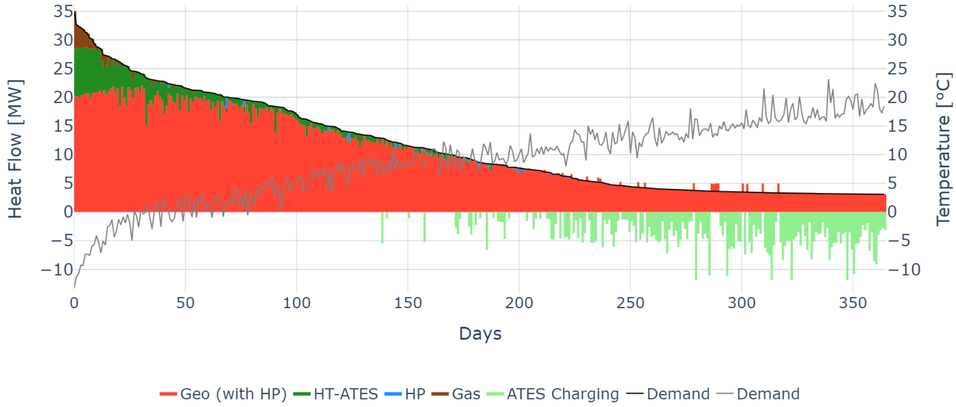

Figure C.7: Load duration curve [dynE-MS-3.5 (w1)]

MS-5

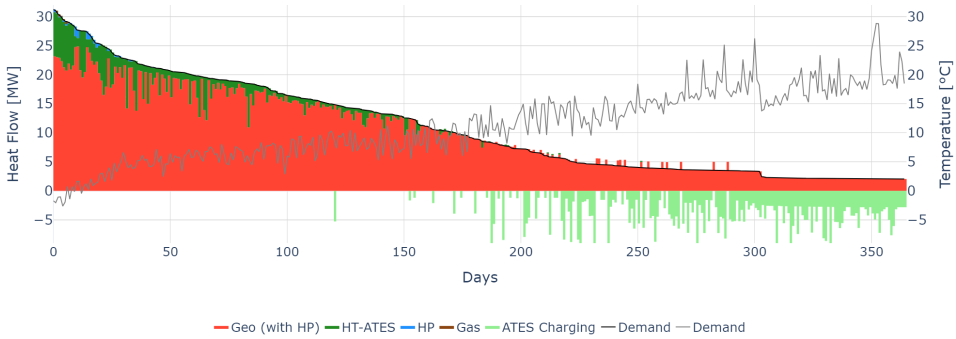

Figure C.8: Load duration curve [dynE-MS-5 (def)]

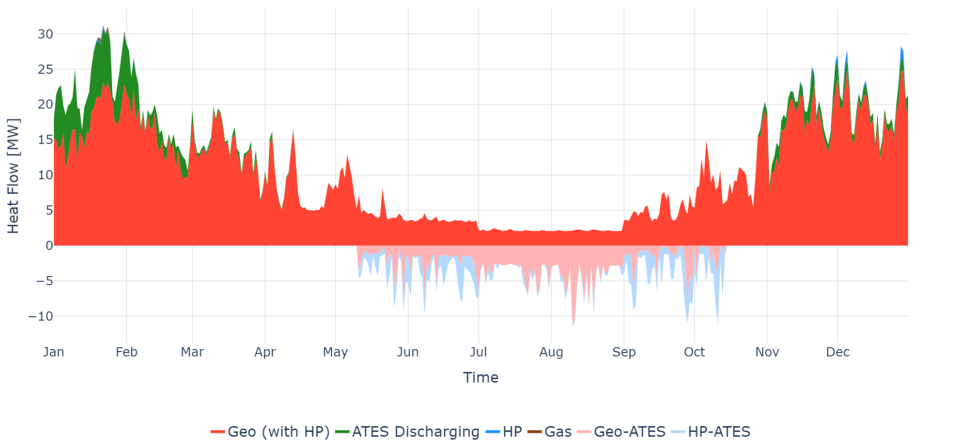

Figure C.9: Daily heat generation [dynE-MS5 (def)]

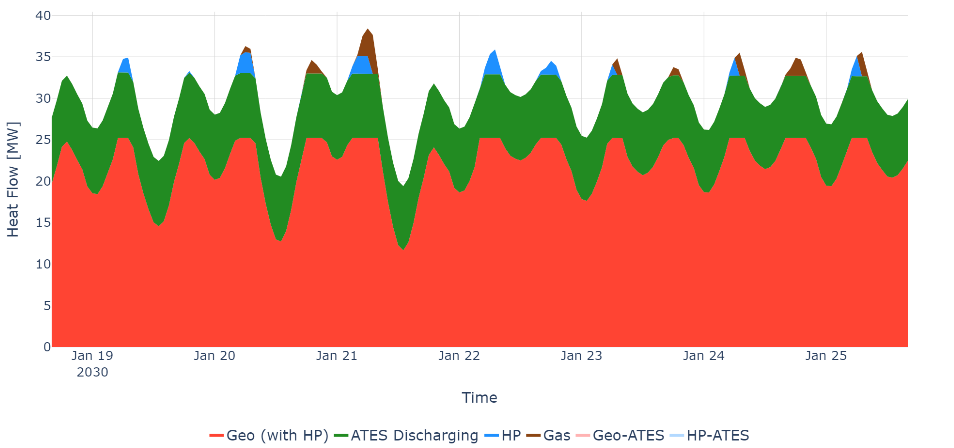

Figure C.10: Heat production during coldest week [dynE-MS5 (def)]

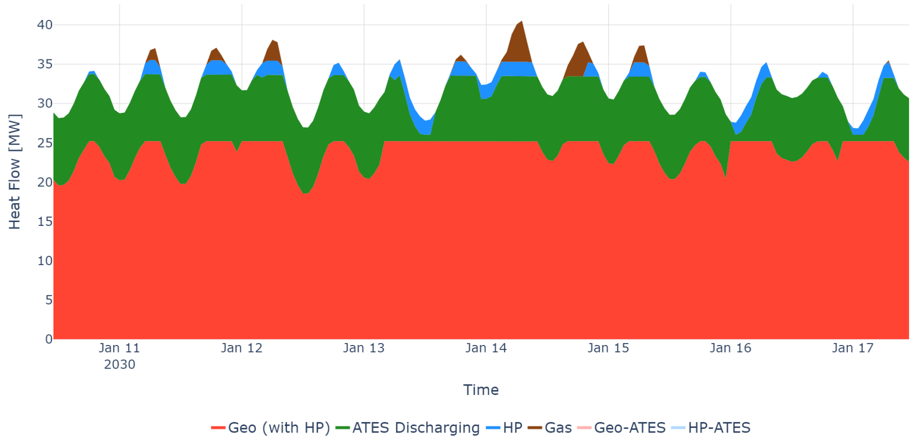

Figure C.11: Heat production during coldest week [dynE-MS5 (w1)]

LS-3.5

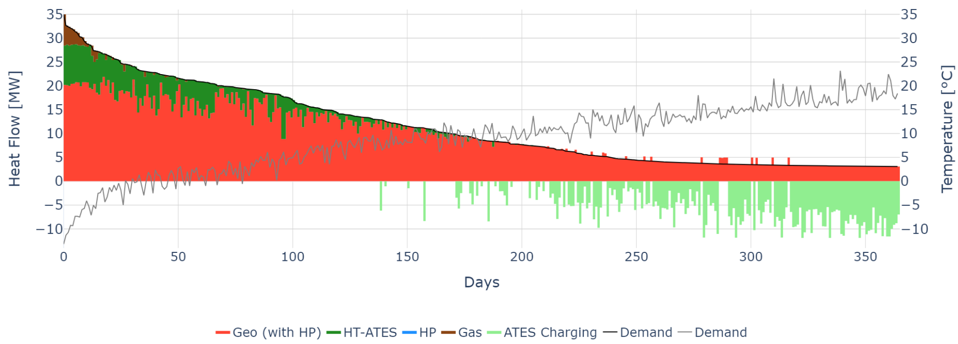

Figure C.12: Load duration curve [dynE-LS3.5 (w1)]

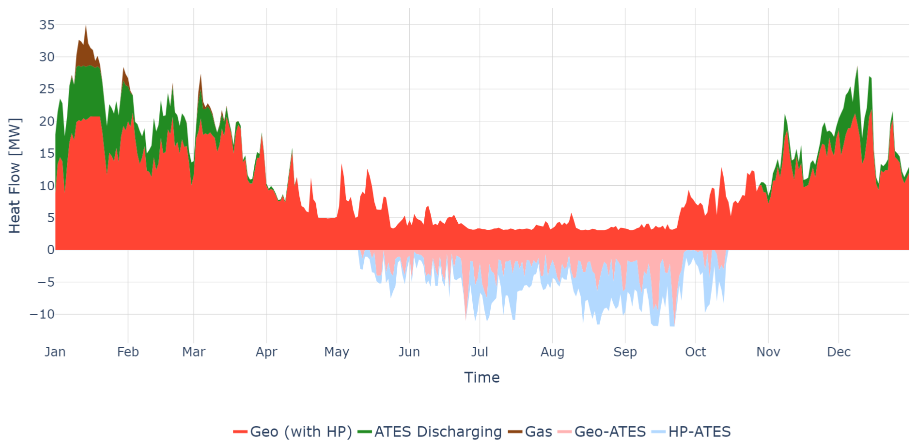

Figure C.13: Daily heat generation [dynE-LS3.5 (w1)]

C.3. Additional Experiments

Injection Temperature Geothermal 35°C

The following figures illustrate the system performance when the geothermal injection temperature is set to 35°C.

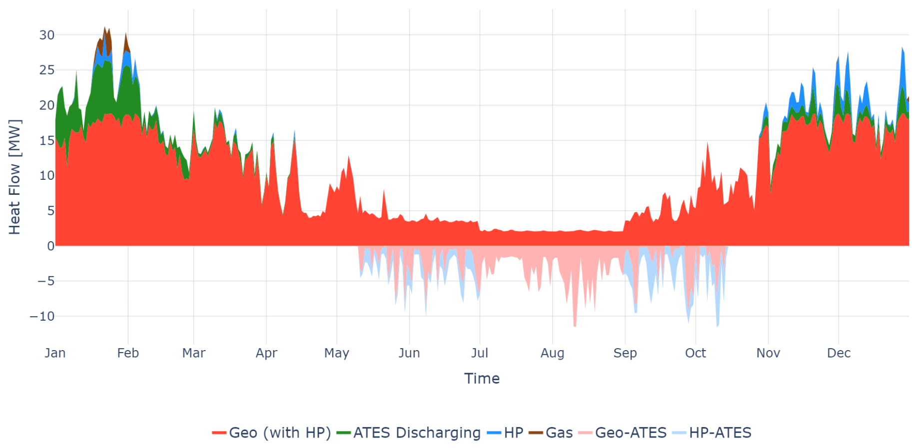

Figure C.14: Daily heat generation [Geo35-MS3.5 (def)]

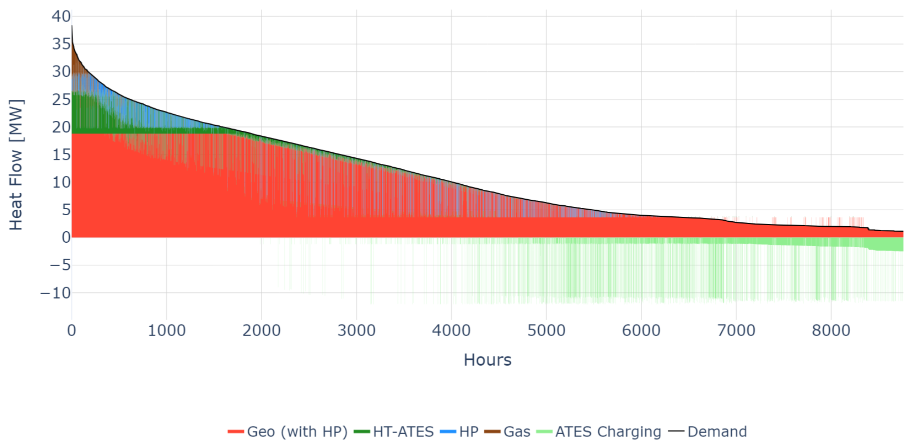

Figure C.15: Load duration curve [Geo35-MS3.5 (def)]

Injection Temperature Geothermal 45°C

This section visualizes how the system operates when the geothermal reinjection temperature is set to 45°C.

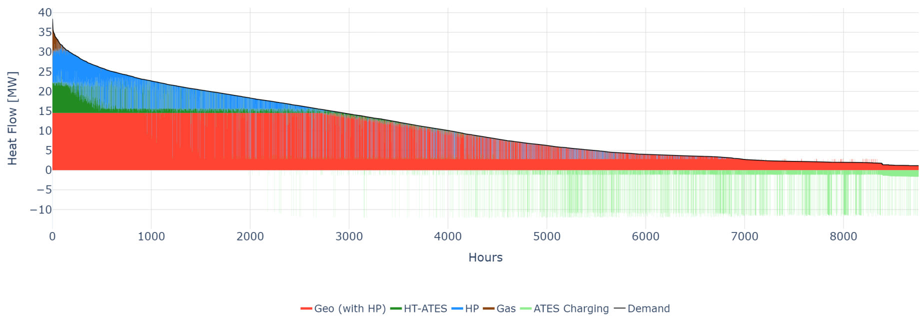

Figure C.16: Hourly load duration curve [Geo45-MS3 (def)]

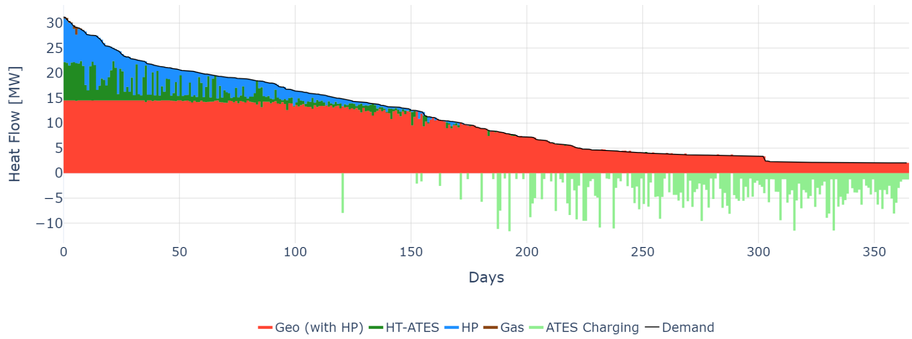

Figure C.17: Load duration curve [Geo45-MS3.5 (def)]

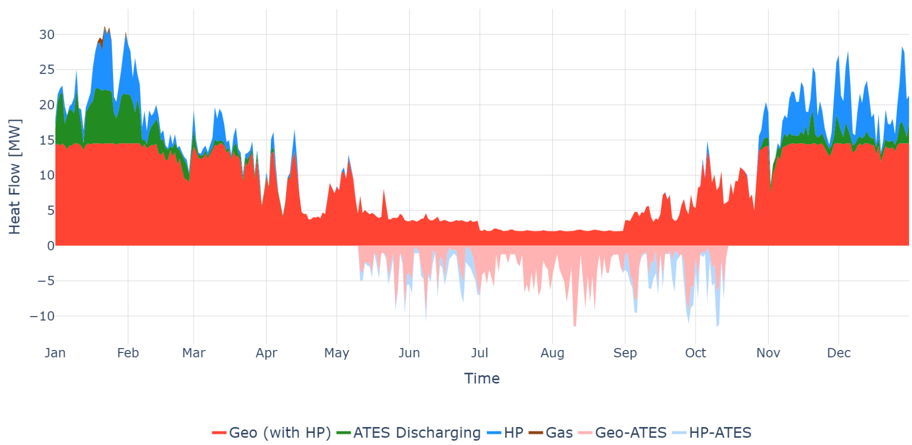

Figure C.18: Daily heat generation [Geo45-MS3.5 (def)]